ENGINEERING ASPECTS OF POLYPYRROLE ACTUATORS AND THEIR APPLICATION IN ACTIVE CATHETERS

by

Tina Shoa Hassani Lashidani

B. Eng. Iran University of Science & Technology, 2000
M. Sc. University of Manitoba, 2004

A THESIS SUBMITTED IN PARTIAL FULFILLMENT OF
THE REQUIREMENTS FOR THE DEGREE OF

DOCTOR OF PHILOSOPHY

in

The Faculty of Graduate Studies

(Electrical and Computer Engineering)

THE UNIVERSITY OF BRITISH COLUMBIA
(Vancouver)

May 2010

ABSTRACT

Polypyrrole has shown potential as an electrochemically driven artificial muscle. It has also been studied as an electromechanical sensor. Despite its potential as an engineering material, its actuation and sensing behaviours have not been fully characterized and modelled. In this thesis, polypyrrole is characterized in terms of electrochemical stability, mechanical stiffness and sensing capability. A link between actuation and sensing is also presented, suggesting a new mechanism of electromechanical coupling. An analytical model is developed to predict the dynamic actuation response. Finally, polypyrrole is applied to actively deform a catheter.

Characterization studies were performed on a PF_6^- (hexafluorophosphate) doped polypyrrole inside an aqueous solution of sodium hexafluorophosphate ($NaPF_6$) - a combination that has shown large repeatable actuation. Polypyrrole is found to be electrochemically stable from -0.4 V to 0.8 V versus an Ag/AgCl reference electrode. Its stiffness is a function of actuation voltage as well as the amplitude and the frequency of the applied load. Its sensitivity as a load sensor is ~ 4×10^{-11} V/Pa and it responds up to at least 100 Hz.

A 2D transmission line model representing polypyrrole electrochemical properties (e.g. ionic and electronic conductivities and charge storage) is used to determine charging and hence actuation as a function of time and position. This model is coupled with a mechanical model to predict deflection and is used to design a polypyrrole driven catheter. The capability of polypyrrole to (1) manoeuvre catheters inside arteries and (2) scan catheter tips for imaging were evaluated by fabricating *in vitro* devices and testing their degree of bending and actuation speed. The feasibility of using the polypyrrole

sensor as a feedback loop element on the catheter was also studied and the sensitivity was found to be insufficient for practical use.

Polypyrrole driven catheters are able to provide the degree of bending needed for manoeuvring; however actuation speed needs to be improved for the imaging application investigated, which requires operation at frequencies > 10 Hz. According to the model polypyrrole electrodes with thin conductive backings on a flexible catheter can provide the required scanning speed. Further work is required to create encapsulated designs which contain the electrolyte needed for actuation.

TABLE OF CONTENTS

LIST OF TABLES

LIST OF FIGURES

GLOSSARY

Ag/AgCl	Silver/Silver Chloride
AQ	Aqueous
CV	Cyclic Voltammetry
EIS	Electrochemical Impedance Spectroscopy
IPMC	Ionic Polymer Metal Composite
MEMS	Microelectromechanical Systems
$NaPF_6$	Sodium Hexafluorophosphate
NMR	Nuclear Magnetic Resonance
OCT	Optical Coherence Tomography
PBS	Phosphate Buffered Saline
PF_6	Hexafluorophosphate
SMA	Shape Memory Alloy
SMP	Shape Memory Polymer

ACKNOWLEDGEMENTS

I would like to express my sincere gratitude to my advisor Dr. John Madden for the continuous support of my Ph.D study and research. His great personality and his immense knowledge have made him a perfect supervisor. He generously granted his time and effort to help me in all the time of research and writing of this thesis.

I would like to thank Dr. Yang, Dr. Munce and Kenneth Lee, for their great collaboration in this research. I would also like to acknowledge members of molecular mechatronics laboratory, Mathew Cole, Arash Takshi, Tissa Mirfakhrai, Eddie Fok, Alex Dimopoulos, Niloofar Fekri, Joanna Lam, Ali Mahmoodzadeh and Dan Yoo, for the valuable discussions we had and their friendship. I would like to thank the Natural Sciences and Engineering Research Council of Canada and British Columbia Innovation Council for funding this research.

I am grateful to my friends; Arghavan Emami, for inspiring me with her passion for science, and Mahsa Pourazad for her constant encouragements. They have been wonderful friends to me and have supported me during the 15 years of our friendship.

My deepest gratitude goes to my family for their unconditional love and support throughout my life; this achievement would be impossible without them. I am indebted to my parents (Zahra Alizadeh and Parviz Shoa) for providing the best possible environment for me to grow up and attend school. I have no suitable word that can fully describe their everlasting love, care and support to me. I am grateful to my dear grandmother who has always given me her prayers and spiritual support. I am proud of my brother (Alireza) for

his exceptional talents and success. We grew up together and had the most special and memorable times. My special thank goes to my husband (Babak) whose encouragements and love throughout this journey have given me the power to go on. His creativity along with his brave and optimistic nature gave me a greater understanding of what it means to create possibilities and fully live my life.

DEDICATION

To my parents,

and

my husband.

CO-AUTHORSHIP STATEMENT

This research was performed by the author under supervision of Professor Madden. Some aspects of the work were done in collaboration with other researchers which are described as follows.

Manuscript 1 (Chapter 2): Polypyrrole operating voltage limits in aqueous sodium hexafluorophosphate: The experimental design, measurements and data analysis of this work were performed by the author. The author has written the manuscript and received valuable suggestions and feedback from her advisor, Professor Madden and the other co-authors.

Manuscript 2 (Chapter 3): Electro-stiffening in polypyrrole films: Dependence of Young's modulus on oxidation state, load and frequency: The experimental work and design of this research was performed by the author. The data analysis was a collaborative work of the author with fellow PhD student Tissa Mirfakhrai, with feedback from their advisor, Professor Madden. The manuscript was written by the author.

Manuscript 3 (Chapter 4): Electromechanical coupling in polypyrrole sensors and actuators: The experimental design and measurements were performed by the author, who received guidance from Professor Madden in interpreting the measured data. This manuscript was written by the author, with input on the modelling section from Professor Madden. Feedback from the co-authors, who had performed separate experiments on trilayer sensors, helped refine the experimental procedure and interpretation.

Manuscript 4 (Chapter 5): A dynamic electromechanical model for electrochemically driven conducting polymer actuators: The experimental design, fabrication of the conducting polymer actuator and the experimental measurements of this study were performed by the author. The transmission line model employed was originally developed by Professor Madden and partly solved by Dan S. Yoo. The author contributed to time domain solution of the impedance model and coupling to a mechanical beam bending model for prediction of the dynamic actuation response. Data analysis and fitting to the model were done by the author. The manuscript was also written by the author who received useful comments from Professor Madden.

Manuscript 5 (Chapter 6): Conducting polymer based active catheter for minimally invasive interventions inside arteries: This research was initiated through discussions with Dr. Victor Yang, from Sunnybrook Health Sciences Center, who is interested in active catheters for intervention inside arteries. The feasibility study of using polypyrrole artificial muscle in developing active catheters was performed by the author. The author conducted experimental design and measurements. Fabrication of the active catheter was performed by the author in collaboration with Nigel Munce (from Dr. Yang's group) who performed the laser machining. The author experimentally demonstrated the manoeuvrability of the catheter. The author performed OCT imaging using the catheter in collaboration with Nigel Munce (the image is shown in Chapter 6). Data analysis and design optimization were performed by the author. The manuscript was also a work of the author who benefited from Professor Madden's comments and feedback.

CHAPTER 1: INTRODUCTION AND OVERVIEW

1.1 Objective

Polypyrrole is a conducting polymer with a range of attractive characteristics, which make it suitable for a variety of applications. Its muscle-like actuation behaviour, in particular, has made it one of the best candidates for artificial muscle technology. In addition to favourable actuation characteristics, polypyrrole also has been recently investigated as a sensor. The sensing ability of this material is another attractive feature which mimics natural muscles, in that all the functional elements are integrated into the actuator. Availability of a muscle-like technology is advantagous for medical implants, human assist devices, and for minimally invasive surgical and diagnostic tools. However, there are some known challenges with this technology (e.g. cycle life, mechanical stability, slow response) that need to be dealt with in order to design practical devices. In this thesis the engineering aspects of polypyrrole material as artificial muscle are studied and are used to demonstrate the feasibility of using this material in developing active catheters for medical applications. The results of these studies will contribute to the understanding of polypyrrole actuation and sensing performances and is extremely useful in designing effective artificial muscle based devices for various applications. The polypyrrole driven active catheter is also an important step towards advanced bio-robotics for minimally invasive surgical procedures.

In this chapter an overview of polypyrrole actuators and sensors as conducting polymer artificial muscles is first presented. The characterization methods and physical modelling used in this thesis to study the engineering aspects of this polymer are then described. Finally application of polypyrrole actuators in active catheters is discussed. This will be followed by highlights of the contributions of the thesis.

1.2 Conducting polymers

Conducting polymers are a class of polymers whose primary attribute is a conjugated backbone structure. Figure 1.1 shows such a structure in polypyrrole, the conducting polymer studied and applied in the present work. The conjugated structure enables some degree of electron delocalization and hence electronic conduction [1]. The electronic conductivity of these polymers can often reach 10^4 S/m [6]. These polymers are typically disordered semiconductors in their neutral state. The effective band gap is reduced in a process known as doping [2]. The polymer is doped by changing its oxidation state (adding or removing electron from the backbone), which, when performed electrochemically, leads to the migration of ions into the bulk polymer, balancing charge. These ions are known as dopants, in analogy to traditional semiconductors. Doping results in creation of states in the band gap and leading to nearly metallic conduction. Figure 1.2 illustrates such a change in oxidation state in polypyrrole.

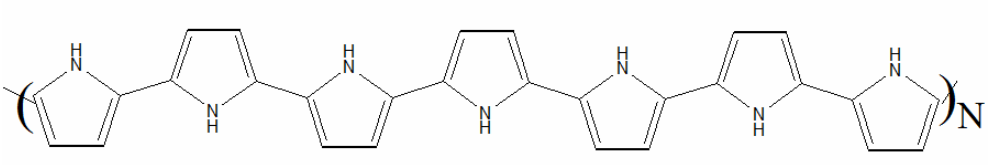

Figure 1.1: The chemical structure of Polypyrrole, showing a conjugated structure (alternating single-double bonds), from [3].

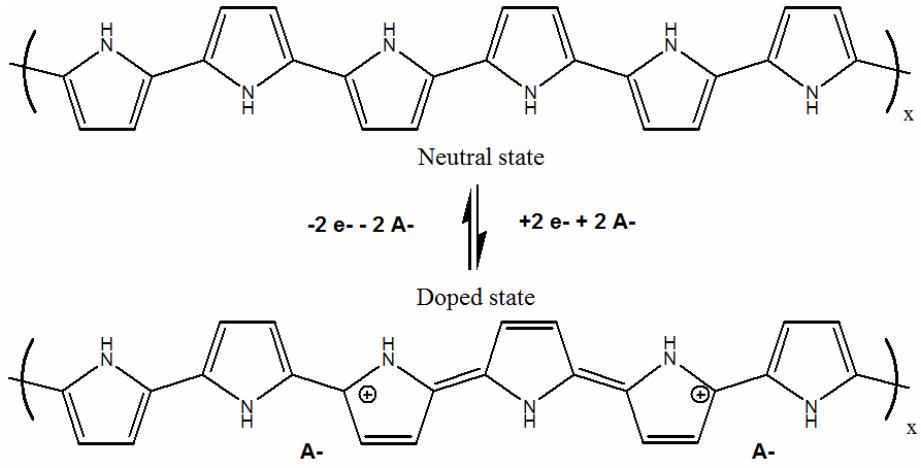

Figure 1.2: Electrochemical redox cycle for polypyrrole. A- represent anions, e- electrons, from[3].

Conductivity is highly dependent on polymer synthesis condition such as synthesis method, dopant employed and the temperature at which synthesis takes place. Electrochemical synthesis of polypyrrole leads to the highest conductivity and the best mechanical properties. As synthesized, the polypyrrole has a backbone configuration shown at the bottom of Figure 1.2, where roughly 1/3rd of the monomers are charged [4,5]. The backbone charge is balanced by the presence of anions (doped state) and the conductivity is ~ 10^4 S/m. Reduction leads to a

semiconducting state, as shown at the top of Figure 1.2, where ions exit the polymer backbone (discharging).

The electrochemically controllable charging of conducting polymers makes them attractive materials to be used as energy storage devices, polymer light emitting diodes, electrochromic windows and drug delivery devices [6]. An interesting property of conducting polymers is that their volume changes as a result of the change in oxidation state and the corresponding charging. Although this effect has been a source of annoyance for the above mentioned applications, it has provided an exciting application for conducting polymers as actuators. In this thesis conducting polymers as electrochemically driven actuators are studied and an example of their application in bio-robotics will be discussed.

1.3 Conducting polymers as artificial muscle actuators

Conducting polymers undergo deformations as a result of changes in oxidation state. This effect was first described by Baughman, Shacklette, and Elsenbaumer who proposed to use conducting polymers as artificial muscle actuators [7]. Key components separating an artificial muscle from a conventional actuator are its flexibility and ability to generate large strains at reasonable stresses (i.e. the attributes of skeletal muscles). Skeletal muscle with a typical Young's modulus of 10-60 MPa, is capable of producing strains of 20%, strain rates greater than 50% per second and stresses of 0.1 MPa [8]. Conducting polymer can generate large strains (typically 6% and maximum 39%), relatively low strain rates (typically 1%/s and maximum 12%/s) and high stresses (typically 5 MPa, and maximum 100 MPa) [8]. The Young's

modulus of these polymers is between 0.2 GPa to 1 GPa [7]. These properties along with biocompatibility, light weight, low actuation voltage and low cost, make them a suitable class of materials to be used as artificial muscle.

1.3.1 Types of artificial muscles

Artificial muscles in general have been divided into two major groups [14]. In the first group dimensional change is in response to electric field. These are commonly known as electronic electroactive polymers. Some of the technologies that fall under this category are dielectric elastomer actuators, relaxor ferroelectric polymers, and liquid crystal elastomers. Although dielectric elastomer actuators are becoming commercially available for certain applications, and exhibit large strains (> 10 %) and high work densities (up to several MJ/m^3) there are some disadvantages with this type of actuator. The materials in this group typically require high voltages (>1 kV) applied to create the electric field required to actuate, which is not desirable in many applications. In addition, the actuation stresses by materials in this group are typically low. Artificial muscles that operate at low voltages and are capable of applying large stresses are therefore of great interest, particularly in catheters, where significant forces are needed to displace devices, and where high voltages, though not strictly forbidden, create safety concerns.

The second group is a class of materials in which the presence and movement of ions is necessary to make actuation possible. This group is referred to as ionic electroactive polymers. For the ions to be able to move an electrolyte phase is necessary, which is often liquid. Actuators in this group include conducting polymers,

and ionic polymer metal composites (IPMC), both of which offer low actuation voltages (<10 V). IPMC actuators can only provide bending actuation and hence are not suitable for linear mode of operation. They can generate large bending displacements and are typically faster than conducting polymers; however, their manufacturing process is often relatively expensive and, unlike conducting polymers, additional energy is usually consumed to hold the actuator in place resulting in low efficiency. Among conducting polymer materials, polypyrrole is found to be the most effective artificial muscle actuator due to its electrochemical stability, low cost, and biocompatibility. In this thesis the engineering aspects of polypyrrole actuators are investigated.

1.3.2 Mechanism of actuation in polypyrrole

As was mentioned in section 1.1, conducting polymer actuation occurs as a result of change in oxidation state. Oxidation state of the polymer can be altered chemically or electrochemically. In electrochemical actuation of conducting polymers, the polymer acts as one of the electrochemical cell electrodes inside an electrolyte containing mobile ions. The actuation voltage (or current) is applied across the polymer electrode and a reference electrode to alter the polymer oxidation state. This change in oxidation state is due to inducing/ removing electrons to/from the polymer backbone in response to the applied voltage (or current). In order to balance the polymer charging, counter ions from the electrolyte enter the polymer matrix (or exit the polymer depending on the sign of the mobile ion and the polymer oxidation state). When the ions enter or leave the polymer, the polymer expands or contracts (see

Figure **1.3**). If both positive and negative ions diffuse into and out of the polymer, expansion due to influx of one ion will be counteracted by contraction due to outflow of the ion with opposite charge [9]. By choosing salts with one small and one very large ion, the influx and outflow are dominated by the smaller ion. Ions in solvents are surrounded by the solvent molecules, so called solvation sphere. In the process of actuation, often, ions enter the polymer with their solvation sphere. In some cases smaller ions are surrounded with a large solvation sphere, thus their total size becomes larger. For instance, in the salt Sodium hexafluorophosphate ($NaPF_6$), the solvated negative ions (the hexafluorophosphate) are smaller and can squeeze between the polymer chains while the solvated cations (the sodium and its accompanying solvation sphere), are too big to diffuse into the polymer bulk. With $NaPF_6$ in water, the expansion and contraction of the polymer appears to be due only to the movement of the negative hexafluorophosphate ions [10-11].

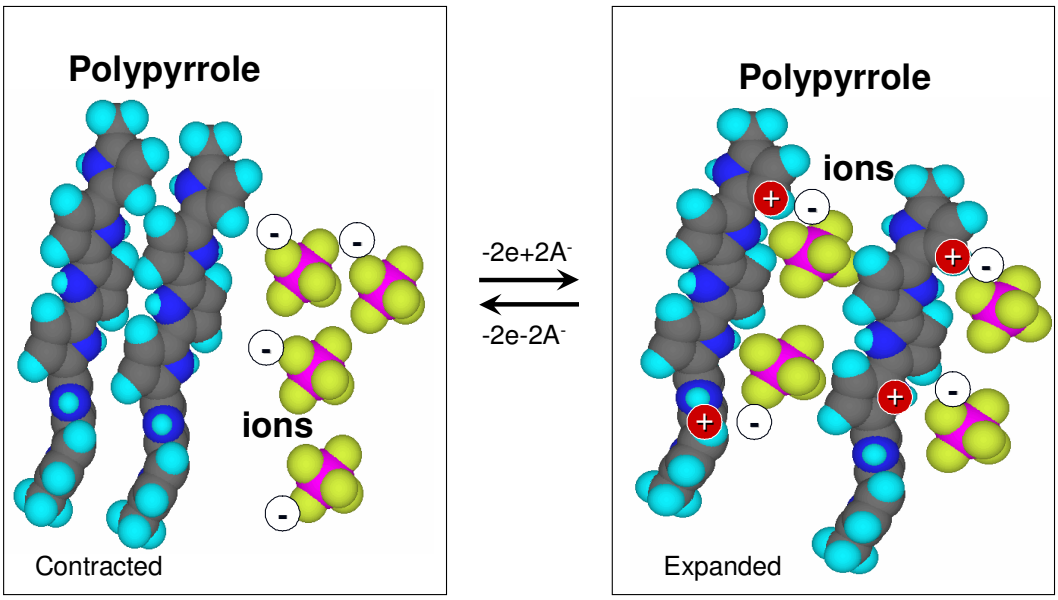

Figure 1.3: Structure and possible mechanism of actuation in response to change in oxidation state inside electrolyte containing mobile ions (anion in this case) from [3].

It has been shown that the actuation strain generated in conducting polymer actuators is proportional to the charge per unit volume, ρ, via the relationship;

$$\varepsilon = \alpha\rho \; . \qquad (1.1)$$

α is an empirically determined strain to volumetric charge ratio [7]. Techniques from electrochemistry, such as cyclic voltammetry (CV) and electrochemical impedance spectroscopy (EIS), described in the following sections, are often used to measure the material charge storage capacitance to estimate the amount of charge. This information can then be used to predict the actuation strain. Electrochemical and mechanical properties of polypyrrole and their variation with operational conditions, significantly affect the behaviour of polymer charging and the performance of the actuator. In this thesis such effects are studied to understand the performance of polypyrrole actuation as an engineering material.

1.4 Conducting polymers as sensors

Actuators such as electric motors and piezoelectrics can also act as sensors, converting mechanical work into electrical energy. Sensing behaviour in conducting polymers was first reported by Takashima *et al.* in 1997 [40]. They achieved a mechanically induced electrochemical current in a free-standing film of polyaniline inside an electrolyte when the tensile load was varied [40] . More recently, Otero *et al.* have shown the sensing capability of polypyrrole bilayer actuators. They found that the potential required to actuate a polypyrrole bilayer actuator under current control based actuation increases when the bilayer touches an obstacle [41,42]. This suggests that conducting polymers can be used as tactile sensors [41,42]. Wu *et al.*

have reported the sensing response of a polypyrrole trilayer, where a bending displacement induces a voltage difference between the conducting polymer electrodes [44]. In another paper, Takashima *et al.* have also recently reported a polypyrrole composite film sensor which detects a step-wise tensioning load by generating spike-wise currents [43]. The sensing behavior of these materials has been recently studied and the mechanism of sensing has not been yet fully investigated. In this thesis the properties of polypyrrole sensors are investigated, enabling the first quantitative demonstration of the link between actuation and sensing, and suggesting a new mechanism of electromechanical coupling that can be exploited in both the electronic and the ionic class of artificial muscles. The hope was that the sensing effect would be sufficiently strong enough to provide force or displacement feedback when polypyrrole actuators are used to drive catheters, but the effect observed so far is too small to be practically useful in this application, as will be discussed in Chapter 4 and 6.

1.5 Synthesis of polyppyrrole

The polypyrrole studied in this thesis was electrochemically synthesised using the method of Yamaura *et al.* [5], which has shown to produce highly conductive polymers with favourable mechanical properties (e.g. tensile strength of 30-50 MPa and Young's modulus of 300-900 MPa). The deposition is done on a conductive surface by polymerizing the pyrrole monomer through electrochemical oxidation [8]. The electrolytic solution is composed of 0.06 M distilled pyrrole, 0.05 M tetraethylammonium hexafluorophosphate and 1 % of solution volume distilled water

in propylene carbonate (from Sigma–Aldrich). The solution is deoxygenated by bubbling with nitrogen before growth. The conductive surface onto which the polymer is to be deposited is used as the working electrode and the counter electrode is a platinum coated glass slide. The reaction occurs at a constant current of 0.125 mA/cm^2 and a temperature of −30 ◦C resulting in polymer deposition with a rate of ~1.6 μm per hour. The resulting polypyrrole is a black and shiny polymer with a conductivity of ~ 10^4 S/m and in the oxidation state of ~ 0.2-0.4 V versus an Ag/AgCl reference electrode.

1.6 Mechanical and Electrochemical characterization techniques

Mechanical and electrochemical characterization of polypyrrole has been previously reported by A. Della Santa *et al*. [50] among others. In this thesis, the aim is to expand the characterization studies for PF_6 doped polypyrrole operating in an aqueous solution of $NaPF_6$ (i.e. the combination used in this thesis), and extend the mechanical measurements to study the actuator's frequency dependent response. In studying the mechanical and electrochemical properties of polypyrrole, different experimental methods have been used throughout this thesis, which are now described.

1.6.1 Strain-stress measurement

Mechanical characterization of polypyrrole, involved measurements of stress and strain on a free standing polymer sample. These measurements were performed using an Aurora Scientific ASI 300 muscle analyzer controlled by LabView-based

software (www.aurorascientific.com). Figure 1.4 is a photo of the apparatus used to apply force to the clamped polypyrrole sample. The polymer sample is mounted between a lower fixed clamp and an upper movable motor arm. The force is applied to the sample and the resulting passive strain is recorded. The precision resolution for displacement using the ASI setup is 1 μm and the uncertainty in the force measurement of the instrument is ±0.3 mN or ±0.03 g.

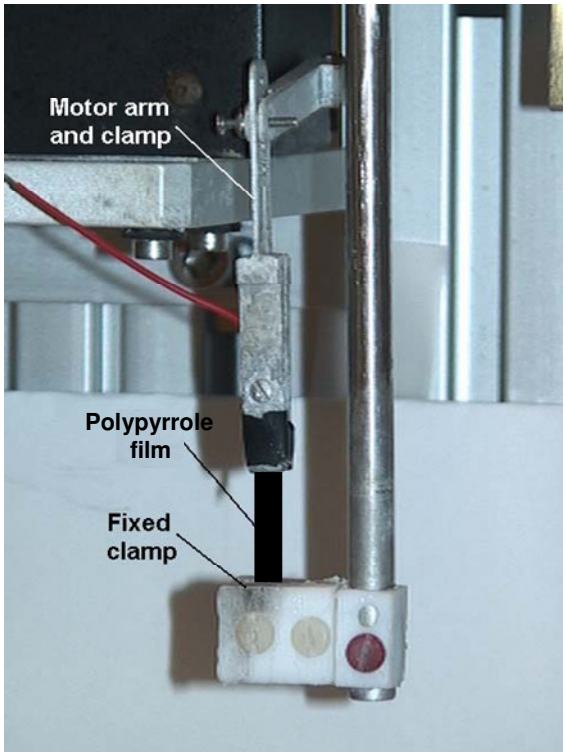

Figure 1.4: A polypyrrole sample mounted in the ASI muscle analyzer clamp [15].

Actuation of the polymer sample was performed in the same experimental setup, but an electrolyte bath was also inserted under the clamp to surround the polymer. The polymer sample is further attached to a gold wire which provides an electrical connection to the actuation voltage source. A computer controlled potentiostat (Solartron 1287), is used to apply voltage or current, in which case polypyrrole is

connected to its working electrode output. The voltage is applied across the working and a counter electrode but measured and controlled against a reference electrode. A data acquisition card (National Instruments 6036E) gathers the force and displacement data from the muscle analyzer and also logs the applied voltage and current. The resolution in measurement of current and potential from the Solatron potentiostat is practically about 100 pA and 5 μV, respectively.

1.6.2 Cyclic voltammetry

Cyclic voltammetry is a widely used technique for measuring the capacitance of an electrochemical cell and acquiring qualitative information about electrochemical reactions. In cyclic voltammetry the potential applied between the polypyrrole electrode and the reference electrode is swept back and forth at a constant rate within the desired range of potentials, forming a triangular voltage waveform, while the cell current is measured. Typically, the current is plotted vs. the applied voltage, forming a diagram known as a cyclic voltammogram. For a purely capacitive material this diagram resembles a rectangle (Figure 1.5). The height of such a rectangle is proportional to the capacitance of the electrode ($i=C\times dV/dt$). In real cases a leakage current is observed due to a parallel leakage resistor which slightly rotates the rectangle as shown in (Figure 1.5).

Any peaks in the cyclic voltammogram of a cell can imply electrochemical reactions taking place in the cell. Such reactions can lead to a loss of charge due to reduction or oxidation of a chemical species at the electrode (i.e. Faradaic reactions), that would be transferred through the electrode/electrolyte interface. Faradaic

reactions may lead to degradation of polypyrrole, if the loss of charge is associated with a change in the polymer chemical structure.

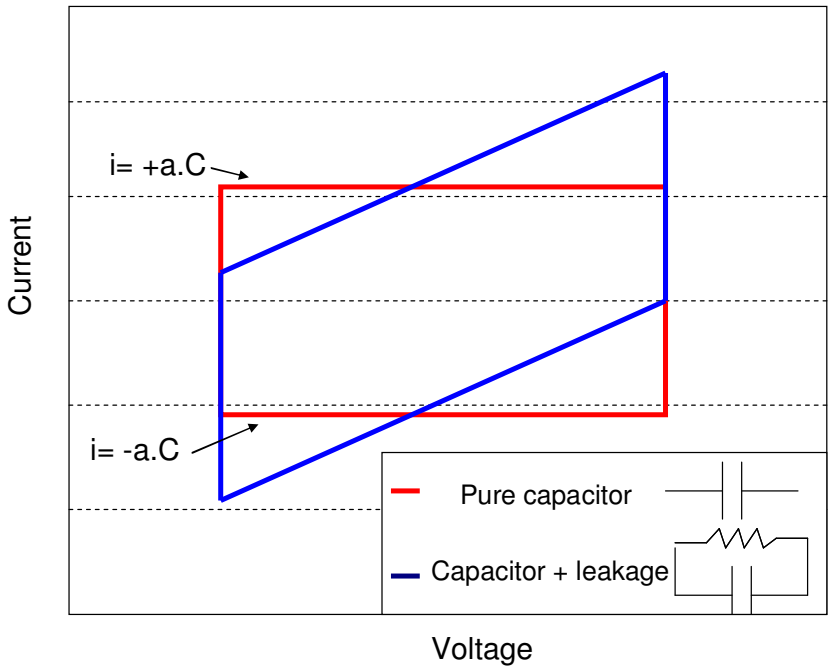

Figure 1.5: The cyclic voltammogram of a pure ideal capacitor, which can model the charge storage behaviour of a polypyrrole actuator to first order and a parallel RC circuit, which can model the charge storage in the actuators in addition to some parasitic currents that may flow into the cell. “a” is the rate of voltage ramp ($a=dv/dt$).

Currents due to Faradaic reactions can sometimes be modelled by adding a parallel resistor to the capacitor model. Such a resistor shows that some charge flows in the cell without being stored in the actuator, and thus does not contribute to the actuation. Since the magnitude of the parasitic current can depend nonlinearly on the applied potential, the resistance of the resistor can also depend on the potential. Often this resistance is lowest at potential extremes, where parasitic reactions are largest, leading to rises in the current magnitude as voltage extremes are approached. When

studying artificial muscles such loss of charge can hinder achieving a good understanding of the actuation mechanisms, since part of the charge entering the cell is not contributing to actuation [15]. Therefore, it is important to study and identify charge storage and charge loss processes and mechanisms. Cyclic voltammetry provides a useful tool for such studies, as will be used in electrochemical characterization of polypyrrole in Chapter 2 of this thesis.

1.6.3 Electrochemical impedance spectroscopy

Electrochemical Impedance Spectroscopy is a method employed to characterise the dynamic behaviour of electrochemical cells. In this method, a small sinusoidal voltage is superimposed on a bias potential applied to the cell. The frequency of the sinusoidal signal is then varied within a desired range and the impedance of the cell is measured by measuring the resulting current at various frequencies. The Bode plots of the impedance are made, and a fitting routine can be used to find an equivalent circuit whose impedance has a similar dependence on frequency as the measured impedance response. By fitting the response of a circuit including a capacitor, the equivalent capacitance of the electrode can be estimated. However, most often the response of a circuit including one capacitor does not provide a good fit for the artificial muscle electrodes and exhibits deviations from the experimentally measured response. In this thesis (Chapter 5), we propose an RC transmission line equivalent circuit to model the dynamic behaviour of the polypyrrole electrode and show that it provides a good fit to the polymer impedance spectroscopy measurements.

1.7 Modelling

A key challenge for the designers of conducting polymer driven devices is the prediction of the actuation response. Modelling of the conducting polymer not only is useful as a design tool, but also can serve to understand the effects of different physical properties on the polymer actuator performance. A diffusive elastic model has been previously developed [1], that predicts the electrical and mechanical behavior of a thin film conducting polymer actuated in an electrochemical cell. The success of this model for polypyrrole suggested that actuation is dominated by ion diffusion through an elastic, metallic polymer matrix. In addition, this model highlighted the relationship between strain and charge and time constants pertinent to polypyrrole actuation, which corresponds to the diffusion time into the polymer and the capacitive charging time of the polymer. An overview of this model is now described as follows.

1.7.1 Diffusive elastic model

As described in [1], by applying a step voltage, V_s, across a highly conductive polymer and a reference electrode inside an electrolyte, ions travel parallel to the applied field and concentrate at the polymer/electrolyte interface. The concentration at the polymer surface creates a potential gradient within the material, thereby inducing a field which pulls the ions into the porous polymer matrix. Although the concentration gradient by itself can contribute to ion diffusion (according to the Fick's Law), an electric field induced diffusion is likely faster than the concentration gradient driven diffusion [45], and thus is the dominant cause of ion transport. The

transport of ions within the polymer pores is described by a finite transmission line [1] shown in Figure 1.6 with a polymer ionic resistance per unit thickness, R_{ion}, and capacitance per unit thickness, C, describing each region of the polymer.

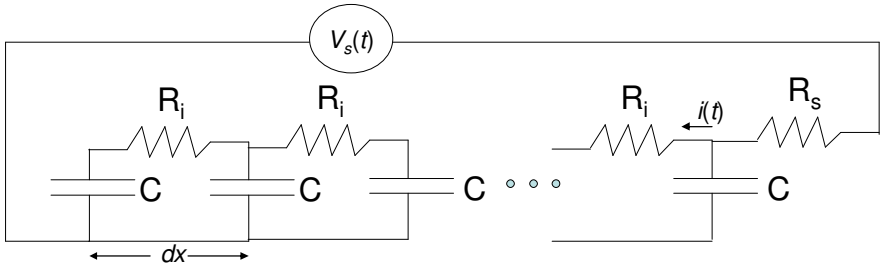

Figure 1.6: Transmission line model representing the ion diffusion into the polymer.

In this case a one-dimensional approach is used, where ions are assumed to diffuse into the polymer thickness in the x direction, leading to an effective diffusion equation:

$$\frac{\partial V(x,t)}{\partial t} = D \cdot \frac{\partial^2 V(x,t)}{\partial x^2}, \qquad D = \frac{1}{R_{ion} C}. \tag{1.2}$$

where the effective diffusion coefficient, D, is equivalently the ionic conductivity divided by the capacitance per unit volume, $D=\sigma/C_v$ (given a cross-sectional area, A, and a thickness, h, the volumetric capacitance is $C_v=C.A^{-1}.h^{-1}$, and R_{ion} is the resistance per unit length is ($R_{ion}=\sigma^{-1}\cdot A^{-1}$). In fact, the potential distribution throughout the polymer electrode "field driven charging" has a response that is of the same form as an ionic diffusion limited behavior, but with the value of the diffusion coefficient being determined by the electrostatic properties rather than by thermal agitation and chemical potential gradients. The ion diffusion into the polymer thickness is

associated with a time delay which is determined by the effective diffusion coefficient, D, and the thickness, h, of the polymer (i.e. $\tau=R_{ion}C_{tot}=h^2/D$[1]).

We later employed this time constant but considered a finite conductivity for the polymer (rather than a pure metallic) [16]. This implied an additional time constant due to the electronic resistivity in the second dimension (through the polymer length). The combination of these two effects (i.e. ionic and electronic delays) is modeled as a 2D transmission line shown in Figure 1.7, where R_e represents the polymer electronic resistance per unit length. A numerical approach was then used to predict the charge propagation through the polymer in 2 dimensions [16].

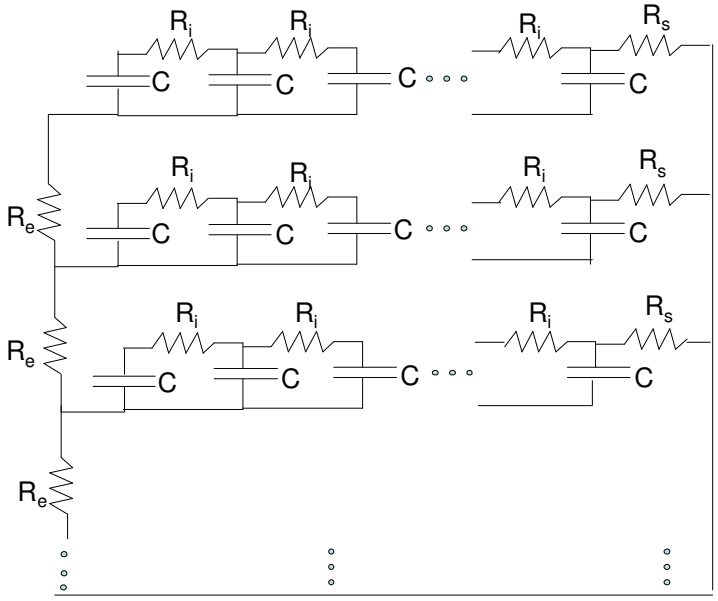

Figure 1.7: 2 dimensional distributed transmission line circuit model

In Chapter 5 of this thesis, an analytical model is proposed which uses the exact solution of the impedance of the 2D transmission line circuit model (as an extension of the model presented in [1]). The analytical model is then coupled to a mechanical model to predict the time-dependent displacement of the actuator. This model

provides a reasonable description of the dynamic actuation response and is very useful for design purposes.

1.8 Application of artificial muscles in active catheters

Studies of polypyrrole properties and the developed analytical model will be used in Chapter 6 to guide the development of an engineering device for biomedical applications. Biocompatibility, miniaturized size and ease of preparation of polypyrrole have made it a good candidate for biological applications such as drug-delivery, blood vessel connectors, cochlear implants, microvalves, and steerable catheter applications [17-21]. Studies of polypyrrole have shown no evidence of acute and subacute toxicity [22]. Also, studies investigating some of the basic biocompatibility issues involved in using polypyrrole as a blood-contacting biomaterial shown that polypyrrole coated polyester fabrics do not cause hemolysis nor did they alter the blood coagulation properties, therefore highlighting the potential of polypyrrole in cardiovascular applications [23]. In Chapter 6 of this thesis a polypyrrole driven catheter for cardiovascular applications will be discussed. An overview of catheters is now described, including the work of other groups to create actively deformable catheters.

1.8.1 Catheters: Background and current applications

A catheter is a thin flexible hollow tube that is inserted into body cavities to provide a channel for fluid passage or an entry for a medical device. Catheters as fluid channels may be used to either remove waste fluids from the body or direct a liquid

into the body. Practical applications include draining urine from the urinary bladder, injecting intravenous fluids and administrating medication or nutrition directly into the body. Catheters are also used to direct a medical device to a particular part of the body for minimally invasive diagnosis and treatment procedures. In angiography for instance, a catheter is used to administer the radio-contrast agent at the desired area to be visualized. In intravascular ultrasound, a catheter based ultrasound transducer is utilized to provide ultrasonic images from the inside of blood vessels. Optical Coherence Tomography (OCT) is another example where an optical fibre is guided through a catheter to a particular part of the body to generate high resolution three dimensional (3-D) images [24].

Catheters have a long history [25]. The earliest catheters were formed from straw and leaves and were used for drainage of urine. Hollow leaves of plants, coated with lacquer, were used as catheters in China around 100 BCE. In 1036 CE Avicenna described the first flexible catheter made from stiffened animal skins. Benjamin Franklin designed a flexible silver catheter in 1752 for patients who suffered from bladder disease. The modern application of the catheter started in 1868 when a catheter with features for controlling the catheter insertion depth was patented by Dr. N. B. Sornborger. The modern disposable catheter was invented in the 1940's by David S. Sheridan [25].

Flexible disposable catheters are used in many applications and their structures and designs have been improved over the last 60 years. The conventional method of handling catheter involves inserting it into the body passively, by pushing it from outside. Guide wires, manipulated externally from the patient, are used for guidance

of the catheter by combinations of push-pull and torque motions. As shown in Figure 1.8, the guide wire is inserted into the selected branch of a blood vessel and approaches the target site. A catheter is then introduced over the guide wire and the guide wire is pulled out leaving the catheter inside the vessel [26].

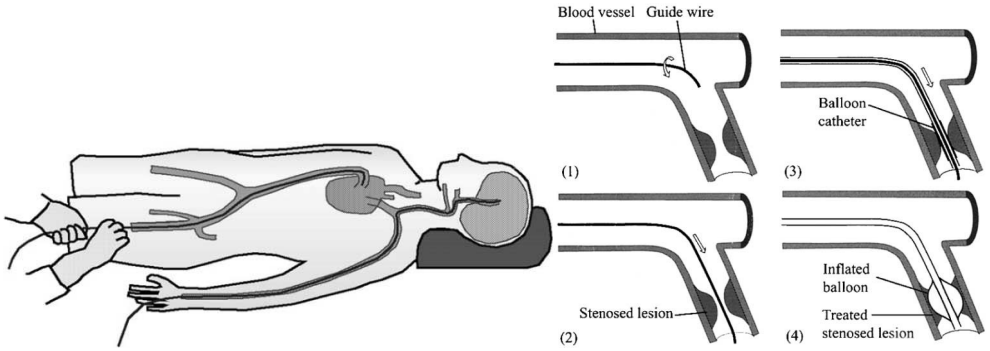

Figure 1.8: Operation of conventional catheter and guide wire. (b) Process of catheter intervention in a blood vessel for treatment of a stenosed (partially occluded) lesion using a balloon catheter [26] (© [2004] IEEE).

Navigation is performed by observing the position of the catheter tip using x-ray fluoroscopy and angiography [26]. However, the x-ray images are two-dimensional (2-D) and lack detailed information about the vessel wall. In addition, the long distance (~ 1 meter) between the operator's hand and the tip of the catheter/guidewire demands a high level of skill from the doctors. Limitations of the current catheter and guidewire designs include long procedural times, and risk of lumen or vessel wall damage, both as a result of slow and inexact guidance. These issues become more critical when dealing with narrow and complex passages such as blood vessels of the brain and tertiary bronchi of the lung [24]. Therefore, advanced active catheter designs with controllable features are required in order to enhance the performance of these devices during minimally invasive medical procedures.

Various active catheters have been suggested, however no active catheters are in wide spread use. Micromotor mounted catheters had been reported for ultrasonography [27,28], but they feature a relatively large size and expensive fabrication process. Shape memory alloy (SMA) and Shape Memory Polymers (SMP) actuators have been used for steerable endoscopes [29-35]. Although these types of actuators are potentially able to provide a large degree of bending, their slow response, high operating temperature and the possibility of electrical current leakage limit their applications [33]. In addition, extra energy is consumed for holding these actuators in a position. Controllable catheters utilizing hydraulic mechanisms have also been developed, where the catheter position is controlled by varying the size of inflatable balloons mounted on its tip using electro-thermally controlled microvalves [26]. This mechanism is cumbersome and controlling the microvalves is slow; hence it is not suitable for many applications. Ionic Polymer Composites (IPMC) actuators have been also suggested to drive active catheters [36-38]. These actuators can generate large displacements at relatively low voltages (<10 V) and moderate speed; however, their manufacturing process is often relatively expensive and additional energy is usually consumed for holding the actuator in a position. A catheter with a MEMS micro-mirror scanner actuated by magnetic field was recently presented [47]. This technique can provide a fast scanning catheter with low voltage, however large currents are used and its miniaturization is challenging since separate magnetic coils are required. In Table 1.1, we summarized characteristics of some of the actuator technologies that can be considered in active catheter application.

Actuator	Advantage	Disadvantage	Potentials in active catheter.
Shape Memory Alloys	- Very high stress (200 MPa). - Moderate to large strain (1-8%). - Low voltage (<4 V). - Great work density (>1MJ/m^3).	- Difficult to control (usually run between fully contracted and fully extended, but not in between). - Large current. - Low efficiency (<5%). - Limited cycle life at large strain. - Typically slow response (seconds).	- Large strain and stress are beneficial for large bending catheters. - High current and high operating temperature is an issue for *in vivo* applications. - Slow response is not suitable for some applications.
Ionic Polymer Metal Composites	- Low voltage (<10 V). - Moderate strain (0.5-3.3%).	- Low coupling and efficiency. - Consumes energy in holding a position. - Requires encapsulation. - Expensive ($500/kg) [8].	- Low voltage is an advantage for catheter application. - Moderate strain is favourable for bending catheters. - Consumes power to hold position, high material cost is not desirable. - Encapsulation is usually needed.
Dielectric Elastomers	- Large strain (20-380%). - Moderate stress (several MPa). - Large work density (10 k-3.4 MJ/m^3. - Low cost. - Low current. -Good coupling (>15%).	- High voltage (>1kV). - Compliant (Y=1MPa). - life time (>3,000,000)[49].	- Large strain is beneficial for bending catheters. - Low current is also an advantage for *in vivo* operations. - High voltage is undesirable. - Compliance may lead to generation of insufficient stress to provide large degree of bending.
Piezoelectric Actuators	- Fast response (~kHz). - Fine controllable positioning (pm). - Low current. - Good coupling	- Low strain (0.1%). - High voltage (100-1000 V). - Rigid.	- Fast response makes it suitable for high speed actuation (e.g. fast scanning catheter for imaging), however substantial mechanical amplification is required. - Its rigidity and low strain is not favourable for large bending catheters. - High voltage may be an issue.
Electrostatic Actuators	- Fast response (ms). - Low current. - Low mass. - Low power consumption.	- High voltage (>1kV). - Low stress (typical10 kPa) . - Rigid substrate. - Complex and expensive in low volume.	- Fast response makes it suitable for high speed actuation - Low stress may be limiting for large bending catheters. - MEMS based electrostatic actuators have problems with brittleness.
Magnetic Actuators	- Low voltage (<3 V). - Fast response.	- Large size (Required separate wired coils). - High power consumption. - Large current [47].	- Fast response is favourable for scanning catheters. - Large volume limits its application. - Large current also is limiting.
Conducting Polymers (e.g. Polypyrrole).	- High stress (5-120 MPa). - Moderate to large strain (2-6% typical). - Low voltage (< 2 V). - High work density (100 kJ/m^3). - Moderate stiffness (0.2-1GPa). - No extra energy required for holding it in place (catch state). - Inexpensive ($3/kg) [8].	- Low electromechanical coupling. - Slow (seconds). - Needs encapsulation. - Limited cycle life (32000 for strain of ~1% [48]).	- Large strain (compared to piezoelectrics) and stress are beneficial for large bending catheters. - Low voltage and low cost are favourable. - Speed increases as miniaturized. - Having a catch state is an advantage for catheterization. - Slow response may limit some applications. - Encapsulation is mandatory.

Table 1.1 Summary comparing actuator technology [from 8].

We chose to study polypyrrole actuators which have shown attractive properties suitable for catheter application. Some of the characteristics include low actuation voltage, small size, ease of fabrication, relatively high strain, compliance and biocompatibility. In this thesis the initial feasibility of a polypyrrole based active catheter for maneuvering inside the blood vessels and for *in vivo* imaging application is investigated. Similar to most of the above mentioned technologies, polypyrrole is a relatively new actuator material, whose properties need to be further characterized and modeled to evaluate its applicability. The focus of this feasibility study is on the following objectives; determination of the potential range for stable operation of the actuator, the significance of variation in mechanical stiffness on actuation, the ability to produce large degree of bending on the catheter, the ability to scan an optical fiber embedded catheter with high speed for imaging applications and the possibility of using polypyrrole sensors to control the catheter position and loading.

Figure 1.9 illustrates the design, composed of a catheter coated with polypyrrole electrodes and equipped with an optical fiber for imaging purposes. The polymer electrodes provide the 2 dimensional bending of the catheter tip. This is done by expanding the polymer electrode on one side and contracting the other electrode on the opposite side as a result of changing their oxidation states. The two vertically facing electrodes provide catheter bending in the vertical direction and the other facing electrode pair is responsible for the bending in the horizontal direction.

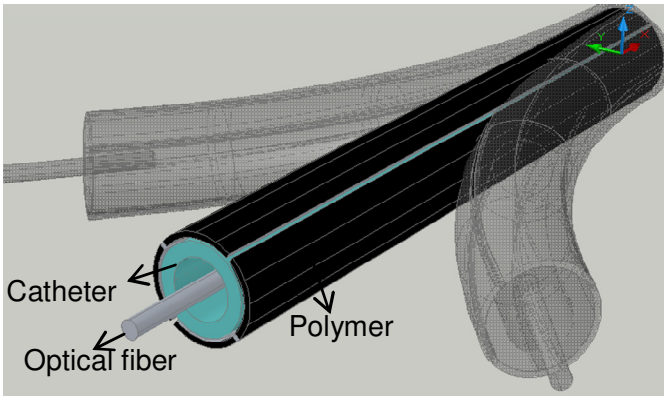

Figure 1.9: Schematic of the active catheter.

As was mentioned in section 1.3, electrochemical actuation of polypyrrole involves using an electrolyte. The polypyrrole driven catheter was originally meant to use the blood itself as the electrolyte; however we found that electrochemical actuation of polypyrrole in blood results in a mixed expansion and contraction of polymer due to presence of multiple ions inside the blood. Also the induced strain is very small. More importantly the current required for actuation is not safe to be directly applied through the blood and therefore encapsulation is needed on the final active catheter (More detailed information of actuation in blood is provided in Appendix 4). An encapsulated version of the active catheter needs to be redesigned and investigated as we suggested in the future work section of Chapter 7.

1.9 Thesis overview

Polypyrrole artificial muscle is a fairly new technology that shows promises for developing medical devices. In its transition from a laboratory curiosity to an engineering material it is critical to understand environmental effects and physical models and develop an appropriate design tool as well as fabrication process. In

characterizing polypyrrole material, electrochemical and mechanical properties are particularly important since the actuation response is mostly dependent on these properties. In this thesis, electrochemical and mechanical characterization of polypyrrole material, using the methods described in section 1.3, are first presented (Chapter 2-4). Polypyrrole as both actuator and sensor is studied in Chapter 4 and the electromechanical coupling in polypyrrole sensors and actuators is described. A dynamic model is presented in Chapter 5 to predict the actuation response of polypyrrole actuators. This model is used in Chapter 6 to design a polypyrrole driven catheter. The device fabrication and performance are also described in this chapter. This will be followed by the conclusions in Chapter 7.

This thesis is in manuscript format, and is a sequence of articles that have been published, are in press or are being prepared for submission. While some minor modifications have been made to the text to help the thesis reader, there is limited scope for changes to the originals allowed by UBC as the manuscripts are to be kept largely intact. As a result there is repetition in the document, for which the author apologizes. What follows, is a detailed summary for the following five chapters, which include the main contributions made in this thesis.

1.9.1 Electrochemical characterization of polypyrrole (Chapter 2)

One important factor in determining the performance of polypyrrole actuators is the electrochemical stability. Our particular interest is in disposable applications where a relatively small number of cycles are needed, and maximum strain is desired. Actuation of polypyrrole in aqueous sodium hexafluorophosphate solution has been

shown to produce relatively large strains [39]. However, little has been published on appropriate potential range of actuation in this electrolyte. This information is clearly crucial for many applications. In Chapter 2, the electrochemical degradation as a function of actuation voltage is investigated by cycling the film between fixed voltages and measuring the charge transfer. Cyclic voltametry (section 1.6.2) was also performed to study the response over a range of voltages. The voltage range for effective operation of the device was suggested in order to achieve stable performance.

1.9.2 Mechanical characterization of polypyrrole (Chapter 3)

Mechanical properties such as the Young's modulus of polypyrrole contribute in determining the amount of strain obtained from the actuation. Therefore investigating factors affecting the modulus is important in designing effective actuators. In Chapter 3 the effects of polymer oxidation state, load and frequency of the applied load on polypyrrole Young's modulus are studied. We chose to study a polymer doped with PF_6^- ions, prepared using electrochemical deposition in propylene carbonate at -30 °C. These growth conditions lead to a highly conductive polymer and provide one of the most effective and repeatable actuator performances for practical devices (particularly when operated in aqueous $NaPF_6$, as first reported by Zama, Kaneto and colleagues [10]). The performance seen to date justifies further careful investigation of its mechanical properties in order to develop practical devices. In this study the "muscle analyzer" made by Aurora Scientific Inc. was used to measure stresses and strains as described in section 1.6.1. The Solartron 1287

potentiostat was also used to control the oxidation state of the polypyrrole sample under test.

1.9.3 Electromechanical coupling in polypyrrole sensors and actuators (Chapter 4)

Most actuators can work in reverse mode to convert mechanical energy to electrical energy. Polypyrrole actuator can also act in reverse, as force and displacement sensors. Polypyrrole sensors enable force and displacement to be measured at relatively large strains (ten times larger than those typical of piezoelectrics) and with relatively little mechanical impedance (elastic moduli are typically < 1 GPa). The deformation of these polymer sensors results in the passing of substantial charge, which can readily be converted to a voltage signal. This effect can have broad applications and in particular for the catheter under investigation it could serve as a position sensor. More interestingly, it might be used to detect a sudden increase in the load applied to the polymer, which likely implies that the catheter has struck the arterial wall. Employing polypyrrole both as actuator and sensor in one device, can be a step towards mimicking natural muscles, where all the elements are made of similar materials.

Previous investigations of polypyrrole sensors and actuators have not established a quantitative relationship between actuation and sensing. In Chapter 4 we propose a model of the electromechanical coupling, which is based on new measurements of polypyrrole sensors. It has also been shown that applying force to

polypyrrole generates a proportional change in voltage. It is shown in Chapter 4 that the same constant of proportionality describes the response in both cases.

In this study the Aurora Scientific muscle analyzer was used to apply force to a clamped polymer sample and the Solartron 1287 potentiostat was used to measure the generated voltage and current in response to the applied force. The Electrochemical impedance spectroscopy method described in section 1.6.3, was also performed to study the response over a range of frequency.

1.9.4 Dynamic analytical model for polypyrrole actuators (Chapter 5)

Since charging of the conducting polymer is the primary effect in electrochemical polypyrrole devices, understanding and modelling the behavior of the charging is important for design purposes. Prediction of time dependent charging is particularly useful for applications where the rate of response is critical. For instance, we are interested in conducting polymer driven catheters for rapidly scanning an optical fiber inside a blood vessel in order to perform imaging. In this case, actuation response at short times governs the device performance. In Chapter 5 an analytical model is presented to predict the actuation response of electrochemically driven structures. A 2D impedance model is first presented which uses the conducting polymer RC transmission line equivalent circuit to predict the charge transfer during actuation. An impedance spectroscopy experiment was also performed and compared with the model which verified its accuracy. The predicted electrochemical charging is then coupled to a mechanical model to find the actuation response of a bending structure. The actuation experiment was also compared with the model prediction,

showing good agreement. The advantage of this model compared to existing models is that it represents the two dimensional charging of the polymer, namely through the thickness of the polymer structure and along its length. An output of the impedance model is the charge density in the polymer as a function of time and position, which is then used to estimate free strain via the strain to charge ratio. Given the modulus of the polymer and of passively deformed structures, time dependent deformation is then determined. The complete electromechanical model is a function of ionic and electronic conductivities, dimensions, volumetric capacitance, elastic modulus, and strain to charge ratio, all of which are measured independently. The full electro-mechanical model is shown to provide a good description of the response of bending polymer structures when compared with experimental results. The model can be effectively used as a design tool for electrochemically driven devices.

1.9.5 Realization of a polypyrrole driven catheter (Chapter 6)

Electrochemical and mechanical characterization of polypyrrole along with the developed dynamic model led to implementation of a polypyrrole driven device described in Chapter 6. This was inspired by the attractive characteristics of polypyrrole and its potential for biomedical application in steerable catheters. The objective is to demonstrate the feasibility of using polypyrrole actuators in developing an active catheter equipped with an imaging tool (here, an optical fiber) which is able to access lesions in narrow and curved blood vessels where a conventional guide wire cannot reach. An advanced imaging technique (here, optical coherence tomography (OCT)) capable of monitoring deep in the lesion, to sub-cellular levels, is then used

for diagnosis purposes. The active catheter combined with the OCT imaging system can provide a new clinical practice where early detection of many diseases such as artery lesions and cancer is possible. This can have a significant impact in medicine and biomedical research.

The developed dynamic model (presented in Chapter 5) was used to design the polypyrrole based active catheter. The design is a commercial catheter with an embedded optical fiber, coated with thin polypyrrole electrodes (as shown in Figure 1.9). Electrochemical actuation of polypyrrole is performed inside an aqueous sodium hexafluorophosphate electrolyte which has been found to generate high and stable strains on polypyrrole. The polypyrrole electrodes are electrochemically activated, leading to bending of the catheter. This enables both positioning of the catheter to the desired region and 2D scanning of the OCT optical fiber for imaging. OCT depth imaging combined with the 2D scanning of the fiber will result in a complete high resolution 3D image, useful for diagnosis purposes.

Initial prototypes of the active catheter have been constructed and tested. A chemical deposition followed by an electrochemical deposition was used to form polypyrrole coating on to the catheter. A laser machining technique was then used to pattern the polypyrrole coating into separate electrodes. The performance of the active catheter was evaluated in terms of its ability to achieve the degree of bending required for navigation and the scanning speed desired for real time imaging. It was shown that polypyrrole can produce large degree of bending to navigate the catheter but the scanning speed is slow compared to that needed for *in vivo* real time imaging. According to the model, an alternative design can be used which benefits from a

flexible tube (instead of the commercial catheter) and a conductive backing on the polymer to achieve the required scanning speed. Effective implementation of this technology *in vivo* will require encapsulation of the electrolyte.

Finally the feasibility of using polypyrrole as a load sensor on the catheter is investigated. The motivation is to use the same material for both actuation and sensing as part of a complete feedback loop controlling of the catheter motion (as in natural muscle). The characterization of polypyrrole sensors and the model presented in Chapter 4 was used in this feasibility study. A preliminary experimental result is also presented showing the ability of polypyrrole actuators in sensing sudden changes in load during actuation. This effect can potentially be useful in detecting the catheter strike on the arterial wall, providing a more accurate and efficient catheterization. It is shown that the sensitivity of the polypyrrole as a mechanical sensor is likely too small at present to be effective for this application.

1.9.6 Contributions

The main contributions of this thesis are summarized as follows:

- The electrochemical stability of polypyrrole actuators was characterized for actuation in aqueous- $NaPF_6$. A safe voltage range is proposed, over which an effective operation of the actuator can be achieved, and a method for determining this range in any electrolyte is presented.
- The complex Young's modulus of polypyrrole as a function of oxidation state is reported and for the first time its components are investigated independently. Studying the real and the imaginary components of the

complex Young's modulus is very useful in characterizing the material viscoelastic behaviour and learning the mechanism of the modulus voltage dependent response. In studying the voltage dependent response we ensured that the polymer has reached the desired oxidation state. The approach we followed will be of benefit to others seeking to measure properties of conducting polymers as a function of oxidation state.

- The effects of load amplitude and perturbation frequency on the measured Young's modulus of PF_6^- doped polypyrrole at various oxidation states were investigated, showing that the modulus is highly dependent on amplitude and frequency of loading. The results of these studies are crucial to designing polypyrrole actuators operating under significant loading and over a large voltage range. Knowing the frequency response of the modulus is also very important in designing actuator systems that operates at mechanical resonance frequency.
- The reverse actuation (sensing) behaviour of polypyrrole is investigated. A semi-empirical model of the electromechanical coupling is proposed that relates sensor output to the effect of polymer deformation on charge insertion. The model is an important step towards the complete description of polypyrrole response in actuators and sensors.
- An analytical model is proposed to predict the dynamic actuation response of electrochemically driven devices. The model used the exact solution of the impedance of a 2-dimensional transmission line equivalent circuit, to predict the dynamic charge distribution along the polymer length. The predicted

charge was then coupled to a mechanical model to find the displacement of the structure. This model enables actuation to be predicted as a function of time. It is shown that the insertion of physically measured properties (modulus, strain to charge ratio, ionic conductivity and capacitance per volume in particular), leads to good predictions of actuation response. Furthermore this model might be generalized to be used in variety of electrochemical based devices, such as supercapacitors and batteries. The model is expected to serve as a powerful design tool for researchers and engineers in the area of electrochemical devices and artificial muscle technology.

- A fabrication method was presented which enables coating polypyrrole directly on to the structure (without the need for a metal layer). This method involves chemical deposition of polypyrrole followed by an electrodeposition.
- An active catheter was shown to meet many of the specifications needed for the OCT *in vivo* imaging application. The design takes advantage of two emerging technologies;

    1) Polypyrrole artificial muscle, which is promising for miniaturized steerable catheter applications,
    2) OCT imaging which has shown great potentials for minimally invasive diagnosis of diseases in very early stages. OCT can serve as the future new generation of biopsy called “optical biopsy”.

Although the polypyrrole driven catheter was primarily designed for cardiovascular applications, its application can likely be extended (with minimal modifications) to other catheterization and endoscopic procedures such as brain catheterization, ablation catheters, bronchoscopy, colonoscopy and so on. Furthermore, the miniaturized active catheter could accommodate multiple imaging tools to work in multimodal imaging. Each mode in a multimodal imaging can provide different information from the tissues that together can play a complementary role in assessing diseases such as cancer. All these potential applications can contribute to a significant advancement in the area of surgical robotics and minimally invasive diagnosis methods.

References

[1] J.D.W. Madden, G. A. Peter, I. W. Hunter, "Conducting polymer actuators as engineering materials" Proceedings of SPIE, Smart Structures and Materials: Electroactive Polymer Actuators and Devices, SPIE Press, pp. 176-190, 2002.

[2] R. Siegmar, One-Dimensional Metals. New York: Springer-Verlag, 1995.

[3] J. D. Madden, "Conducting polymer actuators" PhD thesis, 2000.

[4] C. K. Baker, J. R. Reynolds, "A quartz microbalance study of the electrosynthesis of polypyrrole" Journal of Electroanalytical Chemistry, 251, 307-322, 1988.

[5] M. Yamaura, K. Sato, T. Hagiwara, "Effect of counter-anion exchange on electrical conductivity of polypyrrole films" Synthetic Metals, 39, 43-60, 1990.

[6] T. A. Skotheim, R. L. Elsenbaumer, J. R. Reynolds, Handbook of Conducting Polymers. New York: Marcel Dekker, 1998.

[7] R. H. Baughman, R. L. Shacklette, R. L. Elsenbaumer, "Micro electromechanical actuators based on conducting polymers" Lazarev, P. I., Editor. Topics in Molecular Organization and Engineering, Molecular Electronics. Dordrecht: Kluwer, vol. 7, 267, 1991.

[8] J.D.W. Madden, N.A. Vandesteeg, P.A. Anquetil, P.G.A Madden, A. Takshi, R.Z Pytel, S.R. Lafontaine, P.A. Wieringa, I.W. Hunter, "Artificial muscle technology: physical principles and naval prospects" IEEE Journal of Oceanic Engineering, vol. 29, n 3, pp. 706-28, July 2004.

[9] Q. Pei, O. Inganas, "Electrochemical application of the bending beam method. 1. Mass transport and volume changes in polypyrrole during redox" Journal of Physical Chemistry, 96(25):10507-10514, 1992.

[10] T. Zama, S. Hara, W. Takashima, K. Kaneto, "Comparison of conducting polymer actuators based on polypyrrole doped with $BF4^-$, $PF6^-$, $CF3SO\ 3^-$, and $ClO4^-$", Bulletin of the Chemical Society of Japan 78: 506-511, 2005.

[11] S. Hara, T. Zama, W. Takashima, K. Kaneto, "Artificial muscles based on polypyrrole actuators with large strain and stress induced electrically"Polymer Journal, 36, 151-161, 2004.

[12] J. D. Madden, P. G. Madden, and I. W. Hunter, "Characterization of polypyrrole actuators: modelling and performance," in Proc. SPIE 8th Annu. Symp. Smart Structures and Materials: Electroactive Polymer Actuators and Devices, Y. Bar-Cohen, Ed., Bellingham, WA, 2001, pp. 72–83.

[13] J. Ding, L. Liu, G. M. Spinks, D. Zhou, G. G. Wallace, and J. Gillespie, "High performance conducting polymer actuators utilizing a tubular geometry and helical wire interconnects," Synth. Metals, vol. 138, n 3, pp. 391–398, 2003.

[14] Y. Bar-Cohen, Electroactive polymer (EAP) actuators as artificial muscle, 2nd ed. Bellingham, WA: SPIE, 2004.

[15] T. Mirfakhrai, "Carbon nanotube yarn actuators" PhD thesis, 2000.

[16] T. Shoa, J.D. Madden, N.R. Munce, V.X.D. Yang, "Analytical modelling of conducting polymer driven catheter" Polymer international, Electromechanically Active Polymers for Bioengineering, Mechatronics and Optics, vol. 59, pp. 343-351, 2010.

[17] P. M. George, D. A. Lavan, J. A. Burdick, Chen, Y. Ching, E. Liang, R. Langer, "Electrically controlled drug delivery from biotin-doped conductive polypyrrole" Advanced Materials 18, n 5, 577-581, 2006.

[18] IC. mmerstrand, K. Holmgren-Peterson, K. E. Magnusson, E. Jager, M. Krogh, M. Skoglund, A. Selbing, O. Inganäs, "Conjugated-polymer micro- and milliactuators for biological applications" Source: MRS Bulletin, vol. 27, n 6, pp. 461-464, June 2002.

[19] D. Zhou, G.G. Wallace, G.M. Spinks, "Actuators for the cochlear implant", Synth. Met., vol. 135-136, pp. 39–40, 2003.

[20] Smela, Elisabeth, "Conjugated polymer actuators for biomedical applications", Advanced Materials, vol. 15, n 6, pp. 481-494, March 17, 2003.

[21] A. Mazzoldi, D. De Rossi, "Conductive polymer based structures for a steerable catheter", in 2000 Proc. SPIE–The International Society for Optical Engineering, vol. 3987, pp. 273-80.

[22] X. Wang, X. Gu, Ch. Yuan, Sh. Chen, P. Zhang, T. Zhang, J. Yao, F. Chen, G. Chen, "Evaluation of biocompatibility of polypyrrole *in vitro* and *in vivo*" Journal of Biomedical Materials Research - Part A 68, n 3, 411-422, 2004.

[23] Z. Zhang, R. Roy, F. J. Dugre, D. Tessier, L. H. Dao "In vitro biocompatibility study of electrically conductive polypyrrole-coated polyester fabrics" Journal of Biomedical Materials Research 57, n 1, 63-71, 2001.

[24] T. Shoa, T, J. D. Madden, N. R. Munce, V. XD. Yang, "Biomedical applications of electroactive polymer actuators" John Wiley & Sons, Inc, Chapter 11, 2009.

[25] S. R. Patel, A. A. Caldamone, The history of urethral catheterization, Medicine and Health Rhode Island, 2004.

[26] Y. Haga, M. Esashi, "Biomedical microsystems for minimally invasive diagnosis and treatment" Proceedings of the IEEE, 92, 1, 98–114, 2004.

[27] Salimuzzaman, A. Matani, O. Oshiro, K. Chihara, M. Asao, "Visualization of a blood vessel using a micromotor" Tech. Dig. 14th Sensor Symp. 279–280, 1996.

[28] H. Lehr, W. Ehrfeld, B. Hagemann, K. P. Kamper, F. Michel, Ch. Schulz, Ch. Thurigen, "Development of micro and millimotors," Min. Invas. Ther. Allied Technol. 6, 191–194, 1997.

[29] K. Ikuta, M. Tsukamoto, S. Hirose, “Shape memory alloy servo actuator system with electric resistance feedback and application for active endoscope” Proc. IEEE Int. Conf. Robotics and Automation, 427–430, 1988.

[30] D. Reynaerts,J. Peirs, H. V. Brussel, “Design of a shape memory actuated gastrointestinal intervention system” Proc. 5th Int. Conf. New Actuators, 26–28, 1996.

[31] W. C. McCoy, “Steerable and aimable catheter,” U.S. Patent 4543 090,1985.

[32] S. Kaneto, S. Aramaki, K. Arai, Y. Takahashi, H. Adachi, K. Yanagisawa, “Multi freedom tube type manipulator with SMA plate” Proc. Int. Symp. Microsystems, Intelligent Materials and Robots, 27–29, 1995.

[33] T. Fukuda, S. Guo, K. Kosuge, F. Arai, M. Negoro, K. Nakabayashi, “Micro active catheter system with multi degrees of freedom” Proc. IEEE International Conference on Robotic and Automation 3, 2290-2295, 1994.

[34] M. F. Metzger, T. S. Wilson, D. Schumann, D. L. Matthews, D. J. Maitland, “Mechanical properties of mechanical actuator for treating ischemic stroke,” Biomedical Microdevices 4, n 2, 89-96, 2002.

[35] D. J. Maitland, T. Wilson, M. Metzger, D. L. Schumann, “Laser-activated shape memory polymer microactuators for treating stroke” Proc. SPIE 4626, 394-402, 2002.

[36] S. Gue, T. Fukunda, K. Kosuge, F. Arai, K. Oguro, M. Negoro, “Micro catheter system with active guide wire” Proc. IEEE International Conference on Robotic and Automation 1, 79-84,1995.

[37] S. Guo, T. Nakamura, T. Fukuda, “Microactive guide wire using ICPF actuator-characteristic evaluation, electrical model and operability evaluation” Proc. IEEE IECON 22nd International Conference on Industrial Electronics, Control, and Instrumentation, 1312–1317, 1996.

[38] K. Onishia, Sh. Sewaa, K. Asakab, N. Fujiwarab, K. Ogob, “Bending response of polymer electrolyte actuator” Proc. SPIE 3987, Smart Structures and Materials, 121-128, 2000.

[39] M. Cole, J.D. Madden, “ The effect of temperature exposure on polypyrrole actuation”, Materials Research Society Symposium Proceedings 889, 105-110, 2006.

[40] W. Takashima *et al.*, “Mechanochemoelectrical effect of polyaniline film” Synthetic Metals, 85(1-3), pp. 1395-1396, 1997.

[41] T. F. Otero, M.T. Cortes, “A sensing muscle” Sensors and Actuators, B: Chemical, 96(1-2), pp. 152-156, 2003.

[42] T. F. Otero, M.T. Cortes, “Artificial muscles with tactile sensitivity” Advanced Materials, 15(4), pp. 279-282, 2003.

[43] W. Takashima, K. Hayashi, and K. Kaneto, "Force detection with Donnan equilibrium in polypyrrole film" Electrochemistry Communications, vol. 9, pp. 2056-2061, 2007.

[44] Y. Wu, G. Alici, J. D. W. Madden, G. M. Spinks, G. G. Wallace, "Soft mechanical sensors through reverse actuation in polypyrrole" Advanced Functional Materials, vol. 17, pp. 3216-3222, 2007.

[45] C. H. Tso, J. D. W. Madden, C. A. Michal, "An NMR study of $PF6^-$ ions in polypyrrole", Synth Met 157: 460-466, 2007.

[46] K. Korane, P. Nachtwey, "How hydraulic motion-control measures up", Machine Design. 76- 8: 67-70, 2004.

[47] R.D. Brewer, K. E. Loewke, E.F. Duval, J. K. Salisbury, "Force control of a permanent magnet for minimally-invasive procedures", Proceedings of IEEE/RAS-EMBS, BioRob :580-586, 2008.

[48] J.D. Madden, D. Rinderknecht, P.A. Anquetil. I.W. Hunter, "Creep and cycle life in polypyrrole actuators", Sensors and Actuators, A: Physical, 133: 210-217, 2007.

[49] M. Benslimane, P. Gravesen, P. Sommer-Larsen, "Mechanical properties of dielectric elastomer actuators with smart metallic compliant electrodes", Proceedings of SPIE: 4695:150-157, 2002.

[50] A. Della Santa, D. De Rossi, A. Mazzoldi, "Characterization and modelling of a conducting polymer muscle-like linear actuator", Smart Materials and Structures, 6: 23-34, 1997.

CHAPTER 2: POLYPYRROLE OPERATING VOLTAGE LIMITS IN AQUEOUS SODIUM HEXAFLUOROPHOSPHATE[1]

2.1 Introduction

Conducting polymers such as polypyrrole have been recently used in actuator technology due to their attractive characteristics. These materials are lightweight, inexpensive and can generate large strain [1-4]. Polypyrrole and other conducting polymers can also be driven electrochemically by low operational voltages. In order to determine the range of applications that are appropriate, a key factor is the electrochemical stability of conducting polymers, which in turn will determine lifetime.

In this chapter actuation of polypyrrole in aqueous sodium hexafluorophosphate is studied and the electrochemical degradation as a function of voltage is investigated. Actuation of polypyrrole in aqueous sodium hexafluorophosphate solution has been shown to produce relatively large strains (~ 6%) [5]. Our particular interest is in disposable applications where a relatively small number of cycles are needed, and maximum strain is desired.

This study involves cycling a polypyrrole film within various voltages inside an aqueous electrolyte and analyzing the film response. The dependence of polymer

[1] "A version of this chapter has been published. Shoa, T., Cole, M., Yang, V. and Madden, J. (2007) Polypyrrole operating voltage limits in aqueous sodium hexafluorophosphate, SPIE Smart Structures. 652:652421."

charging on voltage and the reduction in the extent of charging as a function of applied voltage are measured. Since conducting polymer strain is proportional to charge [6], degradation in strain and in charge transferred into the polymer are also correlated, as has been found experimentally in [7]. Therefore the results of charge measurement give direct information about the polymer induced strain in response to the voltage increase. The results of this work will be used in Chapter 6 to determine the extent of voltage and hence strain that can be applied to an active catheter in order for the desired number of cycles to be achieved.

2.2 Experiment

A polypyrrole film was investigated as the working electrode in an electrochemical actuation process. The goal is to study the proper voltage range in which polypyrrole actuators can work effectively. The experimental set up consists of working, counter and reference electrodes inside an aqueous solution of $NaPF_6$. The reference electrode used in this experiment is a Ag/AgCl electrode. Polypyrrole films were electrochemically deposited onto two glassy carbon substrates which are then used as working and counter electrodes.

Polypyrrole was deposited on a polished glassy carbon substrate using the method of Yamaura *et al.* [8] as described in section 1.5 of Chapter 1. The polymer electrochemical deposition was performed for 6 hours to obtain a thickness of approximately 10 μm.

Having the glassy carbon substrate as a backing electrode for the Polypyrrole film ensures good electronic conductivity during the cyclic experiments. Reversible

reduction in electronic conductivity due to change in oxidation state can lead to a slowing of response [9] which can be mistaken for degradation. The use of the conducting substrate reduces the impact of this effect. The disadvantage is that the actuation is not directly observed since the polypyrrole is fixed to a stiff substrate. However, as mentioned, previous work has shown that loss of strain with time is mostly accounted for by a reduction in charge transfer.

2.2.1 Over-oxidation

Polypyrrole as an actuator is often used in bilayer or trilayer structures where it is coated on one or both sides of a structure and is meant to bend the structure. A sequence of potentials is applied to actuate the structure. Our particular interest is in actuating a trilayer back and forth for a number of cycles.

In order to investigate the rate of reduction in the extent of charging in response to different oxidation states, the following experiments were performed:

1. A fixed 0.2 V potential, versus an Ag/AgCl reference electrode, was applied to the working electrode for 20 minutes to bring the polypyrrole film to this oxidation state.
2. A series of square waves from 0 to 0.2 V, versus an Ag/AgCl reference electrode, with the cycling period of 100 seconds were applied between the working and an Ag/AgCl reference electrode and the current was monitored (see Figure 2.1a & b). The amount of charge transferred during experiment 2 is calculated from these data

and will be used later as a comparison to investigate charge transfer reduction.

3. At this point the incremental cycling experiment is begun:
    a. Step 1 is repeated (0.2 V for 20 minutes).
    b. Twenty cycles of a square wave from 0 to v_1=0.25 V, versus an Ag/AgCl reference electrode, are applied to the working electrode with a period of 100 seconds.
    c. Experiment 2 was repeated.
4. Continue experiment 3 by incrementing the cycling amplitude (from v_1 to v_1+0.05V) of step b until the maximum voltage reaches 1V.

Figure 2.1C shows the first 5 cycles of 0 to 0.8 V cycling, applied to the working electrode versus an Ag/AgCl reference electrode, and Figure 2.1b illustrates its corresponding current. The 0.2V square wave of Experiment 2 was reapplied after each cyclic experiment in order to investigate the effect of increase in voltage on the extent of charging. This is done by comparing corresponding charge transfers after each cycling.

Figure 2.2 shows Polypyrrole charging during the last cycle of each cyclic experiment. We can see from Figure 2.2a that the amount of charge transferred during the incremental cyclic experiment is increasing with voltage up to 0.8 V; and according to the plot of Figure 2.2b it decreases dramatically at 0.9V and 1V. During the last cycle the charge amplitude falls by ~ 70% at 0.9V and by about 90% at 1V. This suggests that polymer charge transfer degradation had occurred at 0.9V. It is known from the literature that overoxidation and degradation of Polypyrrole starts

when hydroxyl groups attack the positive charges on the polymer backbone [10]. Oxidation of hydroxylated product yields carbonyl-substituted structures, which have been identified by the use of IR spectroscopy [10-11]. It is possible that this mechanism is the cause of the degradation, particularly as our solvents is water.

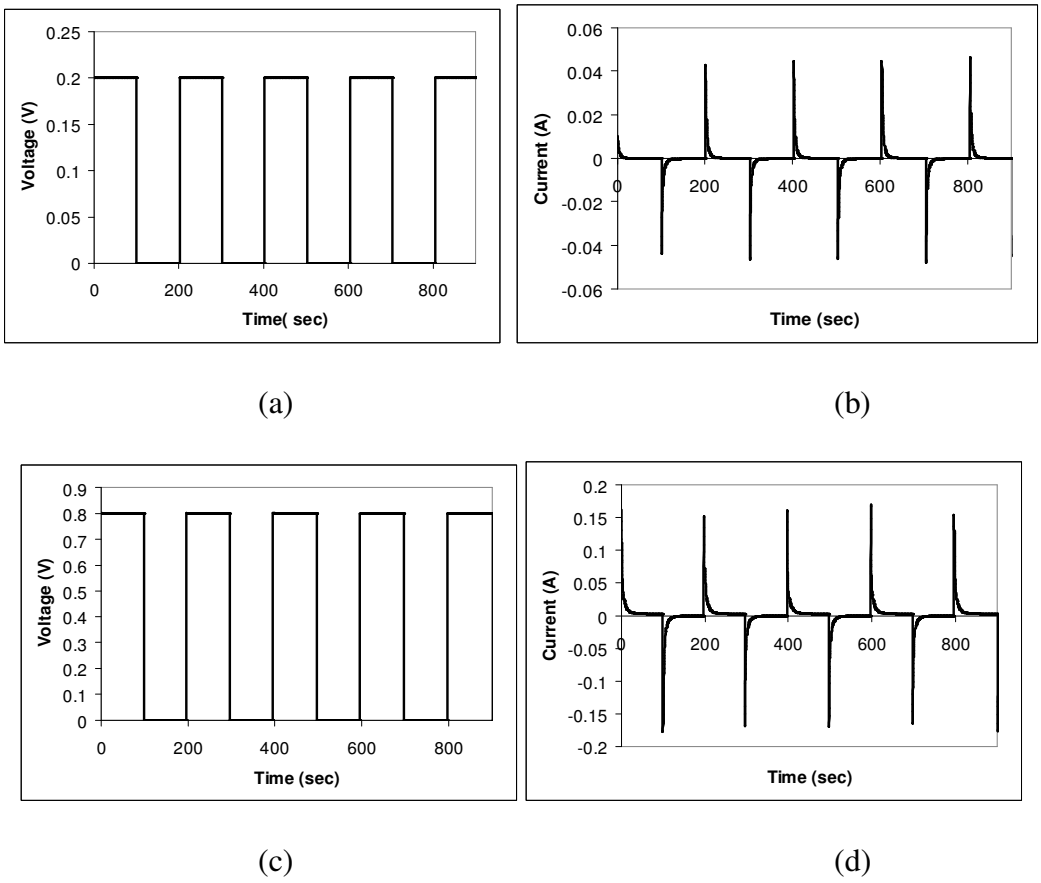

Figure 2.1: a &c Voltage cycling showing 4.5 of 20 cycles, b & c corresponding currents.

At 0.2V cycling shown in

Figure 2.2a, the amount of charge transferred on the last cycle was ~0.1 C. Given that the polypyrrole in this form acts like a capacitor [12], the expected charge transfer at 0.8 V cycling is ~0.4 C. In fact at 0.8 V cycling the measured charge was

0.73 C. This excess charging is due to the parasitic charge which is also increasing with the voltage, as is clear in Figure 2.3, which shows the total charge during cycling to the higher voltages.

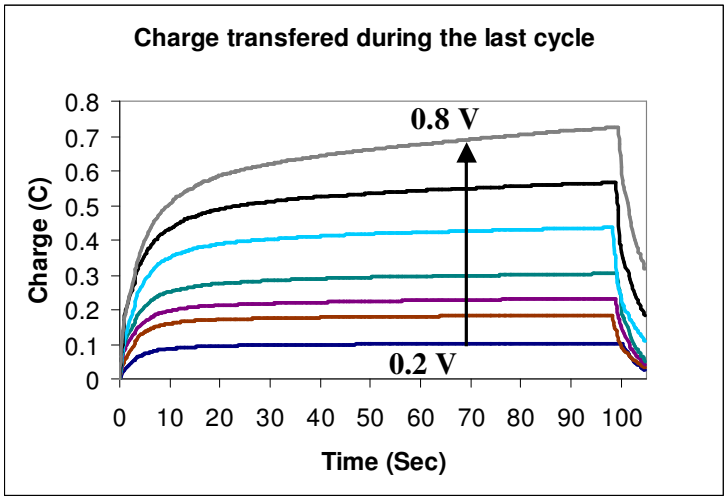

(a)

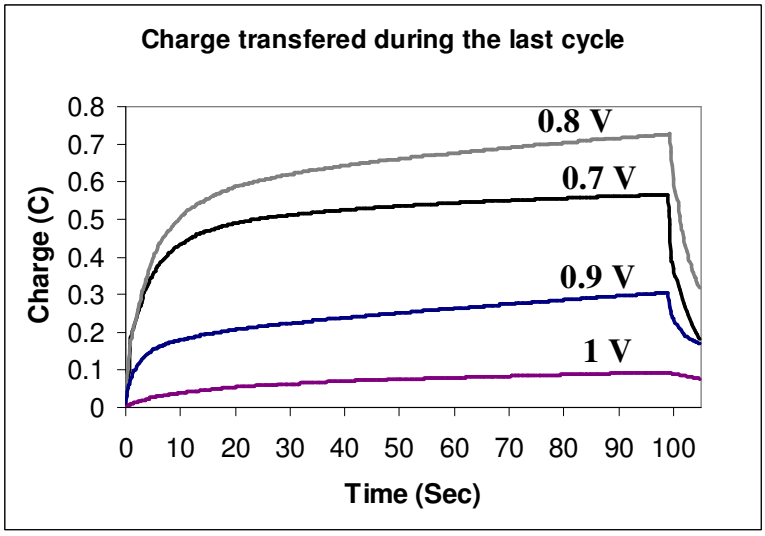

(b)

Figure 2.2: Polypyrrole charging during the last cycle of each cyclic experiment, a) v_1=0.2V to 0.8V. b) v_1=0.8V to 1V.

The drift observed in charge in Figure 2.3 is very likely due to kinetics limited reactions that occur at high voltages. At 0.9 V the charge passed through the polymer during the first two cycles is still increasing, however it starts decreasing over cycles and as shown in Figure 2b, it drops significantly during the last cycle. There is an obvious reduction in the amount of charge transfer at 0.95 V and 1 V cycling suggesting the degradation of the polymeric structure.

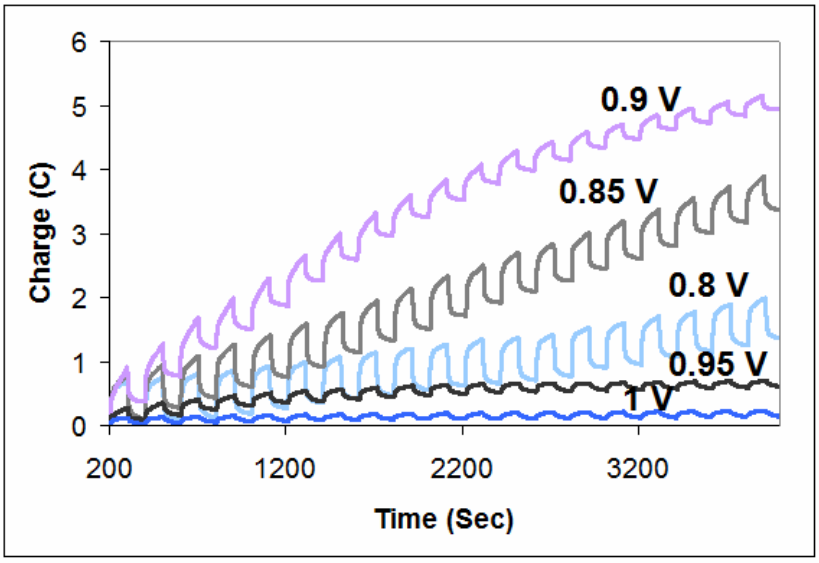

Figure 2.3: Polypyrrole charging over entire cycles

As was mentioned a sequence of 0 to 0.2 V steps, versus an Ag/AgCl reference electrode, was applied after each incremental cyclic experiment. Comparing the amount of charge transferred after each incremental cycling of this experiment also shows charge reduction at 0.9 V. Figure 2.4 illustrates charge reduction behavior after charging (i.e. 0.2 V) and discharging (i.e. 0 V). The result presented in Figure 2.4 shows that cycling the polypyrrole film at voltages below 0.8 V results in

relatively constant charge transfer at 0.2 V cycling. This means that voltages smaller than 0.8 V do not cause noticeable degradation in polypyrrole charge transfer. We can see that the amount of charge transfer decreases by ~30 % at 0.85 V and by ~ 70% at 0.9 V.

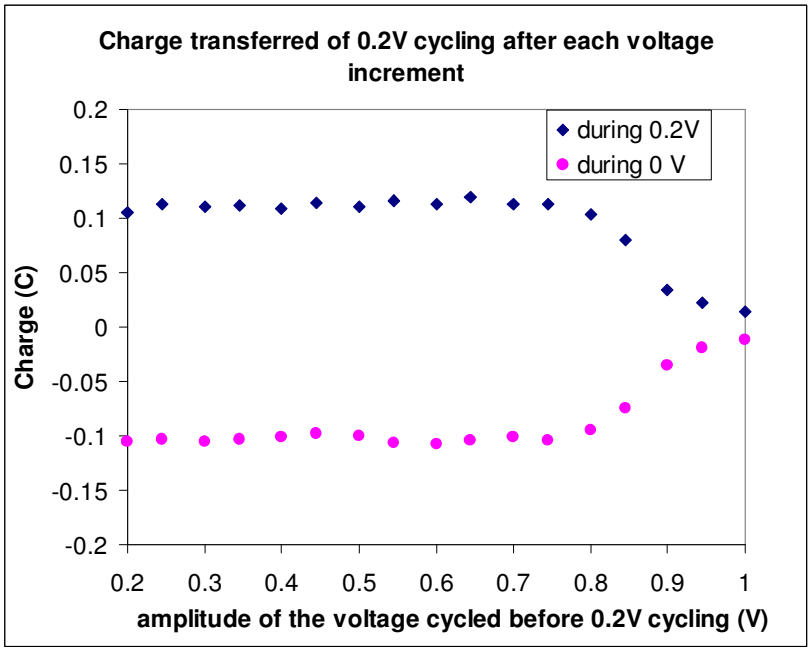

Figure 2.4: Charge transfer at 0-0.2V cycling after each incremental cycling experiment.

The drop in charge transfer at 0.2 V cycling corresponds quite closely with that observed during actuation at higher voltages. This can be seen in Figure 2.5 where the polymer capacitance in these two cases is plotted using the measured charge of Figures 2.2 and 2.4. The parasitic charges have been subtracted from the total charge shown in Figure 2.2 in the capacitance plot of this figure. The parasitic charges have been estimated using the current versus time plot (see Figure 2.1c & 1d). It was assumed that the polymer was completely charged during the period of 100 seconds, and the current responsible for charging the polymer capacitor ideally

reaches zero at the end of each cycle. Therefore any excess current (i_p) at the time t=100 seconds could represent parasitic charge of $q_p = i_p \times t$.

According to Figure 2.5, polypyrrole capacitance is between 1 F to 1.2 F at low voltages. The capacitance measured from 0.2 V cycling drops steeply beyond 0.9 V cycling. The capacitance measured from incremental cyclic experiment starts from 1 F and begins to increase slightly at 0.6 V and shows a peak at 0.85 V. This increase in capacitance may be due to underestimation of parasitic charges at high voltages. More accurate separation of parasitic effects is needed in order to achieve the precise capacitance at highly oxidized states. However this plot still shows the capacitive degradation behavior of polypyrrole qualitatively matches that of 0.2 V cycling. Both plots show that capacitance starts decreasing at 0.9V and suggest that irreversible degradation of the polymer is occurring.

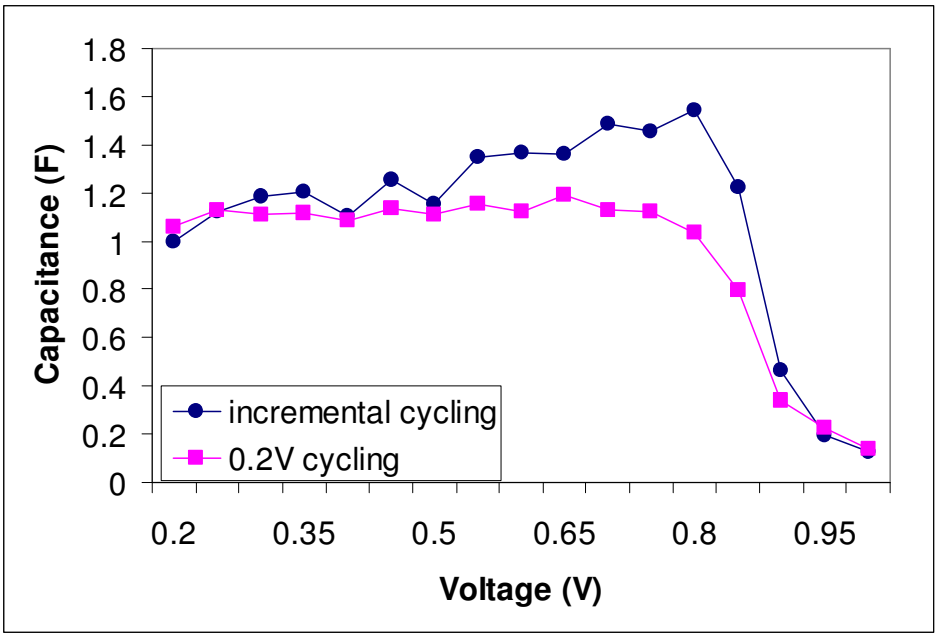

Figure 2.5: Capacitance of Polypyrrole versus the applied voltage.

2.2.2 Over-reduction

The ionic conductivity across the polypyrrole film depends on the electrolyte concentration but also on the degree of oxidation of the film. Also it is believed that in a strongly reduced state, the ions diffuse more slowly than in an oxidized and relaxed state [13, 14, 15]. In order to investigate this effect another set of experiment was performed where the polypyrrole film was initially cycled between 0 and 0.2 V, and then was cycled at reduced states, following the same steps as before but incrementing the voltage, v1, negatively. The film was again cycled between 0 and 0.2 V to see if there is any change in the amount of charge transferred after being reduced.

The resulting charge transfer at different reduced states is shown in Figure 2.6. We can see from Figure 2.6a that the amount of charge transferred during 0 to -0.3 V cycling was about -0.15 C. This amount increases to -0.24 C at -0.4 V cycling and seems to stay constant as the cycling amplitude increases. According to Figure 2.6b the amount of charge transferred is smaller during cycling at more negative voltages. A relatively large charging delay is also observed at reduction potentials (see Figure 2.6). Since the strain in conducting polymers is approximately proportional to the amount of charge transfer, this delay results in a small strain at short cycling periods (i.e. high frequency).

It is possible that low ionic conductivity of polypyrrole at highly reduced state explains the reduction in charge transfer beyond -0.6 V. The effect shown in Figure 2.6 could be due to a change in the polymeric structure which prevents (or at least dramatically slows) subsequent ions from diffusing into the polymer. It could also be

due to irreversible degradation. This will be discussed more in the following paragraphs.

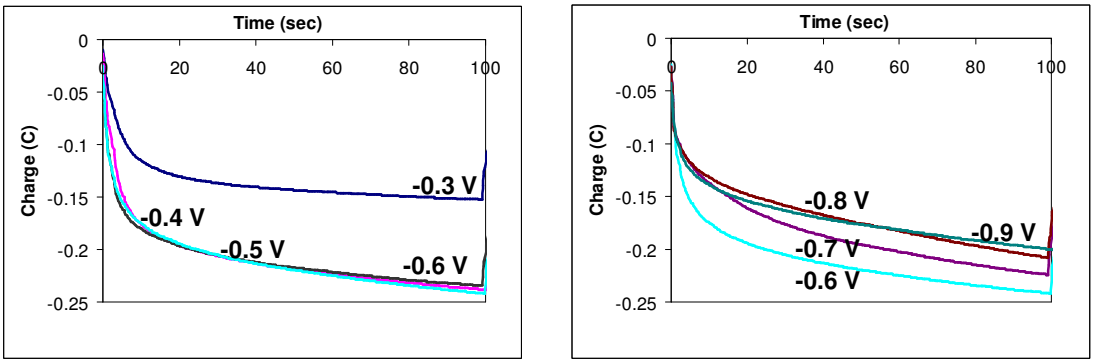

(a) (b)

Figure 2.6: Polypyrrole charging during the last cycle of each cyclic experiment, a) v_1=-0.3 V to -0.6 V. b) v_1=-0.6 V to -0.9 V.

Figure 2.7 shows the amount of charge transfer during 0 to 0.2 V cycling after the polymer had been cycled to various reduced states. This experiment helps determine the effect of cycling at negative voltages on the polymer charging characteristics. The plot in Figure 2.7 shows relatively fast response for initial polymer charging when applying 0 to 0.2 V cycles. After being cycled between 0 and -0.5 V, the polymer charging rate at 0.2V is less steep and as a result the polymer is not fully charged at the end of cycle. This effect is more obvious after larger negative cycling. Warren and Madden have reported a relatively linear relationship between charge and potential within the voltage range of -0.8 V to 0.4 V and with the cycling period of 700 seconds and more [12]. The effect seen in Figure 2.7 could be due to the short cycling period during which the polymer is not fully charged. A drift in charge was also observed during the 0.2 V cycling experiments after polymer reduction, which did not stabilize over cycles. This also supports the idea that the

charging was not complete after 100 seconds and structural degradation is less likely to happen. Otero *et, all* suggested that a highly oxidized potential is required to recover highly reduced polymer [19]. It is likely that the polymer structural change which appears to cause the low ionic conductivity at highly reduced states has not been fully reversed during the 0 to 0.2 V cycling. The polymer is not degraded, but rather transport has slowed, leading to a reduction in charge transfer.

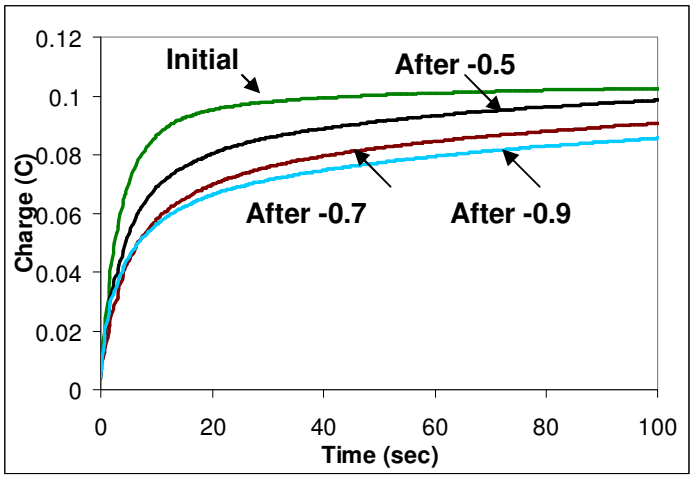

Figure 2.7: charge transfer at 0-0.2V cycling after each incremental cycling experiment.

2.3 Cyclic voltamettry

As was discussed in previous sections, over-oxidation of polypyrrole inside aqueous solution of $NaPF_6$ results in structural degradation at +0.9 V, and its over-reduction seems to reduce the ionic conductivity dramatically at voltage <-0.6 V. In order to confirm these observations cyclic voltammetry was performed on a 10 µm thick polypyrrole film on a glassy carbon versus Ag/AgCl reference electrode. The scan rate was 1mV/s and the voltage range was from -0.8 V to +0.9 V. Figure 2.8 shows sequential voltagrams generated from this experiment. Polypyrrole acts as a

capacitor from -0.2 V to 0.5 V. There is a peak at -0.4 V which drops in amplitude. A similar cathodic peak is observed by others and appears to result from a transient exchange of ions and solvent when the film is first cycled [17-18]. At 0.5 V the current rises steeply, suggesting a kinetics limited parasitic reaction. Presumably this reaction is the same reaction that is degrading the polymer. This current peak is decreasing every cycle, suggesting degradation. In fact the entire CV decreases in amplitude, as would be expected from a reduction in the redox activity. At extreme negative potentials (< -0.4 V) redox activity decreases even more dramatically. This drop is consistent with the results shown in Figure 2.6 which showed that at higher reduced state the amount of charge transferred is limited. As was discussed above (in section 2.2) this effect could be due to either reduction in ionic conductivity at highly reduced state or the short cycling period resulting in an incomplete charging, or a combination of both of these effects.

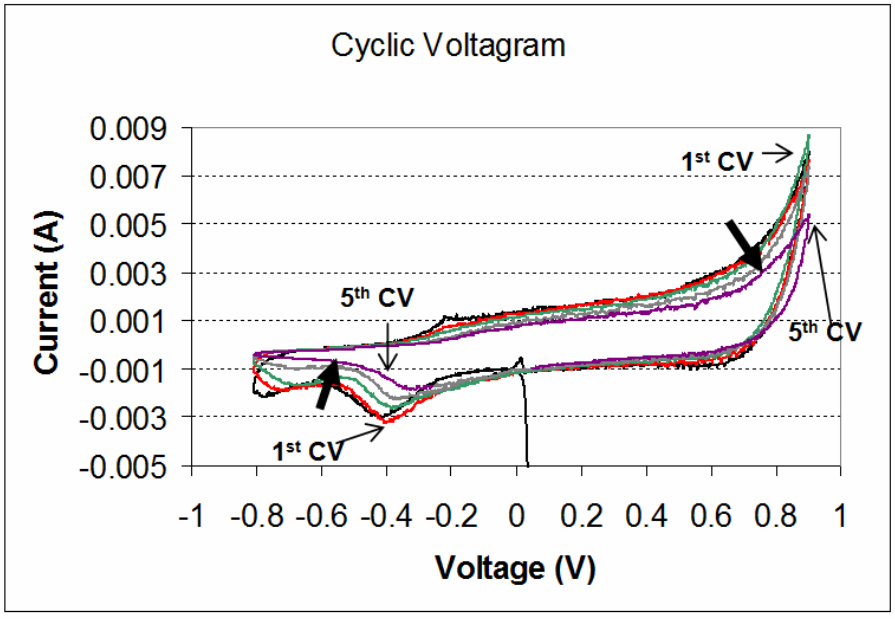

Figure 2.8: Cyclic Voltagramm of polypyrrole inside 1 M of AQ-$NaPF_6$ .Arrows indicate the time sequence.

2.4 Discussion and conclusion

The electrochemical degradation of polypyrrole inside aqueous-$NaPF_6$ as a function of voltage was investigated by stepping the polymer film between fixed voltages and measuring the charge transfer. The dependence of charging on voltage and the rate of reduction in the extent of charging were measured. The result of cycling shows that polypyrrole acts as a capacitor from -0.3 V to 0.8 V. At 0.85 V the amount of charge transferred through the polymer structure decreased by ~ 30% and dropped further to ~ 70% at 0.9 V. According to the charge plots there is not a noticeable increase in the time constant with the voltage at oxidized states. The CV plots also showed a steeply rising current at 0.9 V. These results are consistent with an irreversible degradation of the polymer redox capacity which results from parasitic reactions that are rapid at voltages of > 0.8 V. The mechanisms of degradation at potentials beyond 0.8 V may be the substitution of hydroxyl ions in the polymer backbone, as suggested in reports on degradation of polypyrrole in other electrolytes [10-11]. The result of stepping voltage to reduced states suggested a reduction in polypyrrole ionic conductivity at voltages less than -0.4 V. This reduction in activity at low voltages is confirmed by the CV plot where the amount of charge transfer decreases at reduced states. The effect could be due to a change in the polymeric structure which dramatically slows subsequent ions from diffusing into the polymer. Polymeric degradation at reduced states cannot be ruled out. However the 0.2 V amplitude cycling experiments suggest that charge is gradually recovered. The experiment was not long enough to see if full recovery is eventually achieved.

The voltage range for effective operation of the device was found to be -0.4 V to 0.8 V versus a Ag/AgCl reference electrode in order to achieve stable performance over at least 30 minutes.

References

[1] J.D. Madden, N. Wandesteeg, P. Anquetil, P. Madden, A. Takshi, R. Pytel, S. Lafontaine, P. Wieringa, I. Hunter, “Artificial muscle technology: Physical principles and naval prospects”, IEEE J. Ocean. Eng. 29 (2004) 706–728.

[2] E. Smela, Adv. “Conjugated polymer actuators for biomedical applications”, Mater. 15 (2003) 481–493.

[3] R.H. Baughman, “Materials science: Muscles made from metal “, Science 300 (2003) 268–269.

[4] Bar-Cohen “Electroactive Polymer Actuators as Artificial Muscles” SPIE, Bellingham, WA, (2001).

[5] M. Cole, J.D.W. Madden, “The effect of temperature exposure on polypyrrole actuation”; Materials Research Society Symposium Proceedings, 889 (2006) 105-110.

[6] R. H. Baughman, R. L. Shacklette, R. L. Elsenbaumer, "Micro Electromechanical Actuators based on Conducting Polymers", Topics in Molecular Organization and Engineering: Molecular Electronics, P. I. Lazarev, Ed., 7 (1991) 267, Kluwer, Dordrecht,.

[7] J. D. Madden, D. Rinderknecht, P. A. Anquetil and I. W. Hunter, "Cycle Life and Load in Polypyrrole Actuators", Sensors & Actuators A, 133-1(2007) 210-217.

[8] M. Yamaura, T. Hagiwara, K. Iwata, “Enhancement of electrical conductivity of

polypyrrole film by stretching: counter ion effect", Synth. Met. 26 (1988) 209– 224.

[9] Madden, J.D. ; Warren, M.R.A; "structural, electronic and electrochemical study of polypyrrole as a function of oxidation state" Synthetic Metals, 156-5 (2006) 724-730.

[10] F. Beck, P. Braun, M. Oberst. Ber Bunsenges, " Organic Electrochemistry in the solid state overoxidation of polypyrrole", ,Phys Chem 91 (1987)967-974.

[11] P.A. Christensen, A. Hamnett, "In situ spectroscopic investigations of the growth, electrochemical cycling and overoxidation of polypyrrole in aqueous solution ", Electrochim Acta, 36 (1991)1263.

[12] M. Warren and J.D. Madden, "A Structural, Electronic and Electrochemical Study of Polypyrrole as a Function of Oxidation State", Synthetic Metals, 156, 9-10, (2006) 724-730.

[13] P.Burgmayer, R.W. Murray, in Skotheim TA, ed. The Handbook of Conducting Polymers, 1st ed. New York: Mersel-Dekker, vol1, Ch. 15 (1986) 507-523.

[14] M.J. Ariza, T.F. Otero; "Ionic diffusion across oxidized polypyrrole membranes and during oxidation of the free-standing film"Colloids and Surfaces A (Physicochemical and Engineering Aspects), 270-271 (2005) 226-31.

[15] T.F. Otero, H. Grande, J. Rodrquez, "Role of conformational relaxation on the voltammetric behavior of polypyrrole. Experiments and mathematical model", J. Phys. Chem. B 101 (1997) 3688.

[17] W.L. Trevor; G.M. Spinks,; G.D. Wallace, D. De Rossi; " Investigation of the

applied potential limits for polypyrrole in a two-electrode device" Proceedings of SPIE - The International Society for Optical Engineering, 3669 (1999)272-282.

[18] M. Iseki, K. Satio, M. Ikematsu, Y. Sugiyama,K. Kuhara, A. Mizukami, J. Electroanal. Chem. 358 (1993) 221.

[19] T.F. Otero, H. Grande, J. Rodriguez, "Conformational relaxation during polypyrrole oxidation: From experiment to theory" Electrochimica Acta, 41, n 11-12 (1996)1863-1869.

CHAPTER 3: ELECTRO-STIFFENING IN POLYPYRROLE FILMS: DEPENDENCE OF YOUNG'S MODULUS ON OXIDATION STATE, LOAD AND FREQUENCY [2]

3.1 Introduction

Mechanical properties such as the Young's modulus of the polymer contribute in determining the amount of strain obtained at a given load [9]. When a material is under load, a change in stiffness will lead to a deformation. Therefore investigating factors affecting the polymer Young's modulus is important in designing effective actuators. In this chapter it is shown that the stiffness of polypyrrole is a function of charge state (oxidation state), frequency and load. The magnitudes of the electro-stiffening, frequency dependence and load dependence is important to understand and fully describe the actuation of polypyrrole.

According to previous investigations [9-14], the Young's modulus of the polymer changes in the process of altering the oxidation state. However the reported results show substantial variations in the way the modulus changes with oxidation states. A recent study by Pytel *et al.* [15] observe that typically the elastic modulus is lowest when the largest density of ions is present, regardless of whether the actuation

[2] "A version of this chapter has been accepted for publication. Shoa, T., Mirfakhrai,T. and Madden, J.D.W.(2010) Electro-stiffening in polypyrrole films: Dependance of Young's modulus on oxidation state, load and frequency. Synthetic Metals 160:1280–1286."

response is cation- or anion-dominated. The lower modulus may be due to the reduction of interactions between chains by the dopants, which are mobile, and thus do not form fixed cross-links.

Pytel *et al.* have observed the change in elastic modulus as a function of oxidation state of polypyrrole during actuation [15]. The modulus found by this method may be underestimated due to the effect of ion transport on the material properties. For instance an increase in the rate of the creep has been observed during polypyrrole actuation, perhaps as a result of additional perturbation by the passage of the charge [16]. In addition, the actuation potential was only held for 50 s at each voltage [15]. Although the result obtained using this method provides a reasonable indication of the change in the modulus occurring during actuation over the recorded time interval, it will not give a quantitative description of the modulus as a function of oxidation state since the change in state was not complete over this relatively short time.

In the present study the polymer modulus is measured as a function of oxidation state by applying an external stress to a polypyrrole film, which is first held at an oxidation state for long enough to ensure that steady state is reached. The waiting time was estimated based on the time constants associated with charging of the poylpyrrole material [17-19].

For the first time, the complex Young's modulus of polypyrrole is measured. The effect of load amplitude and perturbation frequency on the measured Young's modulus of polypyrrole at various oxidation states is also measured, showing that the modulus is dependent on these parameters. The results of these studies are crucial to

designing polypyrrole actuators effective for various operational conditions. In our case we are particularly interested in applying polypyrrole actuators in active catheters [17]. Knowing the frequency response and load dependence of the modulus is important in predicting actuator response and, for example, in designing actuator systems that operate at their mechanical resonance frequency in order to response larger amplitudes and strain rates at high frequencies.

The modulus and its changes are a function of synthesis conditions, dopant and electrolyte. In this chapter we study the modulus of polypyrrole doped with hexafluorophosphate (PF_6^-), synthesized following Yamaura *et al.* [20], which can generate stable strains of 6 % when actuated in aqueous electrolyte of sodium hexafluorophosphate ($NaPF_6$) [8]. This combination was chosen based on previous investigations by Kaneto and EAMEX corporation on polypyrrole dopants and electrolytes for effective actuator performance [6,21]. According to these studies, although extremely large strains can be achieved (29-36% [4,5]), the actuator performance is not stable when such strains are generated [22] and practical operating conditions suggest strains of up to 7 % are reasonable where multiple cycles are needed [21,22]. Polypyrrole doped with PF_6^- and actuated in aqueous electrolyte of $NaPF_6$ provides an advantageous combination of large stable electrochemical strain [6,8] and long lifetime [25] potentially suitable for many applications such as steerable devices, robotics, and medical devices [17,21,23,24]. In addition to the effective dopant and electrolyte combination, the polypyrrole actuator of this study is highly conductive due to its low temperature synthesis ($-30^{\circ}C$) – an important factor in enabling fast actuation.

3.2 Synthesis

The polypyrrole film doped with PF_6^- was electrochemically deposited onto a glassy carbon substrate using the method described in Chapter 1 (section 1.5). The polymer film was then peeled off from the glassy carbon and was tested as a standalone film. All experiments were performed on a strip of polypyrrole, with a length of 22 mm, a width of 4 mm, and a thickness of 12 μm. The use of one film enabled uncertainties associated with film dimensions to be minimized when comparing results. The measured stress strain curves for this film are consistent with those taken in other films synthesized under the same conditions.

3.3 Experiment

As depicted in Figure 3.1 the PF_6^- doped polypyrrole film is clamped into an electromechanical test apparatus (Dual Mode Lever System, Aurora Scientific, 300B). A function generator applies the external force control signal to the lever system, which generates force and mechanical movement on the polypyrrole film through a galvanometer and lever arm. The resulting strain is recorded using a data acquisition card.

The polypyrrole sample is also electrically connected to a Solartron 1287 potentiostat which controls its oxidation state during the measurement. Electrical contact was made to the film by attaching gold wires to both ends to increase the speed with which the sample reaches the desired oxidation state when a bias potential was applied. The potential is applied between the clamped polypyrrole film and AvCarb carbon fibre paper (Ballard P75T) counter-electrode. The reference electrode

was Ag/AgCl within a 1 M aqueous solution of $NaPF_6$. An NMR (Nuclear Magnetic Resonance) study on a hexafluorophosphate -doped polypyrrole has shown that the PF_6^- ion content decreases linearly with decreasing the polymer bias potential [26]. Increasing the applied bias potential toward more positive potentials induces positive charges on the polymer (oxidation), and as a result mobile anions (PF_6^-) are attracted into the porous polymer matrix. On the other hand, biasing the polymer at more negative potentials removes the induced charges (reduction) and leads to ions expulsion from the polymer structure.

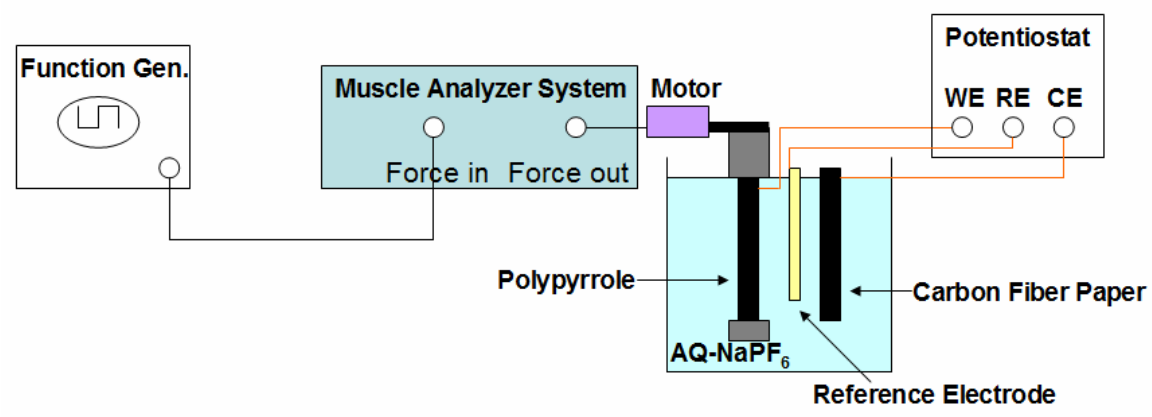

Figure 3.1: Experimental set up for Young's modulus measurement.

3.3.1 Setting polymer oxidation state

Application of a voltage between the polymer and a counter electrode in an electrolyte alters the oxidation state of the polymer by changing its charge content. Electronic charging occurs throughout the volume of the polymer, and is balanced by the insertion of PF_6^- ions into the polymer matrix from the electrolyte (or expulsion of ions from the polymer). The voltage and charge content are related in steady state, so oxidation state is set by applying a fixed voltage and waiting for charging to

complete. As charging of conducting polymers can be slow to finish, we now describe the procedure for determining when charging can be considered complete.

The charging is performed electrochemically and can be thought of as charging a capacitor, C, through a resistance, R, (including electronic resistance along the polymer film, $R_{e,}$ and ionic resistance of mass transport through the polymer thickness, R_i) [17-19]. The time for charging the polymer film is limited by the RC delay, and so it was ensured that the waiting time was significantly longer than the delay time. Based on measured electronic and ionic conductivities for identically synthesized polypyrrole [17], the estimated "upper bound" RC time constants (R_eC+ R_iC) for +0.4 V biasing (versus an Ag/AgCl reference electrode) is ~ 90 sec and for -0.4 V (versus an Ag/AgCl reference electrode) is ~ 300 sec. For this experiment, the bias potential was kept constant for a much longer time (1800 s > 5 × RC) before mechanical measurements are made to ensure the polymer reached the desired oxidation state.

Figure 3.2a plots the charge transferred during biasing at the two extreme oxidation states used in this study, +0.4 V (oxidized state) and -0.4 V (reduced state) versus an Ag/AgCl reference electrode. We can see that polymer charging happens more slowly during biasing at -0.4 V. This is expected due to the higher polymer electronic and ionic resistances at reduced states compared to the oxidized states [17,27,28]. Despite waiting 1800 s the current does not drop completely to zero, but rather settles to a constant value. The steady currents are assumed to be due to parasitic reactions and not to the polymer charging. We believe this is a reasonable assumption based on our previous cyclic voltammetry results for polypyrrole, which

indicate that there is a parasitic current present at extreme potentials [25]. The resistance of the film is sufficiently low, even in the reduced state, [17] that the steady current leads to a negligible voltage drop along the length of the sample, suggesting that oxidation state is homogeneous.

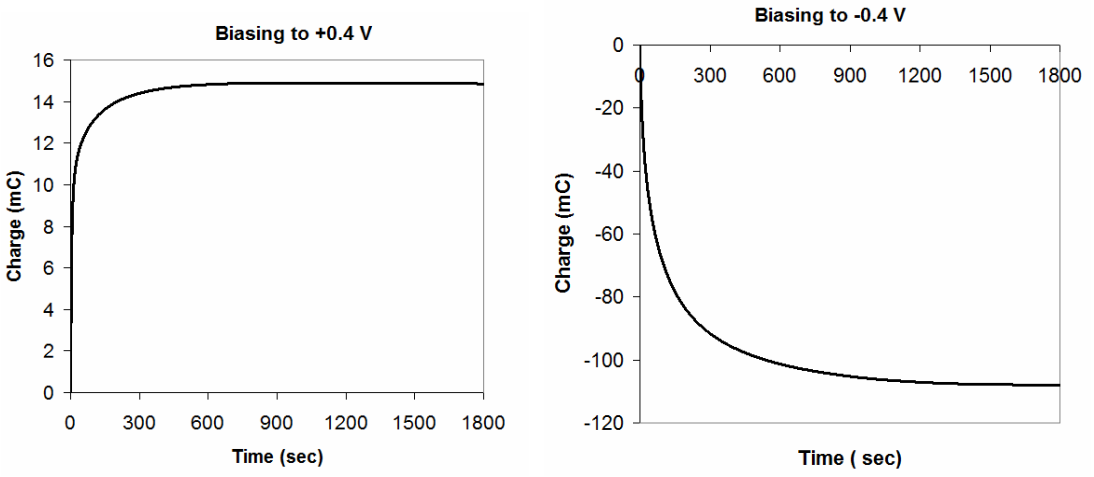

Figure 3.2: Charge transferred during biasing (a) to +0.4 V (from initial potential of +0.32 V), and (b) to -0.4 V (from initial potential of -0.1 V).

After biasing the polymer at a desired potential, the polymer oxidation state is estimated by calculating the number of PF_6^- ions per pyrrole monomer at each potential level assuming that there is one ion inserted per fundamental charge. The initial number of ions per monomer of the as-grown polypyrrole is considered to be 0.23 based on an NMR study of identically synthesized polypyrrole [26]. Figure 3.3 plots the estimated number of PF_6^- ions per pyrrole monomer after each bias potential is reached. In making this estimate a constant current equal to the final steady state current was subtracted from the total current in order to estimate the non-charging component. The number of dopant ions per monomer represents the degree of oxidation, and is very similar in magnitude to that found by NMR [26].

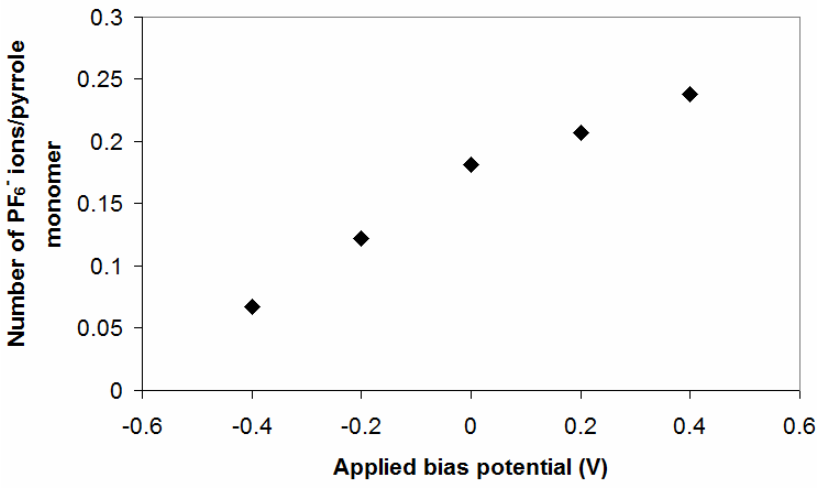

Figure 3.3: Estimated number of PF_6^- ions per pyrrole monomer as a function of oxidation state, with an uncertainty of 10.7 %.

3.3.2 Young's modulus measurement

In order to find the Young's modulus of the polymer film at different loads and oxidation potentials two approaches were followed; (1) applying a constant load with small sinusoidal perturbations superimposed at several frequencies in succession, and (2) gradual ramping of load with a small single frequency sinusoidal perturbation superimposed for the duration of the ramping.

Constant load with superimposed small sinusoidal load (CL-sine)

The load on the clamped polypyrrole sample was first adjusted to the desired value (e.g. 0.7 MPa). Using the function generator, an external sinusoidal load perturbation with a peak amplitude of 1 g (equivalent to 0.2 MPa) was then superimposed for 10 minutes to stabilize the load at the desired value and allow any transient mechanical creep to pass. The film was then biased to an initial oxidation state to +0.4 V, versus an Ag/AgCl reference electrode, using the potentiostat. The

bias potential was kept constant for a period of time longer than the estimated charging time to ensure reaching the desired oxidation state while the load is also maintained constant (1800 s hold time). The following steps were followed:

i. External sinusoidal forces with a peak amplitude of 0.2 MPa and frequencies of f = 0.1 Hz, 1 Hz , 5 Hz and 10 Hz, were superimposed in succession on the constant load (using the function generator). The stresses and the resulting strains were measured and recorded using a data acquisition card. The potentiostat kept the potential constant during each measurement.

ii. The bias potential was then changed sequentially to +0.2 V, 0 V, -0.2 V, and -0.4 V vs. Ag/AgCl reference electrode and the above step was repeated.

iii. The load was then changed to 1.12 MPa and 1.5 MPa, and finally back to 0.7 MPa, and the above steps were repeated at each load.

Based on the data obtained from this method, the complex Young's modulus was calculated by fitting a viscoelastic model (described in section 3.4) to the stress-strain curve found in each experiments.

Ramp with superimposed small sinusoidal (Ramp-sine)

The second approach we pursued in order to measure the Young's modulus is to use ramp loading/unloading with superimposed small sinusoidal perturbation for comparison with the previous method. The major advantage of this method is that all loads between two values are swept during the ramp and thus, the modulus is measured using the perturbation signal at almost a continuum of loads, instead of only

at a few load offset points. Also, the experiment takes a substantially shorter time compared to the method in 3.2.1. The disadvantage of this method is that the load offset is never really constant due to the ramp. However, the load offset may be assumed to be constant if the sweep rate of the ramp is considerably slower than the rate of the perturbation sinusoidal. This method can be summarized as follows;

i. The film was first biased from initial oxidation state to +0.4 V, versus an Ag/AgCl reference electrode, using the potentiostat. The bias potential was kept constant for 1800 s to ensure that the desired oxidation state is reached. The load was also maintained at a constant stress of 0.2 MPa to assure that the film was fully stretched and not slack at the beginning of every test.

ii. The load was then increased slowly at a rate of 10 kPa/s from initial load of 0.2 MPa to 2.4 MPa and was reduced back to 0.2 MPa in a ramp-like fashion, while a sinusoidal load perturbation with amplitude of 20 kPa and frequency of 1 Hz was superimposed on the entire ramp.

iii. The above steps was repeated at oxidation potentials of -0.4 V, -0.2 V, 0 V, and +0.2 V.

An example of the applied stress from the actual experimental data is shown in Figure 3.4.

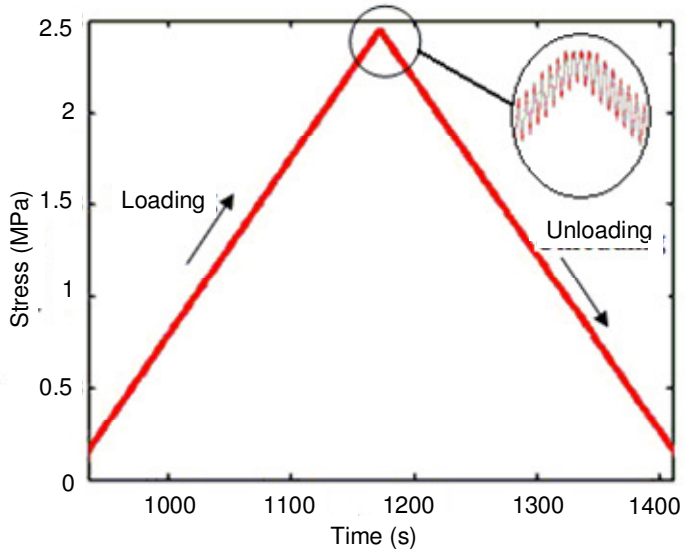

Figure 3.4: The ramp-like applied stress over time. Inset shows a magnification of the top part of the ramp to show the perturbation that is too small to be seen on the big picture.

Based on the data obtained from the ramp method, the Young's modulus was calculated in three ways to find the dependence on the applied load and the oxidation potential:

1. By fitting a viscoelastic model to the stress-strain curve formed by the entire ramp response. This yields one value per each ramp corresponding to the complex Young's modulus at each oxidation state.
2. Using the sinusoid stress and strain during the loading ramp. This way the modulus can be computed at various loads during the rising ramp "loading".
3. Using the sinusoid stress and strain during the unloading ramp. This way the modulus can be computed at various loads during the downward "unloading".

The above experiments were also repeated under open circuit conditions, where the polymer sample was disconnected from the potentiostat after biasing at each potential. This case was studied for conditions where polypyrrole works in open circuit mode. An example could be a polypyrrole sensor where it is employed to generate voltage in response to a detected force. Another example is a polypyrrole actuator that has completed its task in moving an object and is only maintaining the position of the object, in which case potentiostat can be disconnected. The open circuit experiments was challenging, since the relatively rapid drift of open circuit potential in some oxidation states makes them harder to interpret, and thus we believe that these should generally be performed under conditions where such drift is minimized. The detailed procedure for this experiment is described in more detail in Appendix 1.

3.4 Estimation of the complex Young's modulus

At each load, frequency and bias potential, the strain responses to the applied stresses were measured. The applied stress was plotted against the induced strain. For a purely elastic medium, the basic constitutive equation relating the stress, σ, to the strain, ε, is:

$$\sigma = Y \cdot \varepsilon , \qquad (1.3)$$

where Y is the Young's modulus of the material. This implies a line with a slope of Y in the stress-strain curve.

The polypyrrole stress-strain curve shows a hysteresis loop (rather than a straight line), suggesting viscoelastic behaviour and hence a complex value for the

Young's modulus. In order to estimate the complex modulus, the experimental stress-strain responses from CL-sine and Ramp-sine measurements are fitted to that of a Kelvin-Voigt viscoelastic model (Figure 3.5) [29]. This model consists of a Newtonian damper and Hookean elastic spring connected in parallel, as shown in the picture. In a viscoelastic material, the stress response depends not only on the strain but also on the strain rate. The constitutive relation is expressed as a linear first-order differential equation:

$$\sigma(t) = Y \cdot \varepsilon(t) + \eta \cdot \frac{d\varepsilon(t)}{dt}, \qquad (3.2)$$

where σ is the stress, Y is the storage modulus of the material, ε is the strain that occurs under the given stress, η is the viscosity of the material, and $d\varepsilon/dt$ is the time derivative of strain. Y relates to the energy storage and η relates to the energy loss of the material. These two factors were determined by the fitting program.

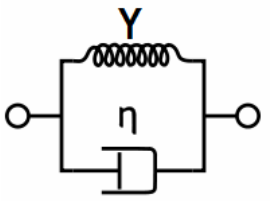

Figure 3.5: Diagram of a Kelvin-Voigt viscoelastic model

The fitting program inputs are the applied stress and the measured strain as a function of time, from which the time derivative of strain is estimated. Using the two parameters (i.e. Y and η), the program fits the data (from the input stress and strain and the calculated strain rate) to Equation 3.2. Figure 3.6 shows an example of fitting an experimental data (obtained from one sinusoidal strain cycle of a CL-sine measurement on a polypyrrole biased at 0.2 V versus an Ag/AgCl reference electrode and a mean applied load of 1.5 MPa at a frequency of 1 Hz) to the Kelvin-Voigt

viscoelastic model. As shown in the figure the stress-strain response of the model using the fit parameters was in close agreement with the experimental data. The waviness of the fit curve is due to the noise in the strain measurement data.

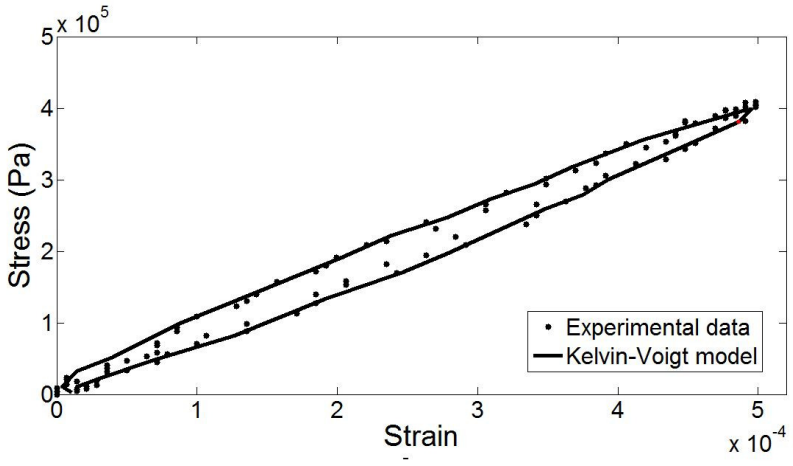

Figure 3.6: Comparison between stress- strain relationships found by experimental data and by fitting to the Kelvin-Voigt model (at 1.5 MPa, at 0.2 V).

The complex Young's modulus is estimated using the fit parameters. The value found by the program for *Y* represents the storage modulus. The value found for η is used to estimate the loss modulus, as is now described.

By taking the Fourier transform of both sides of equation 3.2, the Kelvin-Voigt model can be expressed in the frequency domain:

$$\begin{aligned} \sigma(\omega) &= Y \cdot \varepsilon(\omega) + j\omega.\eta.\varepsilon(\omega), \\ \sigma(\omega) &= Y^{*}\varepsilon(\omega). \end{aligned} \tag{3.3}$$

The complex modulus is then found to be

$$Y^{*}=Y+jY', \tag{3.4}$$

where Y' is the material loss modulus: $Y'=\omega\eta$, and $\omega=2\pi f$, where f is the frequency of the applied load. The values reported for the real and imaginary components of

Young's modulus were determined by averaging over all the cycles in the CL-sine measurements.

3.5 Experimental results

Dependence of the modulus on oxidation state, frequency, and load is studied using both "CL-sine" and "ramp-sine" methods. The complex Young's modulus was estimated for each experiment using the method described above.

3.5.1 Young's modulus: Oxidation potential dependence

Figure 3.7 shows the estimated storage and loss modulus as a function of oxidation potential at f = 1 Hz and at the load of 1.5 MPa. Uncertainties associated with the measurement of the film geometry, and strain and stress are ~ 17 % (every data point may be equally shifted up or down by this amount). The results are found using both methods described in section 3.3.1, (i.e. CL-sine and the Ramp-sine methods). According to this plot, the storage modulus decreases with bias potential. This is also found to be true for other loads and frequencies. As shown in Figure 3.7, the loss modulus also increases as the potential applied to the polypyrrole film is increased. As was discussed in section 3.3, increasing the bias potential increases the polymer ion content, which has been shown to be correlated with lower polymer storage modulus [15], perhaps due to weakening interactions between chains. The PF_6^- anions that are inserted into the polymer matrix during oxidation may also carry solvent molecules with them in a 'solvation sphere'. As a result the solvent content of the polymer may be larger at higher oxidized states. Evidence for this solvent transfer

is provided by Tso *et al.* [26], who have reported that solvent accessibility of PF_6^- ions in the oxidized films are similar to those in the solvent, indicating the ions experience a solvated environment in oxidized states. They also reported a much less solvated ion environment in the reduced film and more tight coupling of the ions with the polypyrrole chains [26]. At higher oxidation states, the solvated ions are free to diffuse into the polymer matrix which may increase the separation between the chains and reduce the forces between them, leading to the observed viscous effect at higher potentials. This explanation also fits with the observed increased creep in polypyrrole at higher oxidation layers reported in [16]. Such softening of polypyrrole due to solvent swelling has been suggested previously [30-32]. Della Santa *et al.* have also observed a longer viscoelastic transient time for a wet polypyrrole sample in comparison with dry samples [33].

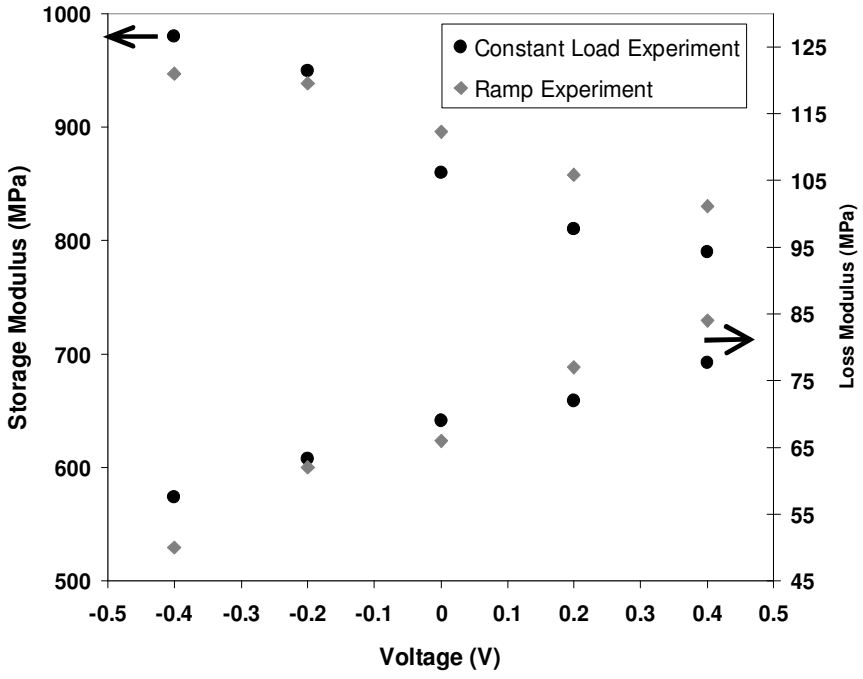

Figure 3.7: Storage modulus and loss factor as a function of polymer potential (vs. Ag/AgCl in 3 M NaCl) found from fitting to the dashpot in Figure 3.5.

3.5.2 Young's modulus: Load dependence

The strain in response to the superimposed sinusoidal load was measured and was used to compute the Young's modulus at various loads during both ramp-sine and the CL-sine experiments. According to our measurement results, increasing the load leads to increasing modulus, as was also observed by Otero, *et al.* [12]. The storage modulus shown in Figure 3.8 illustrates this load dependence of a polypyrrole film biased at -0.2 V, versus an Ag/AgCl reference electrode, at 1 Hz. The increase in modulus with load is also observed at other tested frequencies and bias potentials. Along with some load dependence of modulus there is also a history dependence. Two measurements were performed at 0.7 MPa, one of which was the first constant load measurement, marked 'initial', and another following all the constant load cycles, marked 'end', showing a change in modulus of about 70 MPa over the course of the experiments. The change in modulus with time may be due to gradual stretch alignment of the polymer chains during the application of loads over a long period of time.

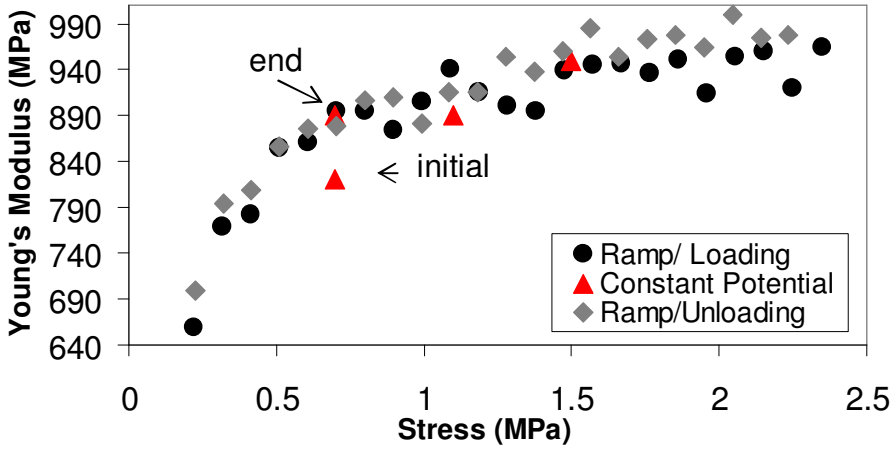

Figure 3.8: Young's modulus as a function of load, found at -0.2 V (a) loading and (b) unloading.

3.5.3 Young's modulus: Frequency dependence

The frequency-dependence of the Young's modulus of the polypyrrole sample was measured by superimposing a sinusoidal variation in the load (amplitude of 0.2 MPa) on the constant loads, at 4 different frequencies (0.1 Hz, 1 Hz, 5 Hz, 10 Hz) and measuring the corresponding displacement. The frequency dependent measurement was only performed through the "CL-sine" experiment. In addition to the above experiments we also performed another set of measurements at a bias of 0.2 V using sinusoidal load input of 0.6 MPa superimposed on a load bias level of 1.35 MPa at frequencies of up to 50 Hz. Figure 3.9 illustrates the storage modulus behaviour as a function of frequency. The result shows that the storage modulus increases with frequency. This is true at all the tested loads and bias potentials (not shown here). The storage modulus and the logarithm of frequency are directly proportional over the range of frequencies studied.

The loss modulus also shows an increasing trend with frequency up to 1 Hz. However, it remains relatively constant over the range of 1 to 50 Hz. The real part of the complex modulus becomes increasingly dominant at high frequencies, with the response becoming more purely elastic. We have also observed this behaviour in stress-strain measurements, which show less loss (smaller loops) at faster scan rates.

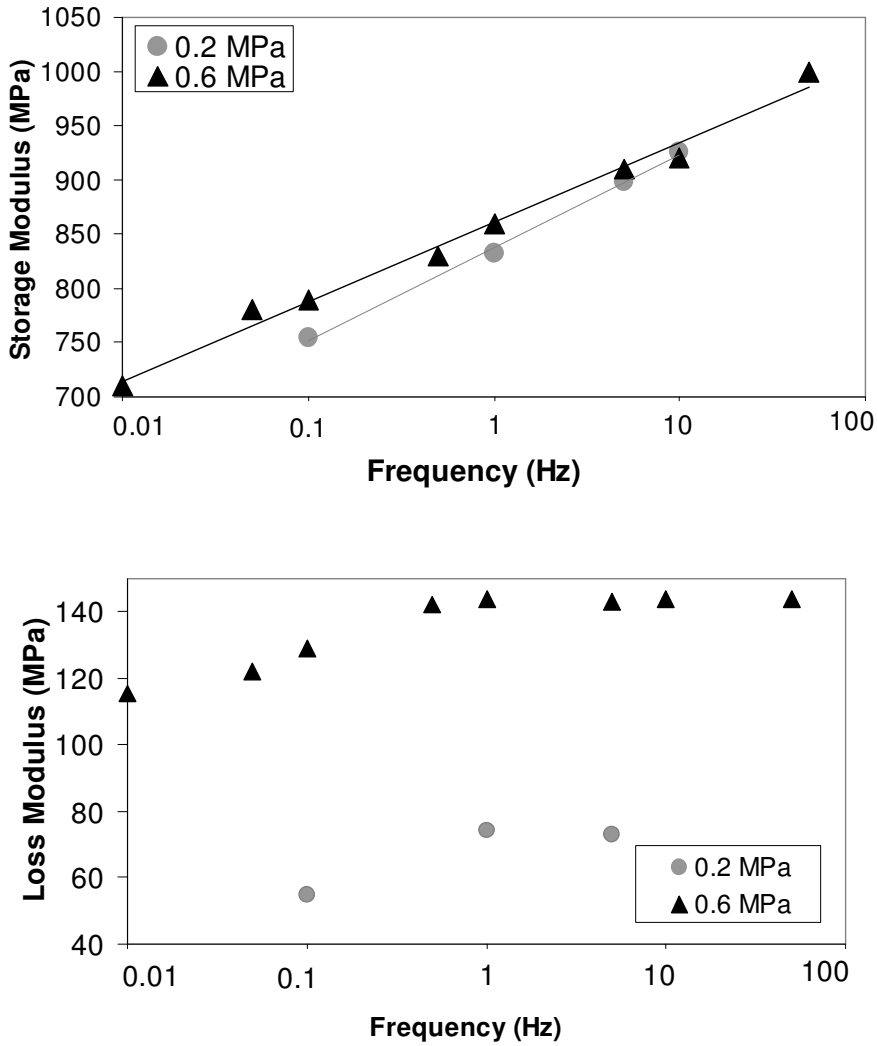

Figure 3.9: (above) Storage Modulus and (below) Loss modulus as a function of log(f) measured by applying sinusoidal loads of 0.6 MPa and 0.2 MPa on a film biased at 0.2 V, and superimposed on loads 1.35 MPa and 1.1 MPa respectively. Linear fits are also shown.

The loss modulus observed at 0.6 MPa amplitude is much higher than that observed in the 0.2 MPa amplitude experiments, as seen in Figure 3.9. The loss modulus during the "CL-sine" experiment is found to increase with each successive experiment (0.7 MPa, 1.1 MPa, 1.5 MPa and 0.7 MPa in the end) (see Figure 3.10). This may be due increased solvent uptake of the film as it spends more time (up to 24

hours between the first and the last experiments) in the electrolyte bath, making its behaviour more viscous. The observed increase in the loss modulus at 0.6 MPa (in Figure 3.9) may be due to the same effect, since this experiment was performed 24 hours later than the 0.2 MPa experiment.

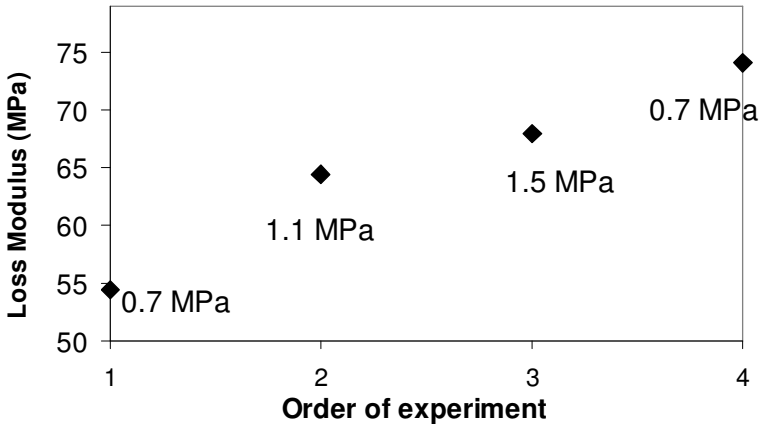

Figure 3.10: Average loss modulus in each experiment as a function of the order of performing the experiments.

3.6 Conclusion

The dependence of the complex Young's modulus of polypyrrole on load, oxidation state and frequency of the applied load is studied. The oxidation-state-dependence experiment shows that the storage modulus is lower at higher oxidation states. The loss modulus of the polypyrrole shows an increasing trend with the oxidation state suggesting that the polypyrrole film's behaviour becomes relatively more viscous at higher oxidation states, where the ion content (and in some cases its accompanying solvent content) of the polymer is higher. An increase in the loss modulus was also observed as a function of order of experiment likely due to polymer gradual soaking.

Polypyrrole modulus is also found to be load-dependent. It increases with increasing the load. The measured modulus also increases with time. This may be due to the polymer chain alignment under tension which causes a permanent change in the polymer structure.

The frequency of the applied load perturbation at each oxidation state was varied and the Young's modulus as a function of frequency was measured. According to this measurement the storage modulus of the polypyrrole increases with frequency.

The results of these experiments show a relatively complex and history-dependent behaviour in the elastic modulus of polypyrrole. The measurements presented here should enable an empirical description of the modulus over a period of several hours under the conditions applied. A precise description over the course of days will require further investigation of the history dependent response.

The results presented in this chapter provide the ground work for modelling the behaviour of polyppyrrole mechanical properties as a function of load, frequency and potential. Actuation of polypyrrole often involves variation of multiple conditions at the same time. For instance, when polypyrrole is used to bend a structure the induced load increases with application of voltage over time. In addition the polymer may face additional perturbation by the passage of the charge during actuation resulting in lower stiffness [16]. Incorporating various dependencies such as voltage, load, time, actuation and history, simultaneously into a model is extremely challenging. Providing the loads involved are not large (< 3 MPa) the changes in strain induced by the effects described here are likely to be less than 0.2 %, which is relatively small compared to the total active strain.

References

[1] T. Mirfakhrai, J. D. Madden, and R. H. Baughman, Materials Today, vol. 10 (2007) 30-8.

[2] E. Smela, Adv. Mater. 15 (2003) 481–493.

[3] R.H. Baughman, Science 300 (2003) 268–269.

[4] S. Hara, T. Zama, w. Takashima, k. Kaneto, Synthetic Metals 149 (2005)199-201.

[5] S. Hara, T. Zama, W. Takashima, K. Kaneto, Synthetic Metals 156 (2006) 351-355.

[6] T. Zama, S. Hara, W. Takashima, K. Kaneto, Bulletin of the Chemical Society of Japan 78 (2005) 506-511.

[7] T. Zama, S. Hara, W. Takashima, and K. Kaneto, Bull. Chem. Soc. Jpn77 (2004) 1425-1426.

[8] M. Cole, J.D. Madden, Materials Research Society Symposium Proceedings 889 (2006) 105-110.

[9] G.M. Spinks, L. Liu, G.G. Wallace, D.Z. Zhou, Adv. Functional Mater. (2002) 437-440.

[10] L. Bay, N. Mogensen, S. Skaarup, P. Sommer-Larsen, M. Jorgensen, K. West Macromolecules (2002) 9345-51.

[11] S. Koehler, A. Bund, I. Efimov. J of Electroanalytical Chemistry (2006) 82-86.

[12] T.F. Otero, J.J. Lopez Cascales, G.A. Vazquez, Materials Science and Engineering: C (2007) 18-22.

[13] P. Murray, G.M. Spinks, G.G. Wallace, R.P. Burford. Synthetic Metals (1998) 117-21.

[14] P. Murray, G.M. Spinks, G.G. Wallace, R.P. Burford, Synthetic Metals (1997) 847-8.

[15] R.Z. Pytel.; E.L.Thomas, I.W. Hunter, Polymer 49 (2008) 2008-2013.

[16] J.D. Madden, P.G. Madden, P.A. Anquetil, I.W. Hunter, Materials Research Society Symposium – Proceedings 698 (2002) 137-144.

[17] T. Shoa, J.D. Madden, N.R. Munce, V.X.D. Yang, Polymer international, Electromechanically Active Polymers for Bioengineering, Mechatronics and Optics, 59 (2010) 343-351.

[18] T. Shoa, J.D.W Madden, E. Fok, T. Mirfakhrai, J. Advances in Science and Technology 61 (2008) 26-33.

[19] J.D.W. Madden, P.G.A. Madden I.W. Hunter, Proc. SPIE International Society for Optical Engineering 4329 (2001) 72-83.

[20] M. Yamaura, T. Hagiwara and K. Iwata, Synth Met. 26 (1988) 209-224.

[21] S. Hara, T. Zama, W. Takashima, K. Kaneto, Polymer, 36(2004)151- 161.

[22] K. Yamato, K. Tominaga, W. Takashima, K. Kaneto, Synthetic Metals 159

(2009) 839–842.

[23] J. Tangorra, P.Anquetil, T. Fofonoff, A. Chen, M. Del Zio, I. Hunter, Bioinsp. Biomim. 2 (2007) S6–S17

[24] K. Kikuchi, S. Tsuchitani, K. Chikatani, Proc. Materials Research Society Symposium 1134 (2008) 55-60.

[25] T. Shoa, M. Cole, V. Yang and J. Madden, Proc of SPIE The International Society for Optical Engineering, Electroactive Polymer Actuators and Devices (EAPAD) 652, (2007) 652421-8.

[26] C.H. Tso, J.D.W. Madden, C.A. Michal, Synth Met 157 (2007) 460-466.

[27] M.R.Warren, J.D. Madden, Synthetic Metals 156 (2006) 724-730.

[28] M. J Ariza,.T. F. Otero, Colloids and Surfaces A: Physicochemical and Engineering Aspects 270-271(2005) 226-231.

[29] Meyers and Chawla, Mechanical Behaviors of Materials, Mechanical behavior of Materials (1999) Prentice Hall, Inc, 570-580.

[30] M.B. Samani, D.C. Cook, J.D. Madden, G. Spinks, P. Whitten, Thin Solid Films 516 (2008) 2800-2807.

[31] M.B. Samani, P.G. Whitten, G. Spinks, Materials Research Society Fall Meeting (2006) 889.

[32] L. Bay, T. Jacobsen, S. Skaarup, K. West, Journal of Physical Chemistry B (2001) 8492-7.

[33] A. Della Santa, D. De Rossi, A. Mazzoldi, Smart Materials and Structures, 6 (1997) 23-34.

CHAPTER 4: ELECTROMECHANICAL COUPLING IN POLYPYRROLE SENSORS AND ACTUATORS[3]

4.1 Introduction

As mentioned in Chapter 1, Polypyrrole is an electronically conducting polymer [1]. It is also porous, enabling small solvent molecules and ions to enter, resulting in changes in volume (actuation). Polypyrrole actuators typically operate at stresses of several megapascals, and can generate moderate strains at loads of 100 MPa [6,7]. The combination of their low voltage operation, moderate strain, high work density (reaching 100 kJ/m^3) and biocompatibility makes them of interest for use in medical devices such as catheters and stents.

These materials also act in reverse, as force and displacement sensors. This effect can have broad applications and in particular for the catheter under investigation it could serve as a position sensor. In addition polypyrrole acting as a sensor and actuator might be useful to detect a sudden increase in the load applied to the polymer, which likely implies that the catheter has struck the arterial wall.

In this Chapter the properties of polypyrrole sensors are investigated, enabling the first quantitative demonstration of the link between actuation and sensing, and

[3] "A version of this chapter has been accepted for publication. Shoa, T., Madden, J. Mirfakhrai,T., Allici, G., Spinks, G., Wallace, G. (2010) Electromechanical coupling in polypyrrole sensors and actuators. Sensors and Actuators A. "

suggesting a new mechanism of electromechanical coupling that can be exploited in materials that are both ionically and electronically conducting.

We have chosen to use polypyrrole grown at low current density and temperature, and actuated in an aqueous solution of sodium hexafluorophosphate because of the relatively large strains achieved (6 %) combined with good electrochemical stability [8,9].

The use of polyporrole as an electrochemically-based strain sensor was first investigated by Takashima and Kaneto [10]. A related effect may have been observed by Otero [11], though the change in voltage with load [12] could well have been due to changes in cell geometry in these cases. Interest in the sensing mechanism and its application has revived recently [13,14], and their use in trilayers has been studied [15,16]. The sensors are potentially useful in instrumentation because they enable force and displacement to be measured at relatively large strains (ten times larger than those typical of piezoelectrics) and with relatively little mechanical impedance (elastic moduli are typically < 1 GPa). The deformation of these polymer sensors results in the passing of substantial charge, which can readily be converted to a voltage signal if more convenient, via an integrator [16]. In this chapter we demonstrate that the sensor response is stable from DC to 100 Hz at least, suggesting that bandwidth can be significant.

Despite the investigations of polypyrrole sensors and actuators, a quantitative relationship between actuation and sensing has not been established. In this chapter we propose a model of the electromechanical coupling, which is based on new measurements of polypyrrole sensors. Before reporting the measurements and

models, some findings from previous work that underlie this new model are presented.

4.2 Background on actuation and sensing

The electrical to mechanical energy conversion in conducting polymer actuators has been extensively investigated. It is generally found that, to a first order approximation, the strain, ε, is proportional to the density of charge transferred, ρ, via the empirical strain to charge ratio, α [17,18]. The strain is positive (lengthening) when ions are inserted [5], with the strain to charge ratio representing the relative change in length per inserted ion. The insertion of an ion leads in general to an expansion in all directions [19,20], with the change in the polymer volume per charge being very similar in magnitude to the volume of ions and their solvation spheres [21,22], suggesting that actuation may at least in part due to deformation of the polymer resulting from the physical insertion of ions and accompanying solvent. The spacing between polymer chains after electrodeposition is found to be proportional to ion size [23], supporting this theory of actuation. However, there is as yet no direct evidence establishing a link between ion size and strain [21,24,25]. A number of other mechanisms may also be involved, including electrostatic interactions between chains, osmotic effects and conformational changes along the polymer backbone that are induced by changes in oxidation state [24]. Whatever the mechanism, the insertion of the ions into the polymer presumably requires some expenditure of energy to deform the polymer matrix. The source of energy for insertion of ions is the

electrical power supply used to drive actuation. It has been suggested that applied stress will influence the ion insertion energy [15,22].

Previous work focuses on two possible mechanisms of sensing. The first suggests that each charge and accompanying solvation sphere occupies a fixed volume [22]. The other suggests that Donnan potential changes are responsible [13,15]. Donnan potential changes result from changes in ion concentration. When the polymer is mechanically stressed, the volume changes, leading to a change in internal ion concentration. As a result the difference between the ion concentration in the polymer and that of the electrolyte is changed, leading to a change in voltage at the interface between the two regions.

We have proposed that tensile stress, which expands the polymer, reduces the force required for ions and accompanying solvent to be inserted into the polymer network, and thus less voltage is needed to pull ions in [15]. For example, when positive ions are present, the expanded network favours the presence of more ions (and solvent), and hence a voltage increase is expected. The quantitative predictions of this model are now shown to be consistent with experimental observations, suggesting that elastic insertion forces are important in explaining the sensor response. The model does not describe the origin of the internal forces that lead to expansion of the polymer as ions are inserted. These mechanisms are described via the empirically derived strain to charge ratio.

4.3 Experiment

In order to examine the performance of polypyrrole sensors, measurements are made on a standalone film immersed in electrolyte, similar to an approach used by Takashima and Kaneto [10,13], and as depicted in Figure 4.1. This approach is chosen because the stresses and strains are then uniform throughout the sample. Also there is no metal layer in contact with the electrolyte, which should reduce any parasitic electrolyte reactions. Voltage is measured between the film and a counter electrode at open circuit, enabling the voltage generated in response to applied stress to be determined. Measurements of current generated in response to stress are also made, with the film held at constant voltage. The results of these measurements are then compared to the inverse process – namely conversion of electrical energy into mechanical work by charging the film electrochemically – and a model is proposed to explain the response.

Three tests were done in order to characterize polypyrrole films as sensors. In the first, time domain measurements were made, relating open circuit voltage to applied stress. The second and third tests investigate the frequency response. In one test, the open circuit voltage is measured in response to a swept frequency stress input, and in the other the transfer function between short circuit current and stress is determined.

4.3.1 Film synthesis

Polypyrrole is polymerized by electrochemical oxidation of the pyrrole monomer as described in Chapter 1 (section 1.5). Polypyrrole is deposited

galvanostatically on glassy carbon at a current density of 1.25 A/m^2 over a period of 8 hours. The resulting films are in a highly doped state of approximately one PF_6^- ion per three monomers [2,25,26].

4.3.2 Sensor characterization

In order to measure the sensor response of polypyrrole, a film was actuated inside an aqueous solution of 1 M sodium hexafluorophosphate and the generated voltage was measured at open circuit. The polypyrrole films used in these experiments were 10 µm thick, 10 mm long and 4 mm wide. As depicted in Figure 4.1 the polypyrrole film is clamped into a motor (Dual Mode Lever System, Aurora Scientific, 300B) and the electrochemical cell is electrically connected to a Solartron 1287 potentiostat via gold wires (that are not in contact with the solution).

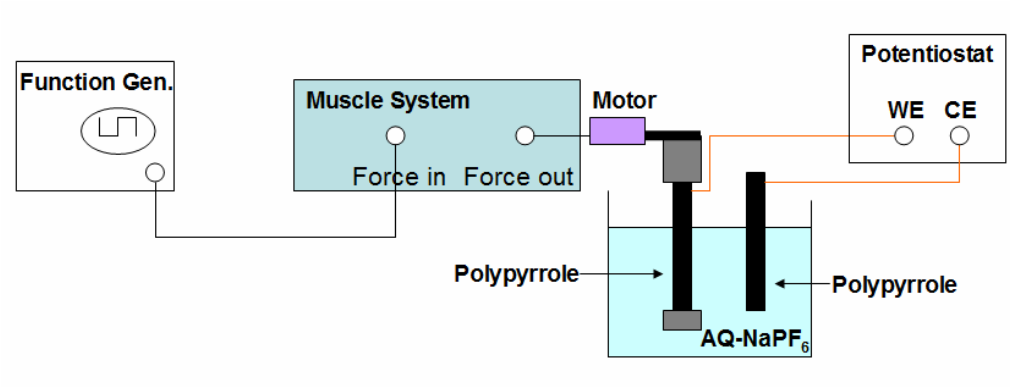

Figure 4.1: Experimental set up of time domain sensor measurement.

In the time domain experiments, the function generator applies a square wave force control signal to the lever system, which generates force and mechanical movement through a galvanometer and lever arm. The resulting strain is recorded

using a data acquisition card, as is the generated voltage. The voltage is measured against an identical but unstressed polypyrrole film that acts as the counter electrode.

The polypyrrole film was also actuated in order to determine the strain to charge ratio of the polypyrrole film. Measurements of strain to charge were obtained by repeatedly stepping the applied current between +4 and -4 mA and determining ratio of the induced strain and the charge transferred per unit volume.

Frequency response experiments were performed at open and short circuit, with voltage or current, respectively, being measured in response to the applied stress. A Solartron 1260A impedance/gain phase analyzer provided the force control input. The input signal was a 0.25 MPa amplitude sinusoid superimposed on a 0.38 MPa constant stress. Frequency was swept from 0.1 Hz to 100 Hz. Measured force and either current or voltage signals were provided as inputs to the gain/phase analyzer, which computed the current to force and the voltage to force transfer functions. In the short circuit case a Keithley 427 Current amplifier was used to convert the current to a voltage at a gain of 10,000 V/A before the signal was input to the gain/phase analyzer. An electrical impedance measurement (transfer function between voltage and current) was also made on the electrochemical cell using the impedance analyzer, thereby determining the 'internal resistance' of the sensor.

4.4 Results

Figure 4.2 shows the stress applied to a polypyrrole sensor and the generated open circuit potential. A strain of about 0.22% was induced in the polypyrrole film by applying a stress amplitude of 0.45 MPa peak to peak in the form of a square wave

superimposed on a constant stress of 1.15 MPa. A voltage signal with an amplitude of approximately 20 μV was generated in response to the induced stress. Change in stress and change in voltage are opposite in sign, as is consistent with previous reports of actuation in aqueous solution where the anions are mobile [15]. The sign of the response is also consistent with both proposed sensor mechanisms. The measured voltage to stress ratio is $4.5 \pm 1.0 \times 10^{-11}$ V/Pa (or equivalently m^3/C). The voltage to stress amplitude matches the measured strain to charge ratio of $3.6 \pm 0.8 \times 10^{-11}$ m^3/C within experimental uncertainty. The correspondence is used to justify the model proposed later in this work.

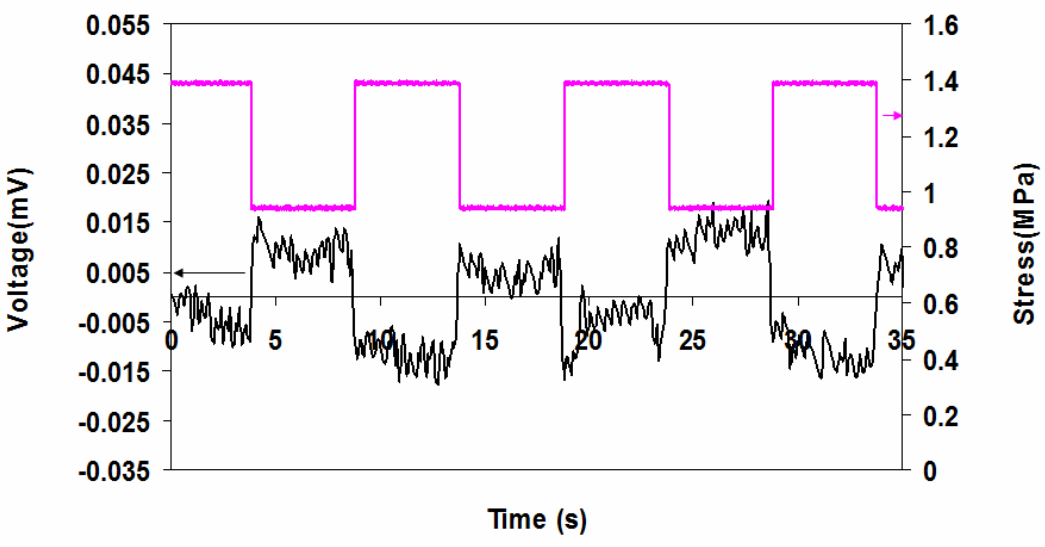

Figure 4.2: Stress and the resulting open circuit potential.

Previous time and frequency domain measurements from trilayer sensors show decays in the sensor voltage response at low frequencies and long times [16], whereas the steps shown in Figure 4.2 do not decay significantly over the 5 s during which they are observed. Previous measurements were done in bending trilayers in which

the electrolyte is in contact with thin platinum layers. The discharge of the sensor voltage in the trilayer studies could be the result of parasitic reactions on the platinum, and the non-uniform stress induced in the polypyrrole – both factors not present in the current experimental approach.

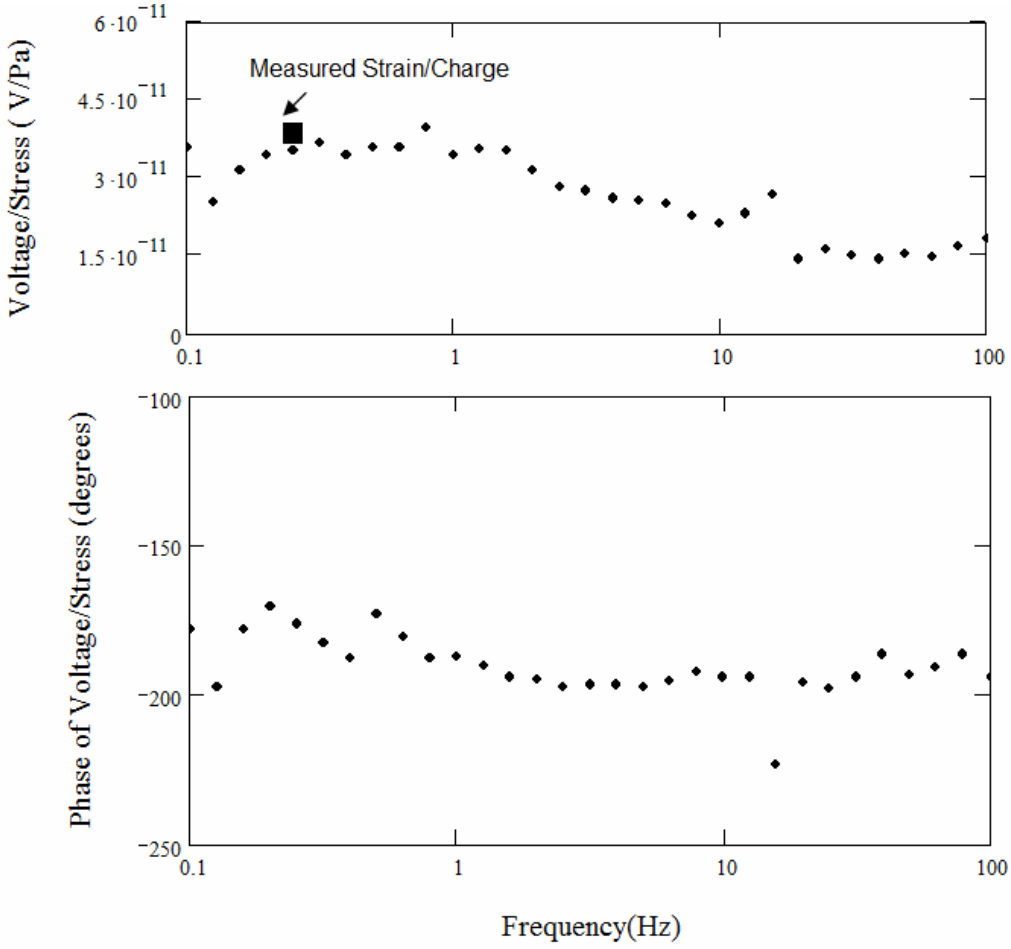

Figure 4.3: Measured voltage to stress ratio gain (top) and phase (bottom), and the measured strain to charge ratio (square).

Figure 4.3 shows the measured voltage to stress ratio as a function of frequency. The measured strain to charge ratio is inserted for comparison (as depicted

by a bold square at the effective frequency at which it was measured). As expected the phase of the voltage to stress ratio is approximately -180°, matching the polarity response observed in the step response of Figure 4.2. Uncertainties associated with the measurement of the film geometry, charge and generated voltage are +/- 20% (every data point may be equally shifted up or down by this amount). The strain to charge ratio and the voltage to stress ratio match within experimental uncertainty.

The origin of the variation in the voltage to stress ratio with frequency is unclear. It has previously been observed that the strain to charge ratio does exhibit some time dependence [27], rising at higher frequencies and shorter times. Figure 4.3 shows that in contrast the generated voltage per unit stress drops somewhat at higher frequencies. The drop may be the result of electrical and mechanical losses which are greatest at high frequencies, where currents and strain rates are highest.

The electrical impedance, *Z*, of the sensor, including the counter electrode, is presented in Figure 4.4. At high frequencies the cell response tends towards a resistive behaviour, and at low frequencies acts as a leaky capacitor, as is common in polypyrrole as grown at low temperatures [22]. The impedance will be used to relate the open circuit measurements (Figure 4.3) to the short circuit response (Figure 4.5).

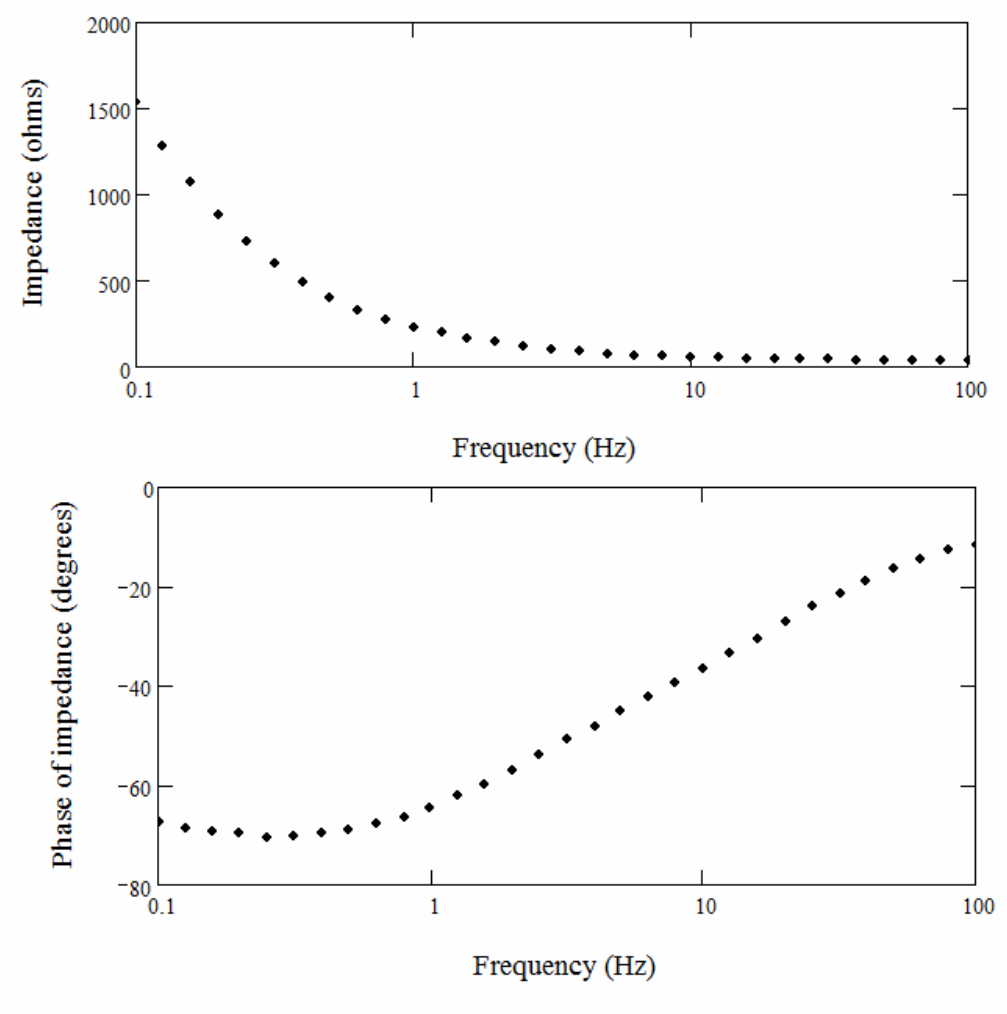

Figure 4.4: Measured impedance of the sensor as a function of frequency, amplitude (top) and phase (bottom).

The current to stress ratio and the corresponding phase are shown in Figure 4.5. Also plotted is the estimated current to stress transfer function, calculated by dividing the measured voltage to stress ratio, presented in Figure 4.3, by the measured cell impedance, shown in Figure 4.4, at each frequency. The measured and estimated data are in close agreement, suggesting that the current generated is simply determined by the sensor voltage observed at open circuit divided by the sensor internal impedance. An equivalent circuit for this response is shown in Figure 4.7.

The magnitude of the sensor voltage is predicted to be $-\sigma \cdot \alpha$, as explained in section 4.5.

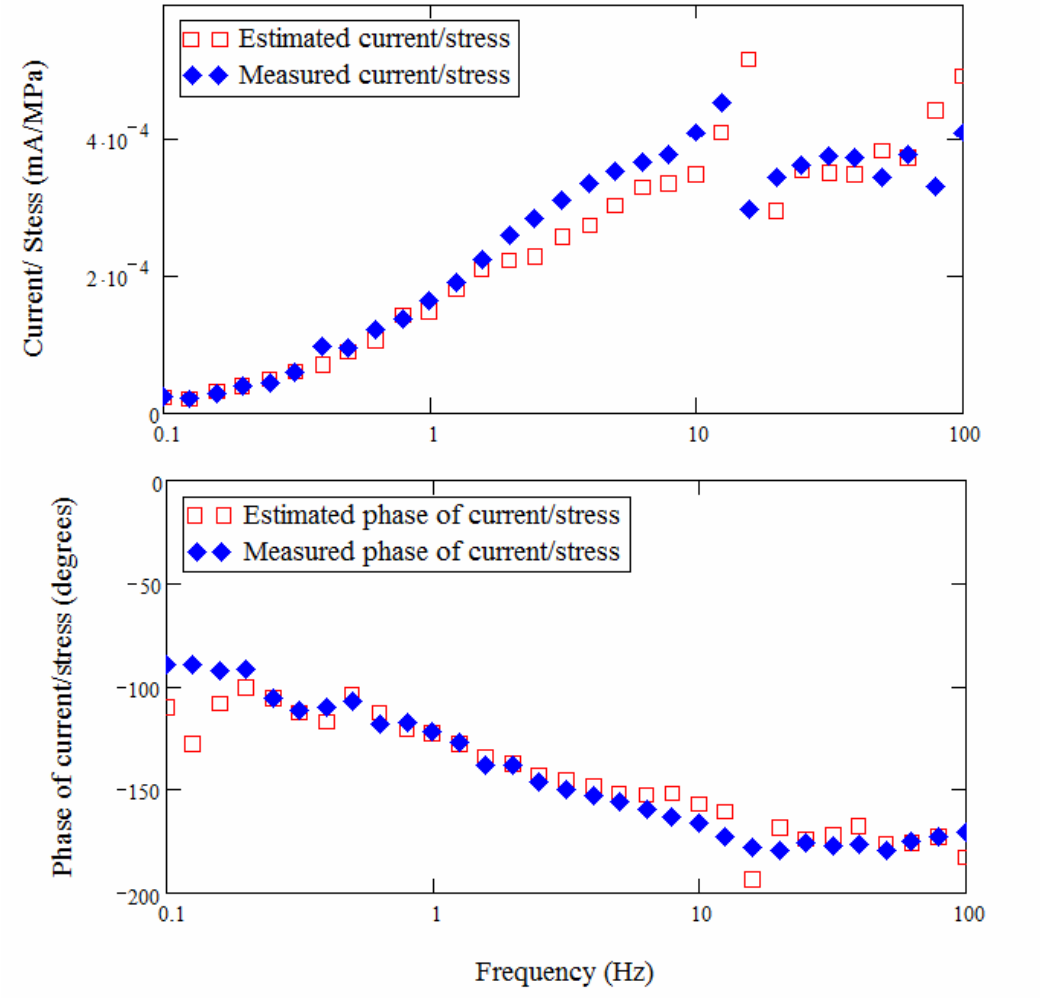

Figure 4.5: Measured current to stress transfer function and the estimated response.

Figure 4.6 shows the relationship between applied stress and sensor output. This result confirms earlier work by Takashima and his colleagues, who show that the current generated in a polypyrrole sensor is proportional to the applied stress [13]. Wu *et al.* also show a linear relationship between input displacement and voltage output [15].

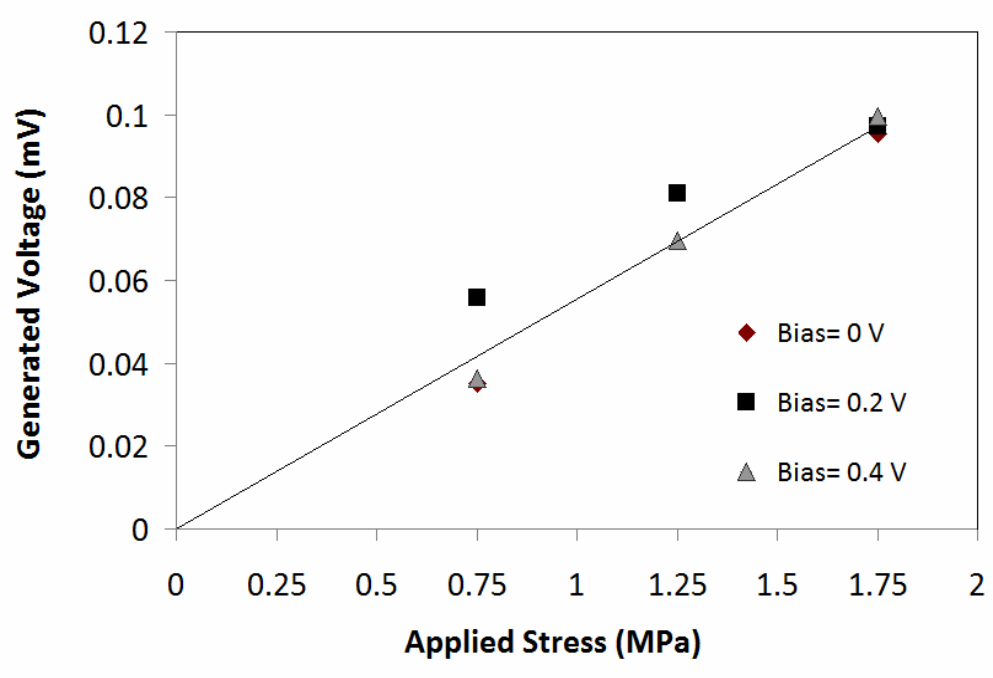

Figure 4.6: The voltage generated in response to load at three polymer biases. The straight line shown is a fit to the data through the origin.

Figure 4.7 graphically summarizes many of the findings presented thus far for polypyrrole sensors, namely that (1) the voltage is proportional to stress, (2) that the constant of proportionality is equal to the strain to charge ratio, within experimental uncertainly, and (3) that sensor's internal 'resistance' is given by the measured electrochemical impedance, *Z*.

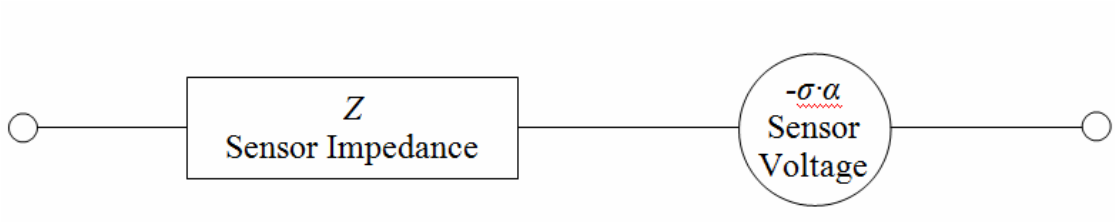

Figure 4.7: Electrical equivalent circuit of the linear polypyrrole sensor, showing the generated voltage, $-\sigma \cdot \alpha$, and the electrode impedance, *Z*. The impedance includes contributions from the solution, contacts and transport of ion and electrons within the polymer.

4.5 Modelling the electromechanical coupling

A model is now proposed that describes the electromechanical response of the polypyrrole sensor/actuators at steady state. The model is depicted in Figure 4.8, with the mechanical portion on the left and the electrical portion on the right.

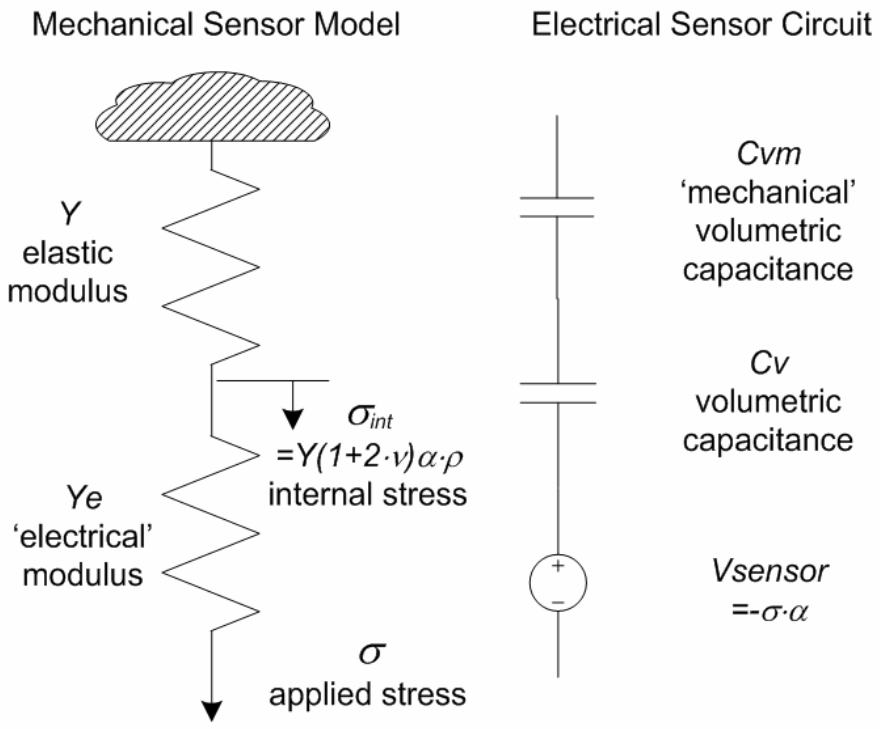

Figure 4.8: Steady state sensor and actuator model including the coupled mechanical (left) and electrical (right) components. Insertion of a volumetric charge, ρ, induces strain, $\alpha \cdot \rho$, and an internal stress, σ_{int}. Application of a tensile stress, σ, acts on the stored charge, producing a sensor voltage, V_{sensor}.

In brief, Y represents the elastic modulus of the polymer, and C_V is the capacitance per unit volume. C_{Vm} is the capacitance resulting from the elastic energy stored during charging, and is very large, reflecting the relatively small elastic energy per unit charge compared to the electrostatic energy per charge. When an external stress, σ, is applied to the material, it is assumed to lead to strain in two ways: (1) by

acting on the polymer chains, against modulus Y, and (2) by squeezing out (compressive stress) or by expanding and assisting the ingress, of ions, producing an strain $\alpha \cdot \rho$. The 'electrical' modulus, Y_e, represents the electrostatic forces needed to move the charge, and is very high as charge imbalance results. The insertion of charge creates an internal stress as the charge expands the material, and this stress is represented by σ_{int}. The C_{Vm} and Y_e components turn out to be very large in value. They are critical to describing the electromechanical coupling. The voltage, $-\sigma \cdot \alpha$, depicted in Figure 4.8 is the sensor voltage.

The model components are now described more fully. As mentioned above, an empirical relationship between charge induced strain, ε_{active} and charge density, ρ, describes actuation reasonably well, even at very high loads [27]:

$$\varepsilon_{active} = \alpha \cdot \rho \,. \tag{4.1}$$

The strain per unit charge, described by the charge ratio, may be due to some combination of electrostatic interactions, physical size of the atoms, and osmotic or Donnan effects. Whatever the precise nature of the interactions, there are balancing forces that bring the polymer back to its original shape following a charging cycle. We postulate that the balancing forces are the result of the materials elastic nature, and thus are the same as those encountered when an external load is applied. In other words the internal stress needed to deform the polymer by charge insertion is given by the product of the elastic modulus, Y, and the charge induced strain. Typically the insertion of ions leads to a deformation in three dimensions [19,20], and thus the stress is modified by Poisson's ratio, v. In an isotropic polymer the charge induced internal stress is then:

$$\sigma_{\text{int}} = Y \cdot (1+2\cdot\nu)\cdot \varepsilon_{active} = Y \cdot (1+2\cdot\nu)\cdot\alpha\cdot\rho\,. \qquad (4.2)$$

The internal stress works against the elastic modulus, *Y*, to expand the polymer. (Alternative expressions can be derived for anisotropic materials such as those that are stretch aligned.) The resulting electrical to mechanical work density in charging the isotropic material is then:

$$\int \sigma_{\text{int}\,ernal}\cdot\alpha\cdot d\rho = \frac{3}{2}\cdot Y\cdot(1+2\cdot\nu)\cdot\alpha^2\cdot\rho^2 = \frac{1}{2}\cdot\frac{\rho^2}{C_{Vm}}, \qquad (4.3)$$

with the factor of three arising from the fact that work is done in three dimensions. The input electrical energy is stored as elastic energy, and can be recovered on discharge, with the effective 'mechanical' capacitance equaling:

$$C_{Vm} = \frac{1}{3\cdot Y\cdot(1+2\cdot\nu)\cdot\alpha^2}\,. \qquad (4.4)$$

The smaller the value of the capacitance, the greater is its influence on the circuit. The mechanical capacitance is small in magnitude when the modulus is high and the strain to charge is large – a situation in which a large amount of elastic energy is stored per charge.

In Figure 4.8, C_{Vm} appears in series with the 'electrostatic' portion of the volumetric capacitance, C_V, as both receive the same charge density, ρ. The capacitive model of charging represented by C_V is based on measurements that show this model provides a good low frequency description of the electrochemical charging of hexafluorophosphate-doped polypyrrole over a wide range of potentials [2,25]. Together the two capacitances shown on the right hand side of Figure 4.8 form an effective capacitance, C_{Veff}:

$$\frac{1}{C_{Veff}} = 3 \cdot Y \cdot \alpha^2 \cdot (1 + 2 \cdot \nu) + \frac{1}{C_V}. \qquad (4.5)$$

Next the origin of the electrical modulus, Y_e, is described. Given that the insertion of ions increases volume, it might be expected that the application of external pressure or compressive stress would lead to an expulsion of ions. Likewise, a tensile stress (which increases polymer volume) might reduce the work needed to insert charge. The applied stress needed to expel charge is given by the derivative of electrical energy density with respect to active strain:

$$\sigma = \frac{d}{d\varepsilon_{active}} \frac{1}{2} \cdot \frac{\rho^2}{C_{Veff}} = \frac{d}{d\varepsilon_{active}} \frac{1}{2} \frac{\varepsilon_{active}^2}{\alpha^2 \cdot C_{Veff}} = \frac{\varepsilon_{active}}{\alpha^2 \cdot C_{Veff}} = \varepsilon_{active} \cdot Y_e. \qquad (4.6)$$

The 'electrical' modulus, Y_e, relating charge induced strain to applied stress, is then:

$$Y_e = \frac{1}{\alpha^2 \cdot C_{Veff}}. \qquad (4.7)$$

The larger the capacitance and strain per charge, the easier it is to add or remove charge by applying force. The overall effective modulus, as seen by an external load, σ, is:

$$\frac{1}{Y_{eff}} = \alpha^2 \cdot C_{Veff} + \frac{1}{Y}. \qquad (4.8)$$

How much charge is expelled when a force is applied to the sensor? For a given applied stress and at constant voltage, the amount of charge per unit volume, ρ_s, that is transferred is $\varepsilon_{active}/\alpha$, or, using Equation 4.6 with $\varepsilon_{acive} = \alpha \cdot \rho_s$ inserted into the second term from the right:

$$\rho_s = -\sigma \cdot \alpha \cdot C_{Veff} . \qquad (4.9)$$

The charge transfer expressed in Equation 4.9 is the predicted sensor charge output at constant voltage. It is the charge transfer that would be expected if a voltage of $-\sigma \cdot \alpha$ were generated, as depicted in Figure 4.8. A voltage of

$$V_{sensor} = -\sigma \cdot \alpha, \qquad (4.10)$$

is predicted at open circuit, matching observed response.

The model shown in Figure 4.8 predicts the measured first order steady state actuation and sensor responses as expected: In response to an applied stress, σ, a voltage, $-\sigma \cdot \alpha$, is produced at open circuit, and a volumetric charge transfer of $-\sigma \cdot \alpha \cdot C_{Veff}$ at constant voltage; The insertion of charge density, ρ, produces a strain of $\alpha \cdot \rho$. The magnitudes of Y_e and C_{Vm} are predicted to be so large that their influence on the mechanical and electrical properties, respectively, is negligible in current materials, as is shown in the paragraph that follows. However, the existence of these coupling elements is critical to describing sensing and actuation.

One element that is missing from the model is the leakage current observed as the polymer drifts back to its equilibrium voltage. This leakage can be represented by a voltage dependent resistor that drains across the capacitors.

What are the magnitudes of Y_e and C_{Vm}? The elastic modulus of polypyrrole is typically between 0.2 and 0.8 GPa [22,28], and α is measured to be between 10^{-11} to 10^{-10} m^3/C [22]. The mechanical capacitance, C_{Vm}, is then predicted to be between $5 \cdot 10^{11}$ and $1 \cdot 10^{13}$ F/m^3. This capacitance is much larger than the measured volumetric capacitance of about 10^8 F/m^3 [3,22]. The relative size of the mechanical capacitance makes it difficult to detect, since the change in voltage induced by its

charging will be small. It is thus possible to neglect on most occasions. Similarly the electrical modulus, Y_e, is predicted to be at least 100 GPa, much larger than the measured elastic modulus.

4.5.1 Electromechanical coupling and generation

Are the sensors useful as generators, and in general what are the implications of the model shown in Figure 4.8 for the operation of polypyrrole and related sensors and actuators? The immediate answer is that electro-mechanical and mechano-electrical coupling in present materials is poor. The model identifies the critical material properties needed to improve coupling.

The electromechanical coupling is the ratio of mechanical energy produced to the input electrical energy. This factor is relevant to actuation – the higher it is, the more electrical energy is converted to work – and vice-versa. The strength of coupling depends on the loading conditions. In the unloaded condition (σ = 0) and without dissipation, the electrical energy transferred to mechanical stored elastic energy in the polymer, $k^2_{internal}$, is:

$$k^2_{\text{int}\,ernal} = \frac{\frac{3}{2}\cdot Y\cdot(1+2\cdot\nu)\cdot\alpha^2\cdot\rho^2}{\frac{\rho^2}{2\cdot C_{Veff}}} = \frac{C_V}{C_{Vm}+C_V} = \frac{1}{1/3\cdot Y\cdot(1+2\cdot\nu)\cdot\alpha^2\cdot C_V + 1}. \quad (4.11)$$

Equation 4.11 is simply the ratio of the mechanical work done by the ions to expand the polymer matrix, to the electrical work performed during charging. Inserting typical values for modulus, strain to charge and volumetric capacitance, the magnitude of the coupling is less than 1 % at present. Although the coupling is poor,

the actuation efficiency can in principle be reasonable if a large fraction of the stored electrical energy can be recovered. The model suggests that to optimize electrical to mechanical coupling the mechanical contribution to the capacitance, C_{Vm}, should be similar to or, preferably, smaller than the purely electrostatic component. Increased coupling might be achieved by employing a very stiff polymer (perhaps highly cross-linked), thereby increasing modulus. Alternatively, increasing the strain produced per ion will maximize coupling.

Generation occurs when a mechanical load is applied that results in a change in voltage and in the output of current. The change in voltage upon application of a load is given by Equation 4.9. The mechanical work done by a load applied in one dimension is $\frac{1}{2}\sigma^2 \cdot Y_{eff}^{-1}$. If we assume that the polymer, once stretched (for example while in the circuit shown in Figure 4.9, with the switch open), and then is discharged across a load until it reaches its original voltage (switch is now closed), and that the lost charge is subsequently replaced at the low voltage (with the switch open), then the fraction of input work converted to electrical potential energy in one cycle is given by:

$$k^2 = \frac{\frac{1}{2} \cdot C_{Veff} \cdot \sigma^2 \cdot \alpha^2}{\frac{1}{2} \cdot \sigma^2 \cdot Y^{-1}} = C_{Veff} \cdot Y \cdot \alpha^2 . \qquad (4.12)$$

Inserting the expression for C_{Veff} from Equation 4.5 it can be seen that the coupling cannot exceed 1. The inclusion of the mechanical contribution to the capacitance ensures the conservation of energy. The magnitude of the coupling is small in polypyrrole. Although electromechanical coupling in polypyrrole is not high, its high compliance and large strain, very high charge density and low voltage

operation relative to piezoelectrics make it suitable for sensing and actuation applications where such properties are needed.

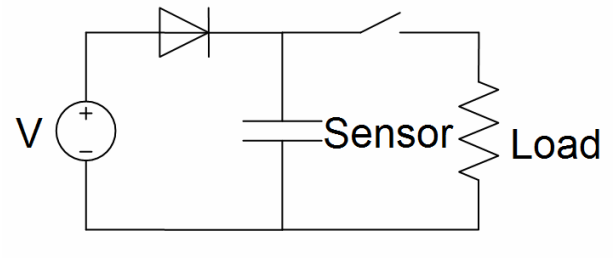

Figure 4.9: A generator configuration. The polymer sensor is represented by the capacitor, which is charged to a voltage, V. A change in load is applied to the sensor/generator such that its voltage increases. The switch is then closed, with the voltage and current discharging across the load resistor. When the voltage drops back to the low voltage value, V, the switch is opened again and the capacitor recharges as the original load is re-applied.

Is it possible to conceive of a material that can be used to actuate and sense by a similar mechanism but where the coupling is high? There are several approaches. One is to increase the modulus, as mentioned. The challenge is to achieve this without reducing the strain to charge ratio. Stretch alignment can increase modulus substantially along the stretch axis, but at the expense of strain to charge in that direction, since expansion occurs perpendicular to the chain orientation [20]. Cross-linking may increase modulus. Increasing the strain to charge ratio, perhaps by using larger ions, should have a dramatic effect since the coupling is a function of the α^2, but the polymer will need to be more porous in order to allow the insertion of substantially larger ions, as in polypyrrole large ions do not enter, or are slow to do so [5,24]. Careful material design with Equation 4.12 in mind may well lead to substantial improvements in low voltage, soft actuators and sensors.

4.6 Conclusion

The voltage generated by loading a free-standing polypyrrole actuator is described by the product of the stress and the strain to charge ratio. The charge per unit volume generated is simply this voltage multiplied by the volumetric capacitance. A model is presented that relates sensor output to the effect of polymer deformation on charge insertion. The model is an important step towards the complete description of polypyrrole response in actuators and sensors.

References

[1] T. A. Skotheim, R. L. Elsenbaumer, and J. R. Reynolds, Handbook of Conducting Polymers. New York: Marcel Dekker, 1998.

[2] C.-H. Tso, J. D. Madden, and C. A. Michal, "An NMR study of PF6- ions in polypyrrole," Synthetic Metals, vol. 157, pp. 460-466, 2007.

[3] J. D. Madden, P. G. Madden, and I. W. Hunter, "Conducting polymer actuators as engineering materials," presented at Proceedings of SPIE, Bellingham, WA, 2002.

[4] J. D. Madden, R. A. Cush, T. S. Kanigan, and I. W. Hunter, "Fast contracting polypyrrole actuators," Synthetic Metals, vol. 113, pp. 185-193, 2000.

[5] Q. Pei and O. Inganas, "Electrochemical applications of the beam bending method; a novel way to study ion transport in electroactive polymers," Solid State Ionics, vol. 60, pp. 161-166, 1993.

[6] J. D. W. Madden, N. A. Vandesteeg, P. A. Anquetil, P. G. A. Madden, A. Takshi, R. Z. Pytel, S. R. Lafontaine, P. A. Wieringa, and I. W. Hunter, "Artificial muscle technology: physical principles and naval prospects," Oceanic Engineering, IEEE Journal of, vol. 29, pp. 706-728, 2004.

[7] S. Hara, T. Zama, W. Takashima, and K. Kaneto, "Gel-Like Polypyrrole Based Artificial Muscles With Extremely Large Strain," Polymer Journal, vol. 36, pp. 933-936, 2004.

[8] T. Shoa, M. Cole, N. R. Munce, V. Yang, and J. D. Madden, "Polypyrrole operating voltage limits in aqueous sodium hexafluorophosphate," presented at Electroactive Polymer Actuators and Devices (EAPAD) 2007, San Diego, California, USA, 2007.

[9] M. Cole and J. D. Madden, "The effect of temperature on polypyrrole actuation," presented at Materials Research Society Fall Meeting, Boston, MA, 2005.

[10] W. Takashima, T. Uesugi, M. Fukui, M. Kaneko, and K. Kaneto, "Mechanochemoelectrical effect of polyaniline film," SYNTHETIC METALS, vol. 85, pp. 1395-1396, 1997.

[11] T. F. Otero and H. S. Nalwa, in Artificial Muscles, electrodissolutoin and redox processes in conducting polymers. Chichester: John Wiley & Sons, 1997, pp. 517-594.

[12] T. F. Otero and M. Broschart, "Polypyrrole artificial muscles: a new rhombic element. Construction and electromechanical characterization," Journal of Applied Electrochemistry, vol. 36, pp. 205-214, 2006.

[13] W. Takashima, K. Hayashi, and K. Kaneto, "Force detection with Donnan equilibrium in polypyrrole film," Electrochemistry Communications, vol. 9, pp. 2056-2061, 2007.

[14] T. F. Otero and M. T. Cortes, "Characterization of triple layers," presented at Electroactive Polymers and Devices, San Diego, 2001.

[15] Y. Wu, G. Alici, J. D. W. Madden, G. M. Spinks, and G. G. Wallace, "Soft mechanical sensors through reverse actuation in polypyrrole," Advanced Functional Materials, vol. 17, pp. 3216-3222, 2007.

[16] M. Bennett and D. Leo, "Ionic liquids as stable solvents for ionic polymer transducers," SENSORS AND ACTUATORS A-PHYSICAL, vol. 115, pp. 79-90, 2004.

[17] A. Mazzoldi, A. Della Santa, and D. De Rossi, "Conducting polymer actuators: Properties and modelling," in Polymer Sensors and Actuators, Y. Osada and D. E. De Rossi, Eds. Heidelberg: Springer Verlag, 1999.

[18] R. H. Baughman, "Conducting polymer artificial muscles," Synthetic Metals, vol. 78, pp. 339-353, 1996.

[19] T. E. Herod and J. B. Schlenoff, "Doping induced strain in polyaniline: stretchoelectrochemistry," Chemistry of Materials, vol. 5, pp. 951-955, 1993.

[20] R. Z. Pytel, E. H. Thomas, and I. W. Hunter, "Anisotropy of electractive strain in highly stretched polypyrrole actuators," Chemistry of Materials, vol. 18, pp. 861-863, 2006.

[21] K. Kaneto, M. Kaneko, and W. Takashima, "Response of chemomechanical deformation in polyaniline film on variety of anions," Japanese Journal of Applied Physics, vol. 34, Part 2, pp. L837-L840, 1995.

[22] J. D. Madden, in Conducting Polymer Actuators. Cambridge, MA: Massachusetts Institute of Technology, 2000.

[23] M. Yamaura, T. Hagiwara, and K. Iwata, "Enhancement of electrical conductivity of polypyrrole film by stretching: counter ion effect," Synthetic Metals, vol. 26, pp. 209-224, 1988.

[24] M. Kaneko, M. Fukui, W. Takashima, and K. Kaneto, "Electrolyte and strain dependences of chemomechanical deformation of polyaniline film," Synthetic Metals, vol. 84, pp. 795-796, 1997.

[25] M. R. Warren and J. D. Madden, "A structural and electrochemical study of polypyrrole as a function of oxidation state," Syntehtic Metals, vol. 156, pp. 724-730, 2006.

[26] M. Yamaura, K. Sato, and T. Hagiwara, "Effect of counter-anion exchange on electrical conductivity of polypyrrole films," Synthetic Metals, vol. 39, pp. 43-60, 1990.

[27] J. D. Madden, P. G. Madden, P. A. Anquetil, and I. W. Hunter, "Load and time dependence of displacement in a conducting polymer actuator," Materials Research Society Proceedings, vol. 698, pp. 137-144, 2002.

[28] G. M. Spinks and V. T. Truong, "Work-Per-Cycle Analysis for Electromechanical Actuators," Sensors and Actuators a-Physical, vol. 119, pp. 455-461, 2005.

CHAPTER 5: A DYNAMIC ELECTROMECHANICAL MODEL FOR ELECTROCHEMICALLY DRIVEN CONDUCTING POLYMER ACTUATORS [4]

5.1 Introduction

Conducting polymer actuators are a class of electrochemically driven "artificial muscle" actuators whose application is being explored in a number of devices including deformable catheters, Braille cells and wet microelectromechanical systems [1-9]. As described in previous chapters, these polymers are electronically conductive, with conductivities typically in the range of 10^3 – 10^4 S/m [10]. Conducting polymers are also ion conductors, enabling ion transport between polymer chains. Application of a voltage to the polymer in an electrolyte alters the charging of the polymer through oxidation or reduction processes. The electronic charging occurs throughout the volume of the polymer, and is balanced by the insertion or removal of ions that are taken from (or given to) the electrolyte, depending on the polarity of the mobile ions inside the electrolyte. This charging process is associated with changes in volume, where increase in volume generally occurs when ions are inserted into the polymer matrix. Actuator characteristics

[5] "A version of this chapter has been accepted for publication. Shoa, T.,Yoo, D., Madden, J. A. (2010) Dynamic electromechanical model for electrochemically driven conducting polymer actuators. IEEE Transactions in Mechatronics."

include low actuation voltage (<2 V), ease of fabrication, relatively high strain (2% or greater) [11], and biocompatibility [12,13].

A key challenge for the designers of conducting polymer driven devices is the prediction of the actuation response. This is particularly challenging for applications where the rate of response is critical. For instance, we are interested in conducting polymer driven catheters for rapidly scanning an optical fiber inside a blood vessel in order to perform imaging [14,15]. In this case, actuation response at short times governs the device performance. A dynamic model is needed in order to predict the time dependent actuation response. The modelling of conducting polymer driven actuation has been previously reported [16-20], however these models were focused on static operating conditions. Y Fang *et al.* predicted the dynamic displacement response by employing electrical admittance of the polymer structure and coupling it to the mechanical displacement [21]. In this model the polymer is considered to be a perfect conductor and the effect of electronic delay has not been considered in the prediction of the time dependent response. In some structures, potential drop due to the finite conductivity of the polymer is very significant, and thus needs to be considered. In this chapter we use an equivalent transmission line model for the polymer that considers the finite electronic conductivity as well as other electrochemical characteristics such as ionic and solution resistances and the capacitance of the porous polymer. The equivalent circuit, in fact represents the distribution of the actuation potential and current in 2 dimensions; namely through the polymer thickness and along its length. We present an analytical solution for the

impedance of the polymer 2D circuit model and couple it to a mechanical model to predict the dynamic actuation response.

In our previous work [22], we used time constants obtained from a transmission line model to describe ionic charge transport and electronic charge propagation into the polymer actuator. The predicted currents as a function of position are then related to mechanical deformation, which is achieved by numerically solving a discrete model in order to relate the time dependent charge transport to the local mechanical deflection of the actuator structure. Although this model enabled prediction of a dynamic actuation response, there was an uncertainty in estimating the initial element for the discrete mechanical modelling, which influenced the accuracy of the model in predicting the response in short times. In addition the discrete numerical modelling could be slow when predicting high frequency responses, and provides less insight into the rate limiting mechanisms.

In this chapter we use the exact solution of the 2D transmission line impedance and use it to predict the transient current in response to the applied actuation potential. The charge transport corresponding to the transient current is then converted to the time dependent electrochemical strain and is used to predict the structure dynamic actuation response. The advantage of this model compared to existing models is that it represents a two dimensional charging through the polymer structure by considering both ion diffusion through the thickness and electron propagation along the length. In addition it provides an exact analytical expression to accurately predict the dynamic actuation response and clearly distinguish the effects of different variables on the actuation. The need for fitting is also minimized by

measuring the relevant physical properties. This model can serve as a design tool for electrochemical based conducting polymer devices. In this thesis it is used to describe the deformation of a deflecting polymer driven catheter through time.

5.2 Transmission line model

As was mentioned in Introduction, electrochemical excitation of conducting polymers inside an ionic electrolyte results in an insertion of ions into the porous polymer structure, which leads to mechanical deformation. The induced strain is proportional to the number of ions per unit volume inserted and the strain rate is also related to charging rate [10]. In order to model the deformation of a conducting polymer it is important to determine the charge as a function of position, which in turn enables an estimate of strain. The approach presented here is to employ transmission line models to predict this charging through time and space.

Substantial previous work has been devoted to describing the electrochemical impedance of conducting polymers for prediction of the charging behavior [24-42]. A number of transmission line equivalent circuits have been developed, emphasizing different aspects of conducting polymers such as a homogeneous structure, where ionic transport is modeled by means of diffusion mechanisms [36-42] or as a distributed polymer/electrolyte interface [24-35]. Here we use the distributed transmission line depicted in Figure 5.1, to model the 2 dimensional charge distributions in polypyrrole. In this circuit model, R_i represents the ionic resistance of a small section through the polymer thickness (h), R_e represents the electronic resistance of a segment along the polymer length (L), R_s is a portion of the electrolyte

resistance and C is the capacitance associated with charging of a segment of the polymer. This simulates a long segment of polypyrrole immersed in electrolyte, electrically connected at the top, and in contact with electrolyte down its length.

Conducting polymers as electrochemical actuators are often designed as thin and long structures, so during actuation the ion insertion through the thickness enables a large displacement along the polymer length. For this type of structure, although the electronic charging occurs in 3 dimensions, it is mostly limited by the polymer electronic resistance along its length, since the resistance across the thickness is negligible and we assume that the electrode is connected such that the potential is uniform across the width, as shown in Figure 5.1. We also assume (and confirm experimentally) that the ionic conductivity within the polymer is always much lower than the electronic conductivity, so that we do not need to account for electronic resistance through the thickness. Finally, ion transport along the length is small since the distances are large and ionic conductivity is poor, so this component is neglected.

In some actuator design, the conducting polymer is coated on a conductive substrate eliminating the electronic resistance along the polymer length. Therefore a one dimensional model, only considering the ionic transport through the thickness, is sufficient to predict the electrochemical actuation response.

Ionic transport is assumed to be field driven – hence ionic resistance combined with capacitance is used to model it. However it can also be by diffusion. Conveniently, the RC transmission line model is able to describe either mass transport mechanism. Our previous work suggests that in polypyrrole as we grow it,

field driven mass transport is dominant [43], and this is reinforced by the relatively good agreement in this model between experimentally fit and measured values of ionic conductivity, as will be discussed. The model shown in Figure 5.1 will not work if both diffusion and field driven transport are significant. Such a situation could emerge at low doping levels [43].

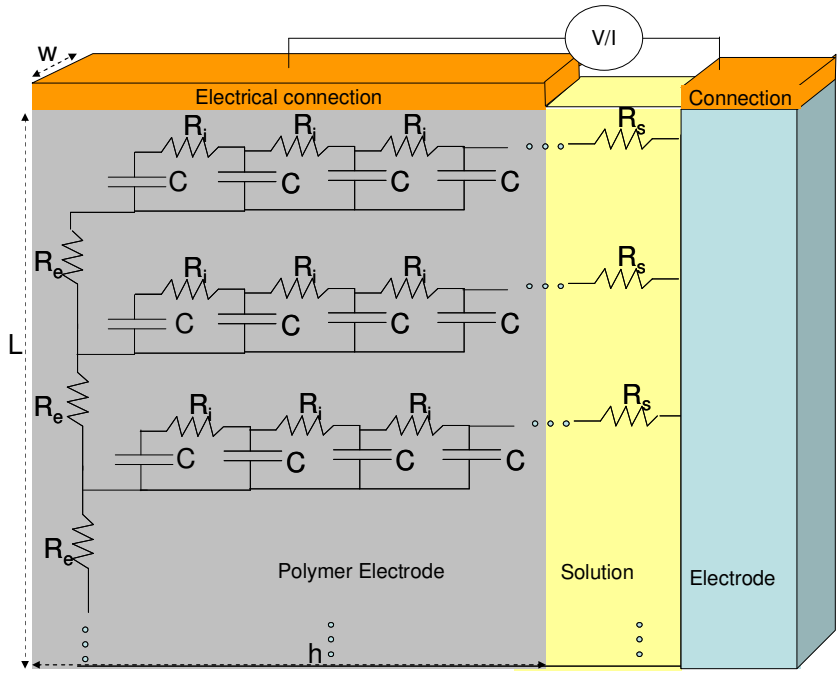

Figure 5.1: 2 dimensional distributed transmission line circuit model. V/I represents the applied voltage /current. (Note that, in the real device h<<w<L, and in this figure, the scale of thickness (h) is exaggerated to accommodate the circuit model.)

In the following two sections the impedance of the transmission line model is found analytically. We start with the solution to the one dimensional case and then derive the impedance of the 2 dimensional circuit model. We will use the impedance to predict the current in response to an actuation potential. The amount of charge transfer will then be calculated from the predicted current. This time-dependent

charging can be converted to mechanical actuation response which will be described in section 5.3.

5.2.1 1D model

In solving for the impedance of the conducting polymer transmission line model the impedance through the thickness is first determined. In the 1D model shown in Figure 5.2, x is along the polymer thickness, and h is the total thickness of the polymer. It is assumed that a voltage (or current) is applied across the polymer electrode, at $x=0$ and a reference electrode inside an electrolyte located at $x=h+d$, (d is the distance between the reference electrode and the conducting polymer). The circuit model consists of, the ionic resistance per thickness, $R_i = \frac{1}{\sigma_i A}$ (σ_i is the ionic conductivity of the polymer and A is the area (width × length)), the capacitance per thickness $C = C_v A$ (C_v is the volumetric capacitance of the conducting polymer), and the electrolyte resistance, $R_s = \frac{d}{\sigma_s A}$ (σ_s is the electrolyte conductivity).

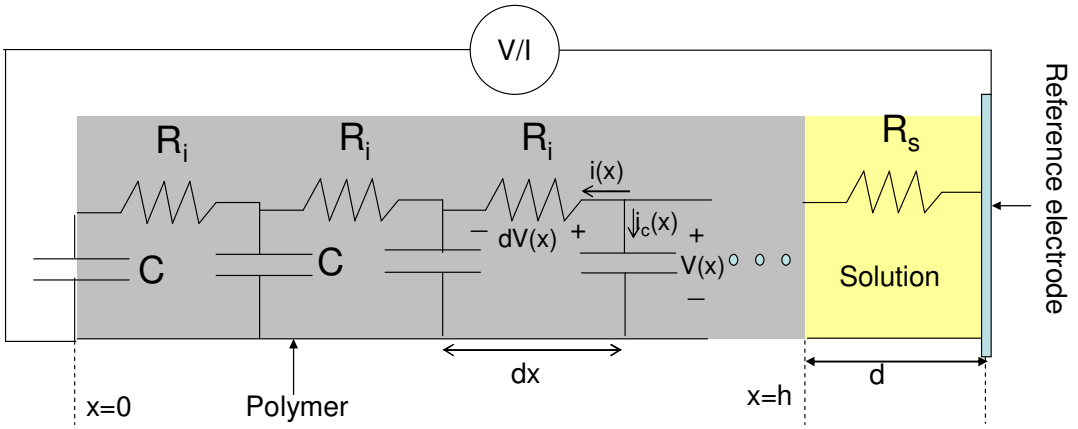

Figure 5.2: 1 dimensional transmission line circuit modelling the mass transport of ions through the polymer thickness.

The impedance of the transmission line plus the solution resistance as a function of the Laplace variable, *s*, is:

$$Z_{1D}(s) = \sqrt{R_i Z_c}.\coth(\sqrt{\frac{R_i}{Z_c}}.h) + R_s,$$

or

$$Z_{1D}(s) = \frac{\coth(\sqrt{\frac{s.C_V}{\sigma_i}}.h)}{A.\sigma_i\sqrt{\frac{s.C_V}{\sigma_i}}} + \frac{d}{\sigma_s A}. \qquad (5.1)$$

5.2.2 2D model

The effect of electronic resistance is now added to the model, accounting for voltage drop along the length. This model is a transmission line, with the *RC* transmission line ladders in the thickness direction (x) described Z_{1D} blocks (i.e. the impedance of the 1D model). This configuration is shown in Figure 5.3 (rotated 90 degrees from the orientation in Figure 5.1). In this circuit R_e is the electronic resistance per unit length, $R_e = \frac{1}{\sigma_e w.h}$, where σ_e is the electronic conductivity of the polymer. The resistance describes the effect of finite electronic conductivity along the polymer length (y).

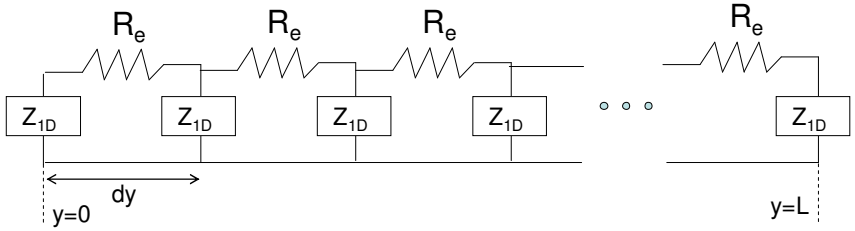

Figure 5.3: Simplified representation of the 2D model of Figure 5.1.

As can be seen From Figure 5.3, the 2D circuit model is now similar to the circuit of Figure 5.2 with the capacitors being replaced by Z_{1D}. Following the same approach used to derive Equation 5.1 the impedance of this 2D transmission line model is found to be:

$$Z_{2D}(s) = \sqrt{R_e Z_{1D}}.\coth\left(\sqrt{\frac{R_e}{Z_{1D}}}.L\right), \tag{5.2}$$

$$Z_{2D}(s) = \sqrt{\frac{1}{\sigma_e w.h}\left(\frac{\coth\left(\sqrt{\frac{s.C_V}{\sigma_i}}.h\right)}{A.\sigma\sqrt{\frac{s.C_V}{\sigma_i}}} + \frac{d}{\sigma_s A}\right)}.\coth\left(\sqrt{\frac{\frac{1}{\sigma_e w.h}A.\sigma_i\sqrt{\frac{s.C_V}{\sigma_i}}.\sigma_s A}{\coth\left(\sqrt{\frac{s.C_V}{\sigma_i}}.h\right).\sigma_s A + dA.\sigma_i\sqrt{\frac{s.C_V}{\sigma_i}}}}.L\right).$$

The validity of this expression in predicting the polypyrrole impedance frequency response was confirmed and is presented in Appendix 1.

The analytical expression for the impedance in Laplace domain enables the calculation of time dependent charging in response to actuation voltage (or current). In the device considered in this chapter, voltage controlled actuation is used where polymer charging occurs in response to a step in voltage, $V(t)=V_o$ for time greater than zero. The current in response to a step in voltage is calculated as follows:

$$V(t) = V_o \qquad \Rightarrow V(s) = \frac{V_o}{s},$$

$$i(y,s) = \frac{\frac{V_o}{s}}{Z_{2D}(s)}\left(\frac{e^{\sqrt{R_e/Z_{1D}}(s).y} - e^{-\sqrt{\mathrm{Re}/Z_{1D}(s)}.y}}{e^{\sqrt{R_e/Z_{1D}(s)}.L} - e^{-\sqrt{\mathrm{Re}/Z_{1D}(s)}.L}}\right). \tag{5.3}$$

Here, $i(y,s)$ is the current as a function of frequency and position along the length of the polymer. The current in Laplace domain is then inverted into time domain and the time dependent charging per volume as a function of position is found by:

$$Q_{vol}(y,t) = \frac{1}{h.w}\int_0^t \frac{di(y,t)}{(L-y)}.dt \,. \qquad (5.4)$$

This determines the strain which is a function of charge. The strain is then entered into the mechanical model to predict deflection, as now described.

5.3 Mechanical model

In this section, the time dependent charge transfer, found from the impedance model, is coupled with the mechanical model to predict the dynamic actuation response. The electrochemically driven conducting polymer actuator produces strain, ε, that is proportional to the amount of charge transfer per volume of the material, via the following relationship;

$$\varepsilon(y,t) = \alpha Q_{vol}(y,t) \,. \qquad (5.5)$$

α is an empirically determined strain to volumetric charge ratio [24,44,45]. Equation 5.5 is used to couple the impedance model to the mechanical model. If the polymer actuator is designed in a linear mode of operation, its dynamic mechanical displacement can be easily found by substituting the time dependent charging of Equation 5.4 into Equation 5.5. For the bending mode of operation, however, a more sophisticated modelling is needed.

We are particularly interested in conducting polymer based bending catheter where polymer electrodes are formed onto a tube beam (i.e. the catheter). A voltage is applied across the polymer electrodes inside an electrolyte containing mobile negative ions (see Figure 5.4). As a result one polymer electrode is oxidized and the other is simultaneously reduced. During oxidation mobile negative ions enter the polymer from the electrolyte, therefore expand the structure. During reduction they exit the polymer to the electrolyte and contract it. Expansion on one side and contraction on the other side induces a stress gradient on the polymer/catheter interfaces and causes the whole structure to bend in one direction.

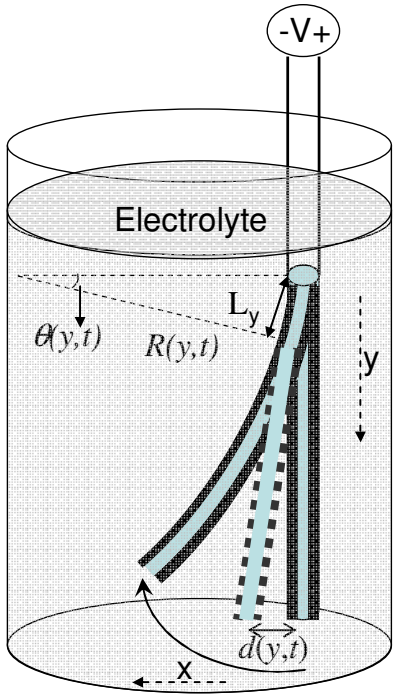

Figure 5.4: Actuation of the polymer coated catheter by applying voltage inside an electrolyte.

A mechanical beam bending model for conducting polymer bilayer actuators has been developed previously [19]. We have extended this model by adding time and position dependent variables and developed a dynamic mechanical model for a

polypyrrole driven catheter [22]. The model uses the fundamental formulas of force and torque balance and considers the polymer electrochemically induced strain on the catheter (from Equation 5.5) and the cantilever beam condition to find the curvature of the catheter and thus its tip displacement. Equation 5.6 and 5.7 illustrates the radius of curvature of the catheter structure, R, and angle of bending, θ, at any position y along the length, and time, t, (depicted in Figure 5.4).

$$R(y,t) = \frac{3}{32}\pi \frac{Yb^4 - Y_p(a+2h)^4 - Ya^4 + Y_p a^4}{Y_p \varepsilon(y,t)\left[(a\ )^3 - (a+2h)^3\right]}, \tag{5.6}$$

$$\theta(y,t) = \frac{L_y}{R(y,t)}. \tag{5.7}$$

Here a and b are the outer and inner diameters of the catheter and h represents the thickness of the polymer. Y and Y_p are the Young's modulus of the catheter and the polymer respectively. L_y represents the position along the catheter length.

The catheter tip displacement, d, resulting from the curvature at each position and time is found to be:

$$d(y,t) = R(y,t)\left(1 - \cos\left(\theta(y,t)\right)\right) + (L - L_y)\sin\left(\theta(y,t)\right). \tag{5.8}$$

The first term of Equation 5.8 is the displacement of the L_y segment due to actuation and the second term represents the mechanical amplification through the extension of the catheter length (L-L_y), which has not yet been charged (actuated). The final step is to first find the x components of the segments' displacements, $d(y,t)$, and then add them at each time interval to find the total tip displacement as a function of time.

5.4 Experiment

In order to validate the developed dynamic model, experimental actuation results are compared with the model predicted response. Conducting polymer coated catheters were fabricated in two configurations; 1) a gold coated catheter with one conducting polymer electrode, and 2) a catheter coated with two polymer electrodes. The first configuration was tested to evaluate the accuracy of the 1D model, where a gold coated catheter acts as a conductive backing for the polymer, eliminating the need for considering the electronic resistance along the actuator length. The second configuration of polymer coated catheter was compared with the 2D model.

5.4.1 Fabrication

The catheter used in this experiment was a Micro Therapeutics Inc. (Irvine, CA) UltraflowTM HPC. The catheter used for comparing with the 1D model has outer and inner diameters of a=0.9 mm and b=0.28 mm respectively. The Young's modulus of this catheter was measured using a dynamic mechanical analyzer (DMA Q800 V7.1) to be Y=65 MPa. A 50 nm gold layer was deposited on to one side of the catheter using ebeam evaporation technique. A 10 μm thick conducting polymer (here polypyrrole) was then deposited onto the gold layer using electrochemical deposition forming a polymer electrode along one side of the catheter (Figure 5.5). This process is done following the method of Yamaura [46] as described in Chapter 1 (section 1.5). The resulting polymer is in the oxidized state with the doping level in as-grown polypyrrole of approximately one charge per three monomers [47]. The Young's

modulus of a free standing polypyrrole film during actuation was measured to be Y_p=350 MPa.

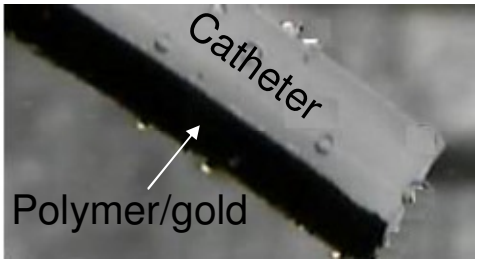

Figure 5.5: The catheter tip coated with one polymer electrode on one side (gold layer is underneath the polymer).

The second catheter has an inner and outer diameter of 0.28 mm and 0.5 mm respectively. Polymer deposition on the catheter was done in two steps. First a thin layer of polymer was deposited using electroless deposition by chemical polymerization of pyrrole monomer in the presence of oxidizing agent [48]. The film deposited by this method provides a seed layer for electrochemical deposition of polypyrrole. The polypyrrole film is then electrochemically grown onto the seed layer from the same solution and under the same condition as described above. Polymer coating was then divided into 2 electrodes using laser ablation (Figure 5.6) [15]. A more detailed description of laser ablation is provided in Chapter 6.

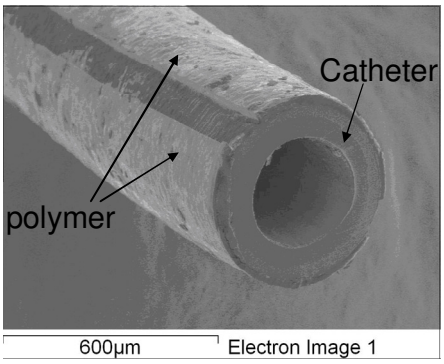

Figure 5.6: The polymer coated catheter tip showing the laser machined 2 separate polymer electrodes.

5.4.2 Actuation of conducting polymer based catheters

Gold coated catheter/polymer

The response of the conducting polymer actuated catheter to a step input of voltage was measured and compared with model predictions. A 35 mm long gold coated catheter with 10 µm thick polymer electrode was actuated inside an aqueous solution of sodium hexafluorophosphate ($NaPF_6$) by applying a step potential of ±0.5 V across the polymer electrode and an Ag/AgCl reference electrode. The model is compared with the experimental results to check if it provides a reasonable description of the response. The 1D impedance expression of Equation 5.1 was used in Equation 5.3 to predict the current in response to the step in potential. In this model, the ionic conductivity of $\sigma_i = 2.2\times10^{-3}$ S/m, the volumetric capacitance of $C_v = 2\times10^{8}$ F/ m^3, and a solution conductivity of $\sigma_s = 8$ S/m were used from the previously measured electrochemical parameters [23]. Figure 5.7 shows the experimental and modelled transient current in response to the actuation potential.

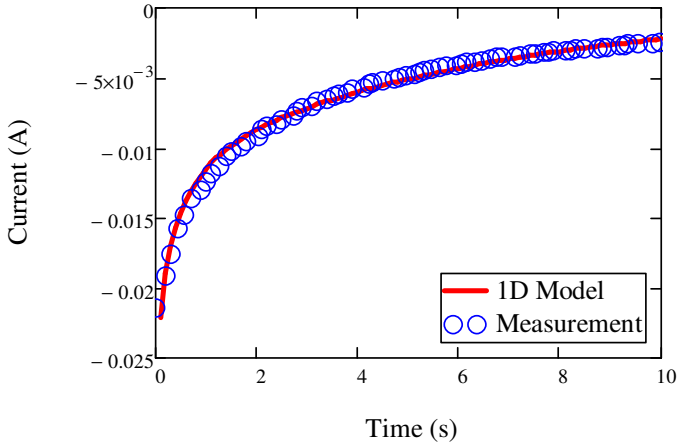

Figure 5.7: Current during the step in voltage (+0.5 V to -0.5 V) on the polymer/gold coated catheter.

The polymer time dependent charging was then calculated using Equation 5.4, where Z_c(s) is replaced with Z_{1D} (s), R_i with R_e and Z_{1D}(s) is replaced with Z_{2D}(s). The calculated charge was entered to the coupling equation (Equation 5.5). The mechanical modelling explained in section 5.3 was modified for a simpler case of "one polymer electrode on the gold coated catheter" and the resulting time dependent displacement was calculated. In this model, the measured values of 65 MPa and 350 MPa were used for the Young's modulus of the catheter and the polymer electrode, respectively, and a measured strain to volumetric charge ratio of 4×10^{-11} m^3/C was used in the coupling equation (Equation 5.5). The catheter tip displacement as a function of time is shown in Figure 5.8.

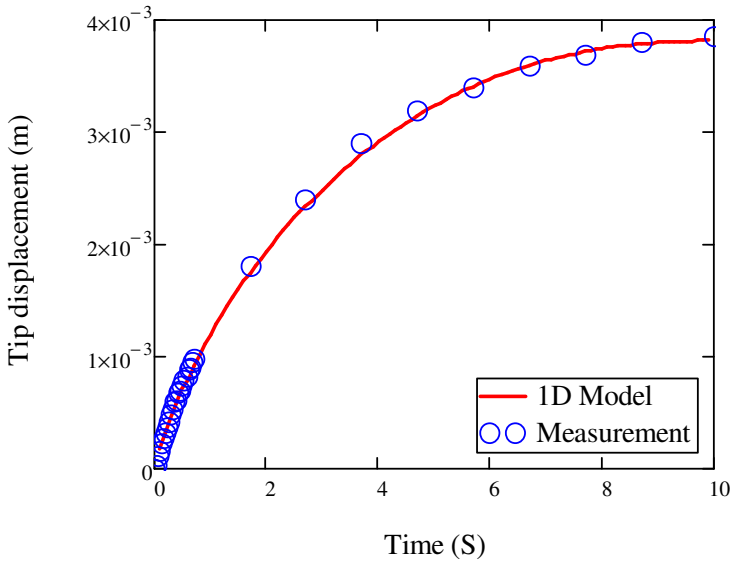

Figure 5.8: Tip displacement of the gold coated catheter with one polymer electrode in response to the step in voltage from +0.5 V to -0.5 V.

We can see from the above figures that the model predictions match with the experimental results, confirming the accuracy of the proposed 1D impedance model.

This dynamic modelling can be very useful in designing actuator devices with a highly conductive backing.

Polymer/catheter/polymer

The validity of the 2D model is now investigated for designing conducting polymer devices with limited electronic conductivities. A 22 mm long catheter coated with two polymer electrodes (with no additional conductive backing) was actuated inside an aqueous solution of $NaPF_6$. The actuation potential was a step voltage of ±1 V across the two polymer electrodes. Since the second electrode is also a conducting polymer, the equivalent circuit model can be thought of as two transmission lines (of Figure 5.1) in series. We solve for the half-cell impedance assuming a step potential of ±0.5 V across one polymer electrode and a reference electrode. The half-cell potential (between each polymer electrode and an Ag/AgCl reference electrode) was measured during actuation to alternate between -0.5 V and +0.5 V confirming this assumption. The 2D expression for impedance of Equation 5.2 was used in Equation 5.3, to find the transient current in response to the step potential of ±0.5 V. Figure 5.9 shows the measured actuation current along with the prediction of the 1D and 2D models. We can see that the 1D model overestimates the magnitude of initial current since it neglects the resistance along the polymer length. By overestimating the initial current, the 1D model predicts faster charging of the polymer and shorter time constant during which the current drops to zero. An electronic conductivity of 8000

S/m for the polymer was used in the 2D model and shows a good agreement with the experimental results.

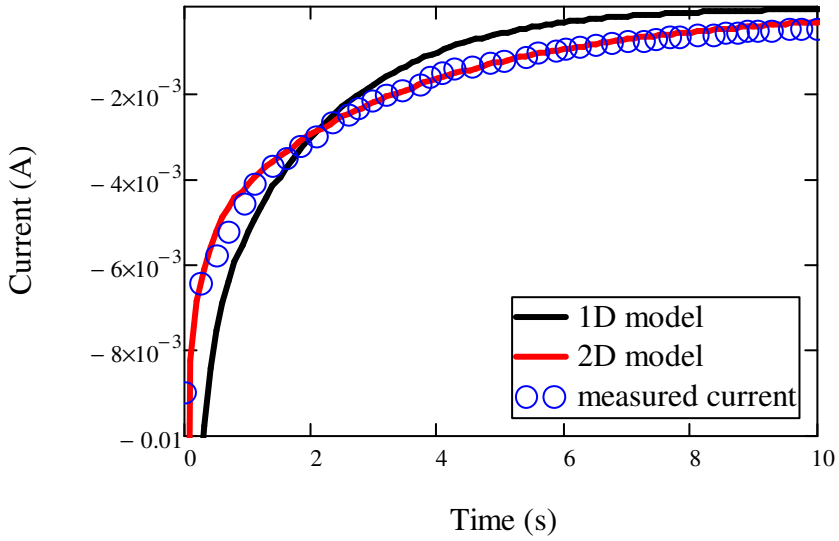

Figure 5.9: Current during the step in voltage from +0.5 V to -0.5 V on the polymer/catheter/polymer trilayer.

The time-position dependent charging was then found from Equation 5.4 which allows the prediction of charge and its corresponding strain along the polymer length as a function of time. The degree of bending was predicted by coupling the charge transferred during the actuation with the mechanical model, using the measured mechanical properties of the actuator. Figure 5.10 depicts the model predictions and the experimental results. We can see that, the 1D model overestimates the speed of response by ignoring the effect of electronic resistance along the polymer length. The necessity of the 2D model for accurate prediction of the actuation response, particularly at short times is clear.

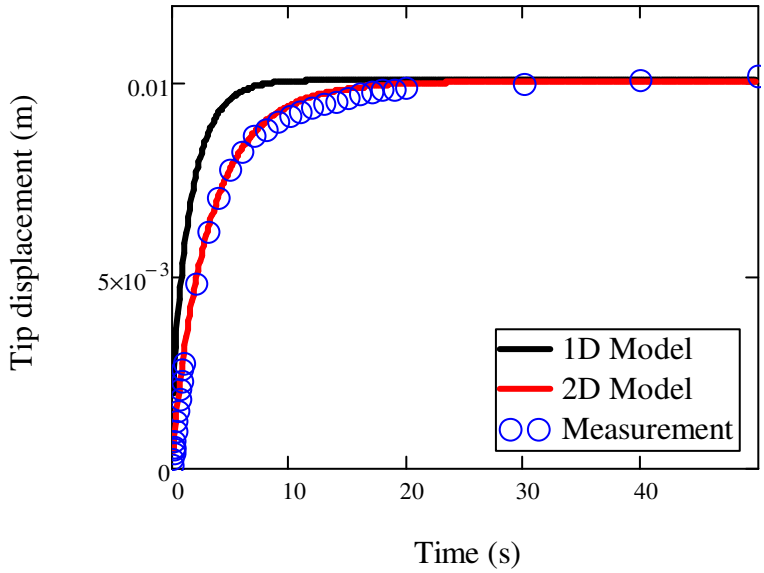

Figure 5.10: Tip displacement of the polymer/catheter/polymer in response to the step in voltage from +0.5 V to -0.5 V.

5.5 Conclusion

An analytical model was presented to predict the dynamic actuation response of electrochemically driven actuators. The model used the exact solution of the impedance of a 2 dimensional transmission line equivalent circuit to predict the charge distribution along the polymer length as a function of time. The predicted charge was then coupled to a mechanical model to find the displacement of the structure. This model enables the effects of device geometry, capacitance per unit volume, ionic conductivity, and electronic conductivity on degree of actuation to be determined. The need for fitting is minimized by directly measuring ionic conductivity, electronic conductivity and volumetric capacitance. The model was used to predict the bending response of two polypyrrole driven catheters; polymer/gold coated catheter and polymer/catheter/polymer structure. A 1D model

was used to predict the dynamic response of the former, and a 2D model was used for the latter. The results show a good match with the experimental observations, confirming the accuracies of the models in predicting the dynamic actuation responses.

References

[1] A. Mazzoldi, D. De Rossi, "Conductive polymer based structures for a steerable catheter," Proceedings of the SPIE (The International Society for Optical Engineering), vol. 3987, pp. 273–80, 2000.

[2] Della, A. Santa, A. Mazzoldi, D. de Rossi, "Steerable microcatheters actuated by embedded conducting polymer structures," J. Intelligent Mat. Syst. Struc., vol. 7, 3, pp. 292–300, 1996.

[3] D. Zhou, G.G. Wallace, G.M. Spinks, "Actuators for the cochlear implant", Synth. Met., vol. 135-136, pp. 39–40, 2003.

[4] A. Gursel ; G. Daniel, "A bio-inspired robotic locomotion system based on conducting polymer actuators" IEEE/ASME International Conference on Advanced Intelligent Mechatronics, AIM, pp. 998-1004, 2009,

[5] K. Kaneto, "Conducting polymer soft actuators based on polypyrrole films", Proceedings of SPIE - The International Society for Optical Engineering, Smart Structures and Materials: Electroactive Polymer Actuators and Devices (EAPAD), vol. 6168, 2006,

[6] M. Fuchiwaki, K. Tanaka, K. Kaneto, "Planate conducting polymer actuator and its application," Proceedings of ASME Fluids Engineering Division Summer Meeting FEDSM2006, vol. 2 FORUMS, pp. 849-854, 2006.

[7] K. Ren, S. Liu, M. Lin, Y. Wang, Q.M. Zhang, "A compact electroactive polymer

actuator suitable for refreshable braille display" Proceedings of SPIE - The International Society for Optical Engineering Electroactive Polymer Actuators and Devices (EAPAD), vol. 6524, 2007.

[8] G. Spinks, G. Wallace, J. Ding, D. Zhou, B. Xi, J. Gillespie, "Ionic Liquids and Polypyrrole Helix Tubes: Bringing the Electronic Braille Screen Closer to Reality" Proceedings of SPIE - The International Society for Optical Engineering, vol. 5051, pp. 372-380, 2003.

[9] K. Asaka, T. Sugino, "Robotic applications of ionic conductive polymer actuators" Polymer Preprints, Japan, vol. 54, n 2, pp. 4670-4671, 2005.

[10] J.D.W. Madden, P.G.A. Madden, and I.W. Hunter, "Conducting polymer actuators as engineering materials", Proceedings of SPIE, Smart Structures and Materials: Electroactive Polymer Actuators and Devices, vol. 4695, pp. 176–190, 2002.

[11] J.D.W. Madden, N.A. Vandesteeg, P.A. Anquetil, P.G.A Madden, A. Takshi, R.Z. Pytel, S.R. Lafontaine, P.A. Wieringa, I.W. Hunter, "Artificial muscle technology: Physical principles and naval prospects," IEEE J Ocean Eng 29: 706-28 (2004).

[12] P.M. George, D.A. Lavan, J.A. Burdick, Y. Chen Ching, E. Liang, R. Langer," Electrically controlled drug delivery from biotin-doped conductive polypyrrole," Advanced Materials, vol.18, pp. 577-581, 2006.

[13] X. Wang, X. Gu, Ch. Yuan, Sh. Chen, P. Zhang, T. Zhang, J. Yao, F. Chen, G. Chen, "Evaluation of biocompatibility of polypyrrole *in vitro* and *in vivo*," Journal of Biomedical Material Research - Part A vol. 68, pp. 411-422, 2004.

[14] T. Shoa, J.D.W. Madden, N.R. Munce, V.X.D. Yang, "Steerable Catheters in Biomedical applications of electroactive polymer actuators," Ed by Carpi F and Smela E, John Wiley& Sons Ltd. UK, pp 229-246, 2009.

[15] K. Lee, N.R. Munce, T. Shoa, L.G. Charron, G.A. Wrigh, J.D. Madden, V.X.D. Yang, "Fabrication and characterization of laser-micromachined polypyrrole-based artificial muscle actuated catheters," Sensors and Actuators, A: Physical, vol. 153(2), pp. 230-236, 2009.

[16] Ph. Metz, G. Alici, G. M. Spinks, "A finite element model for bending behaviour of conducting polymer electromechanical actuators," Sensors and Actuators, A: Physical, 130-131: 1-11 (2006).

[17] A.D. Santa, D. De Rossi, A. Mazzoldi, "Characterization and modelling of a conducting polymer muscle-like linear actuator," Smart Materials and Structures, vol. 6, pp. 23-34, 1997.

[18] G. Alici, B. Mui, C. Cook, "Bending modelling and its experimental verification for conducting polymer actuators dedicated to manipulation applications ," Sensors and Actuators, A: Physical, vol. 126, pp. 396-404, 2006.

[19] M. Christophersen, B. Shapiro, Smela E, "Characterization and modelling of PPy bilayer microactuators. Part 1. Curvature ," Sensors and Actuators, B: Chemical, vol. 115, pp. 596-609, 2006.

[20] G. Alici, N. N. Huynh, "Predicting force output of trilayer polymer actuators," Sensors and Actuators, A: Physical, vol. 132, pp. 616-625, 2006.

[21] Y. Fang, X. Tan, Y. Shen, N. Xi, G. Alici, "A scalable model for trilayer

conjugated polymer actuators and its experimental validation," Materials Science and Engineering C, vol. 28, pp. 421-428, 2008.

[22] T. Shoa, J.D. Madden, N.R. Munce, V.X.D. Yang, "Analytical modelling of conducting polymer driven catheter ," Polymer international, Electromechanically Active Polymers for Bioengineering, Mechatronics and Optics, vol. 59, pp. 343-351, 2010.

[23] T. Shoa, D.S. Yoo, D, J. Madden, "Analytical Impedance Model for Electrochemically driven Conducting Polymer devices", submitted to journal of electrochemical society, 2010.

[24] X. Ren, P. G. Pickup, "Impedance study of electron transport and electron transfer in composite polypyrrole+polystyrenesulphonate films," Journal of Electroanalytical Chemistry, vol. 420, pp. 251-257, 1997.

[25] W.J. Albery, C.M. Elliot, A.R. Mount, J. "Transmission line model for modified electrodes and thin layer cells," Journal of Electroanalytical Chemistry, vol. 288, pp. 15-34, 1990.

[26] S. Fletcher, "Contribution to the theory of conducting-polymer electrodes in electrolyte solutions," Journal of Chemical Society, Faraday Trans. vol. 89, pp. 311-320, 1993.

[27] G. Paasch, K. Micka, P. Gersdorf, "Theory of the electrochemical impedance of macrohomogeneous porous electrodes," Electrochim. Acta vol. 38 pp. 2653-2662, 1993.

[28] G.S. Popkirov, E. Barsoukov, R.N. Schindler, "Investigation of conducting

polymer electrodes by impedance spectroscopy during electropolymerization under galvanostatic conditions," Journal of Electroanalytical Chemistry, vol. 425, pp. 209-216, 1997.

[29] K. Rossberg, G. Paasch, L. Dunsch, S. Ludwig, "Influence of porosity and the nature of the charge storage capacitance on the impedance behaviour of electropolymerized polyaniline films," Journal of Electroanalytical Chemistry, vol. 443, pp. 49-62, 1998.

[30] G. Paasch, "The transmission line equivalent circuit model in solid-state electrochemistry," Electrochemistry Communications, vol. 2 pp. 371-375, 2000.

[31] J. Bisquert, G. Garcia-Belmonte, F. Fabregat-Santiago, N.S. Ferriols, M. Yamashita, E.C. Pereira, "Application of a distributed impedance model in the analysis of conducting polymer films," Electrochemistry Communications, vol. 2, pp.601-605, 2000.

[32] G. Garcia-Belmonte, J. Bisquert, E.C. Pereira, Switching behaviour in lightly doped polymeric porous film electrodes. "Improving distributed impedance models for mixed conduction conditions," Journal of Electroanalytical Chemistry, vol. 508, pp.48-58, 2001.

[33] R.P. Buck, M.B. Madaras and R. Mackel, "Simple hierarchical impedance functions for asymmetric cells: Thin-layer cells and modified electrodes," Journal of Electroanalytical Chemistry, vol. 362, pp. 33-46, 1993.

[34] G. Garcia-Belmonte, J. Bisquert, "Impedance analysis of galvanostatically

synthesized polypyrrole films. Correlation of ionic diffusion and capacitance parameters with the electrode morphology," Electrochim. Acta, vol. 47, pp. 4263–4272, 2002.

[35] M. Warren, J.D.W. Madden, "Electrochemical switching of conducting polymers: A variable resistance transmission line model," Journal of Electroanalytical Chemistry, vol. 590, pp.76-81,2006.

[36] W.J. Albery, Z. Chen, B.R. Horrocks, A.R. Mount, P.J. Wilson, D. Bloor, A.T. Monkrnan and C.M. Elliott, "Spectroscopic and electrochemical studies of charge transfer in modified electrodes," Faraday Discuss. Chem. Soc., vol. 88 pp. 247 ,1989.

[37] M.A. Vorotyntsev, J.-P. Badiali, G. Inzelt, " Electrochemical impedance spectroscopy of thin films with two mobile charge carriers: Effects of the interfacial charging," Journal of Electroanalytical Chemistry, vol. 472 pp. 7, 1999.

[38] R.P. Buck, "Diffusion, migration impedances for finite, one-dimensional transport in thin layer and membrane cells," Journal of Electroanalytical Chemistry, vol. 219, pp. 23-48, 1987.

[39] M.F. Mathias, O. Haas, "An alternating current impedance model including migration and redox-site interactions at polymer-modified electrodes," Journal of Physical Chemistry, vol. 96, pp. 3174-3182,1992.

[40] C. Gabrielli, O. Haas, H. Takenouti, "mpedance analysis of electrodes modified with a reversible redox polymer film," Journal of Applied Electrochemistry, vol. 17, pp. 82-90, 1987.

[41] G. La´ng, G. Inzelt, Electrochim. Acta 44 (1999) 2037.

[42] B.W. Johnson, D.C. Read, P. Christensen, A. Hammet, R.D. Armstrong, J. Electroanal. Chem. 364 (1994) 103.

[43] C. Tso, J.D.W. Madden, C.A. Michal, "An NMR study of PF6- ions in polypyrrole ," Synthetic Metals, vol. 157, pp. 460-466, 2007.

[44] A. Mazzoldi, A. Della Santa , and D. De Rossi, "Conducting polymer actuators: Properties and modelling ," Polymer Sensor and Actuators, Ed by OSada Y and De Rossi DE, Springer Verlag Polymer: Chapter 7, 1999.

[45] R.H. Baughman, R.L. Shacklette, R.L. Elsenbaumer, "Microelectromechanical actuators based on conducting polymers ," Topic in Molecular Organization and Engineering, vol. 7, pp. 267, 1991.

[46] M. Yamaura, T. Hagiwara, K. Iwata, "Enhancement of electrical conductivity of polypyrrole film by stretching: Counter ion effect," Synthetic Metals, vol. 26, pp. 209-224, 1988.

[47] R.S. Kohlman, A.J. Epstein, "Insulator-metal transition and inhomogeneous metallic state in conducting polymers", in Handbook of Conducting Polymers: Marcel Dekker, second edition: pp 85–122, 1998.

[48] R.V. Gregory, W.C. Kimbrell, H.H. Kuhn, "Conductive textiles ," Synthetic Metals, vol. 28, pp. 823-835, 1989.

CHAPTER 6: CONDUCTING POLYMER BASED ACTIVE CATHETER FOR MINIMALLY INVASIVE INTERVENTIONS INSIDE ARTERIES [5]

6.1 Introduction

In this Chapter an example of the polypyrrole artificial muscle in biomedical application is discussed. We employ the results of the characterization studies and the developed models presented in previous chapters to realize a polypyrrole driven active catheter for minimally invasive diagnosis procedures. An overview of this application, its potential benefits and justification of using polypyrrole in developing active catheters are described as follows.

Recent advancements in micro devices and robotics have made it possible to replace traditional open surgery with minimally invasive medical procedures. These procedures offer many benefits including more accuracy of operation, faster recovery and less pain and risk to the patient. Diagnosis procedures that are minimally invasive have allowed earlier detection of many diseases such as cancer, which substantially increases the chance of treatment. Conducting polymer actuators are a class of "artificial muscle" actuators, with particular characteristics which are advantageous

[5] "A version of this chapter will be submitted for publication. Shoa, T., Munce N.R., Yang V.X.D., Madden, J. (2010) Conducting Polymer Based Active Catheter for Minimally Invasive Interventions Inside Arteries."

for application in minimally invasive surgical and diagnostic tools. Some of the characteristics include low actuation voltage (<2 V), ease of fabrication, relatively high strain (typically 2% or greater), and biocompatibility [1]. These polymers have been used in medical applications such as blood vessel connectors, Braille displays, cochlear implants, biosensors and microvalves [2-7]. One of the interesting applications of these types of actuators is to convert passive catheters into active ones, hence providing controllable catheter manipulation inside the body [8]. Catheters are extensively used in many medical procedures such as angiography, stent deployment, intravascular ultrasound, and treatment of thromboembolic diseases (blot clots). They are used to provide a channel for fluid passage or an entry for a medical device. In angioplasty and stenting, for instance, catheters are employed to guide a therapeutic device to open a blockage inside a vessel. Traditionally, guide wires manipulated external to the patient are used for guidance of the catheter by combinations of push-pull and torque motions [9]. In situations where complex manoeuvring is required within the vascular system, long procedural times, lumen or vessel wall damage, and subsequent medical complications can result. For these reasons application of catheters and endoscopes in narrow and complex passages such as blood vessels of the brain and tertiary bronchi of the lung has been limited.

Recently, advanced catheter designs exploit active tip bending for more controllable and efficient minimally invasive medical procedures. Although various active catheters driven by shaped memory alloys (SMA) [10-13], piezoelectric materials and MEMS based devices [14-15] have been presented, no active catheters are in wide spread use.

Conducting polymer actuators have shown attractive properties, which make them promising to be employed extensively in active catheter application. IPMC (ionic polymer metal composites), another type of artificial muscle actuators, has been used in steerable catheters [16-18]. These actuators can generate large displacements at relatively low voltages (<10 V) and are typically faster than conducting polymers; however, their manufacturing process is often relatively expensive, stresses are smaller and unlike conducting polymers, additional energy is usually consumed to hold the actuator in place. Conducting polymers offer higher stiffness than IPMCs, an attribute which is often important in catheter design [19]. Their efficiency can be higher as maintaining deflection does not require energy expenditure.

In this chapter conducting polymer actuated catheters for minimally invasive intervention inside arteries are designed and demonstrated. Two designs are presented, as shown in Figure 6.1. One active catheter,"scanner", is employed for scanning an optical fibre over a distance of 1 mm, with a relatively high speed to provide forward viewing images from an artery lesion, as depicted in Figure 6.1 A. This catheter is placed inside a rigid encapsulation containing the electrolyte. The second catheter, the "positioner", is meant to actively bend to reach the target lesion and guide a wire through the lesion, potentially with the first fibre optic mounted catheter monitoring the procedure in real time, as suggested in Figure 6.1 B.

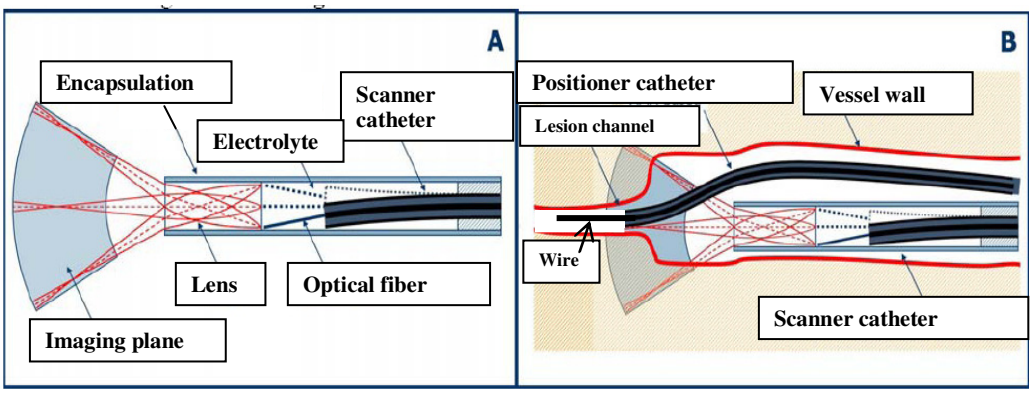

Figure 6.1: Schematic of the positioner and scanner catheters inside the blood vessel. A) The scanner catheter is moving an embedded optical fiber back and forth, and a lens amplifies the angular scanning range. The reflected light is collected by the same optical fibre and processed by the OCT system. B) the positioner catheter is bent to reach the lesion while the scanner catheter is monitoring the operation. A wire is inserted through the positioner catheter to open a channel through the lesion.

Real time forward viewing is done by a technique called optical coherence tomography (OCT) which performs depth resolved imaging by sending wide band near infrared light into tissue and observing the backscattered light interferometrically [20]. OCT depth imaging combined with the conducting polymer based scanning catheter shown in Figure 6.1 (which provides planar 2D scanning of the optical fiber), will result in complete high resolution 3D images. This technique could serve as an important diagnostic adjunct, enabling the detection and the monitoring of changes in tissues, and therefore could be useful for assessment of vascular disease and cancer tissue progression [20], and surgical guidance.

The scanner catheter needs to scan an optical fiber over a 1mm distance with a speed of 10-30 Hz and a lens amplify the angular scanning range (see Figure 6.1). Imaging is expected to require up to 50000 cycles before disposal. The positioner

catheter needs to produce a curvature radius of 10 mm. The catheter length is limited to 35 mm and its outer diameter to 2 mm. These specifications were defined by our clinical collaborator Dr. Yang, to meet the requirement of cardiovascular catheterization and imaging applications.

Previously an electrostatic scanner [21] has been reported for scanning a fibre for an OCT systems. However the high fabrication cost, device fragility and large driving voltage (1-3 kV) limits its application. Y.Wang *et al.*, has developed a hand-held OCT probe driven by an IPMC actuator for clinical oral and skin *ex vivo* imaging. They demonstrated scanning rate of 1Hz by applying 2V actuation potential [33], however the manufacturing cost is relatively high.

In this work we employ low cost polypyrrole actuators which requires low actuation voltage (<1 V) for *in vivo* applications. Polypyrrole electrodes coated on the catheters are used as the conducting polymer active elements and are electrochemically actuated in an electrolyte. Blood, which contains mobile ions, was initially considered to be used as an electrolyte; however the presence of multiple mobile ions inside the blood results in a mixed expansion and contraction of the polymer. The induced strain is also very small and there are safety issues as well as regulatory constraints in applying current through the blood (see Appendix 4). The electrolyte we chose is aqueous$NaPF_6$, with mobile ions of PF_6^-, which has been shown to produce large strain in polypyrrole actuators. In addition, actuation of polypyrrole in this electrolyte seems to be stable at body temperature at least for 3 hours of operation (see Appendix 3). The final active catheter needs to be

encapsulated to encompass this electrolyte, a task that has been accomplished in other polypyrrole driven devices [36, 37], and is left to future work.

The catheter used to demonstrate the bending is Micro Therapeutics Inc. (Irvine, CA) Ultraflow^{TM} HPC (0.5 mm OD/0.28 mm ID), which is a neurointerventional catheter with a thin, flexible tip that allows manoeuvring through narrow and curved arteries. Using our initial design, which is similar to a design suggested by Mazzoldi and De Rossi [8], we demonstrate that the polymer can provide sufficient force and displacement to achieve the desired bending as a positioner. The performance of the polypyrrole driven catheter in scanning an optical fiber and generating an OCT image is also presented. An optimum design is suggested based on the dynamic model (presented in Chapter 5) to achieve higher speed of scanning (10-30 Hz), desired for real time imaging. Finally the feasibility of using polypyrrole as a load sensor to control the position and to detect the catheter strike on the arterial wall is investigated, suggesting that it is not sensitive enough for the application.

6.2 Conducting polymer actuator driven catheter

The conducting polymer, in this work polypyrrole, is electronically conductive. It is also porous, enabling ion insertion. Application of a voltage to the polymer in an electrolyte alters the charging of the polymer. The electronic charging occurs throughout the volume of the polymer, and is balanced by the insertion of ions from the electrolyte. This charging process is associated with changes in volume, where increase in volume generally occurs when ions are inserted into the polymer matrix.

Figure 6.2 illustrates the mechanism of the dimensional change as a result of the electrochemical activation.

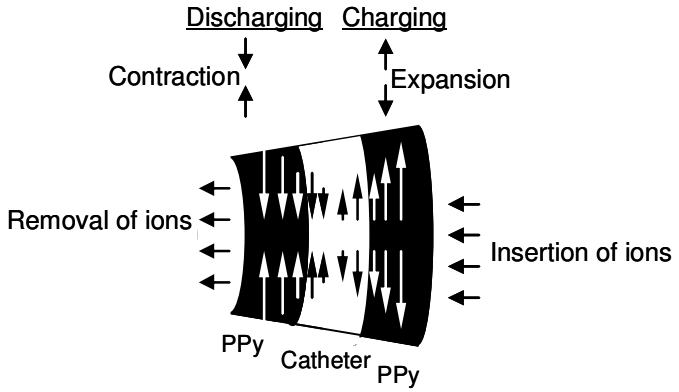

Figure 6.2: Compressive and tensile stress upon insertion and removal of ions from the polymer.

As shown in the figure a substrate (here a catheter) coated with conducting polymer electrodes on both sides is in an electrolyte solution containing mobile negative ions and large immobile positive ions. An alternating voltage is applied across the two polymer electrodes resulting in charging and discharging of the polymer electrodes. During charging the mobile negative ions enter the polymer from the electrolyte, expanding the structure. During discharging they exit the polymer to the electrolyte and contract it. Expansion on one side and contraction on the other side induces a stress gradient in the polymer and catheter, causing the whole structure to bend in one direction. Alternating expansion and contraction will result in bending with both positive and negative radii of curvature. Coating the catheter with four polymer electrodes, as in Figure 6.3, enables actuation in 2 dimensions.

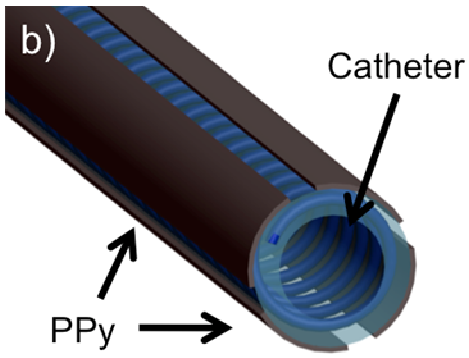

Figure 6.3: Design of polypyrrole actuated catheter showing four polymer electrodes on a catheter and enabling two degree of freedom deflection.

The relative amount of dimensional change or "strain" ,ε, is proportional to the volumetric charge per volume, ρ, via the relationship: $\varepsilon = \alpha\rho$ (α is an empirically determined strain to volumetric charge ratio) [22-24]. Therefore a higher amount of charge transferred results in a larger degree of bending (i.e. suitable for the positioner catheter). The amount of charge transferred is determined by the polymer capacity to store charge (i.e. volumetric capacitance C_v) and the actuation voltage ($\rho = C_v \times V$).

The rate of actuation of polypyrrole is proportional to the rate of ion insertion and hence to the current. In order to achieve high speed of actuation for the scanner catheter, large current is needed. The current can be limited by the ionic and electronic resistivities of the polymer electrode. For a long device the total polymer resistance along the length of the catheter, R_e, can significantly limit the rate of charging and hence actuation [24], with the predicted time constant being of the form $\tau = R_{ppy} C = \frac{C_v L^2}{\sigma_e}$ [24], where σ_e is the electronic conductivity of the polymer, C_v is the polymer volumetric capacitance and L is the length. For a thick device the ionic resistance through the thickness, h, is the rate limiting factor, with the time constant

of $\tau = \frac{C_v . h^2}{\sigma_i}$ [24], where σ_i is the effective ionic conductivity of the polymer. In some electrolyte, the solution resistance can also be a rate limiting factor, however, the electrolyte solution we use here (1M aqueous $NaPF_6$), is highly conductive and thus is found not to be the primary limiting factor.

6.2.1 Design of the active catheters

In our previous work [25] (presented in Chapter 5), an RC transmission line model is proposed that describes for rate of charging and actuation, assuming these are limited by ionic resistance, electronic resistance and solution resistance. The model suggests the impedance is in the form of a transmission line (Z) (as shown in Figure 5.1) and is a function of polymer electrochemical properties such as electronic conductivity, σ_e ,ionic conductivity, σ_i , and volumetric capacitance, C_v. The model can then be used to calculate charging in response to the applied voltage. The time dependent charging was used to predict free strain of the polypyrrole and input to a mechanical bending model used to find the dynamic actuation response of a catheter-like structure. The detailed description of the model can be found in Chapter 5 [25]. This model is now employed to estimate optimum geometries for both the positioner and the scanner catheters.

In Chapter 5 an expression for the catheter radius of curvature, R as a function of device geometry, Young's modulus and electrochemical strain was presented (Equation 5.6). By substituting the strain with $\varepsilon = \alpha\rho = \alpha C_v V$, the expression relating the catheter radius of curvature, R, to the actuation voltage, V, is:

$$R(V) = \frac{3}{32}\pi \frac{Yb^4 - Y_p(a+2h)^4 - Ya^4 + Y_p a^4}{Y_p \alpha . C_v . V\left[(a\ )^3 - (a+2h)^3\right]} . \qquad (6.1)$$

Here a and b are the outer and inner diameters of the catheter, h represents the thickness and of the polypyrrole electrodes, Y and Y_p are the Young's modulus of the catheter and the polymer respectively. This equation will be used in designing the positioner catheter which is required to provide a radius of curvature of R< 10 mm. This radius of curvature is sufficient to manoeuvre through most vessels' branches (e.g. the smallest radius of curvature of the left anterior descending coronary artery is 10 mm [26]).

The catheter displacement as a function of frequency (ω=$2\pi f$) was also calculated based on the impedance of the RC transmission line model ($Z(\omega)$) presented in Chapter 5 [25] and was used to predict the actuation speed of the scanner catheter. This was done using the expression of Equation 5.6 and relating the catheter radius of curvature to the frequency dependent electrochemical strain. As was mentioned in section 6.2, the electrochemical strain is proportional to volumetric charge, ρ, via the relationship: $\varepsilon = \alpha\rho$, thus can be estimated from Equation 6.2

$$\rho(\omega) = \left(\frac{1}{j\omega} \frac{V}{Z(\omega)} \right) \frac{1}{Vol} \ . \qquad (6.2)$$

The radius of curvature $R(\omega)$ is then described as a function of frequency by:

$$R(\omega) = \frac{3}{32}\pi \frac{Yb^4 - Y_p(a+2h)^4 - Ya^4 + Y_p a^4}{Y_p \alpha . \rho(\omega)\left[(a\ )^3 - (a+2h)^3\right]} . \qquad (6.3)$$

Equation 6.4 shows the relationship between the frequency dependent catheter tip displacement ($d(\omega)$) and the radius of curvature ($R(\omega)$),

$$d(\omega) = R(\omega) - R(\omega).\cos(\frac{L}{R(\omega)}). \qquad (6.4)$$

Providing that the actuation voltage is within the range proposed in Chapter 2 (-0.4 V to +0.8 V, versus an Ag/AgCl reference electrode) and according to Equation 6.1 a thickness of > 40 μm is required to achieve the large degree of bending (i.e. the requirement for the positioner catheter). The model (Equation 6.4), however, suggests that a polymer thicknesses of ~ 10 μm results in maximum tip displacement at high actuation rate (i.e. the requirement for scanner catheter). Therefore the positioner catheter was coated with 40 μm thick polypyrrole and the scanner catheter was coated with 10 μm thick polymer, and their performances were tested separately as now described.

6.3 Fabrication

The catheter used in this experiment was a Micro Therapeutics Inc. (Irvine, CA) UltraflowTM HPC, with inner and outer diameters of 0.28 mm and 0.5 mm respectively. The maximum allowable length for the active element on the catheter tip is 35 mm. Polypyrrole deposition on the catheter was done in two steps. First a thin layer of polymer was deposited using electroless deposition by chemical polymerization of pyrrole monomer in the presence of oxidizing agent [27]. Then polypyrrole films are electrochemically grown as described in Chapter 1 (section 1.5), following the procedure of Yamaura [28].

Effective patterning of the polypyrrole electrodes, shown in Figure 6.4, is critical to the success of this design. Patterning of polypyrrole electrodes has

previously been achieved using photolithography [31], but this method is not practical for non-planar geometries. Instead, laser micromachining was employed which is a mature technology that can be used for shaping tubular structures such as laser-cut stents. Excimer laser micromachining, in particular, is very well established as a tool for machining of polymers. Excimer laser ablation at 248 nm was used to pattern polypyrrole into 4 separate electrodes (Kr:F excimer laser, GSI Lumonics plus beam expansion optics, a photomask, focusing optics and an xyz programmable stage). An important benefit of using ablation is that there is no thermal damage and minimal debris, as is evident in the clean cut depicted in Figure 6.4. The connections from the polymer electrodes to the potential source were via 100 μm thick gold wires attached to the banana-shaped cuts at the end of the catheter (Figure 6.5). This shape of cut facilitates proper connections to the polymer electrodes avoiding a short circuit connection between separate electrodes. The laser patterning work was performed by Nigel Munce at Sunnybrook research institute under the guidance of Tina Shoa.

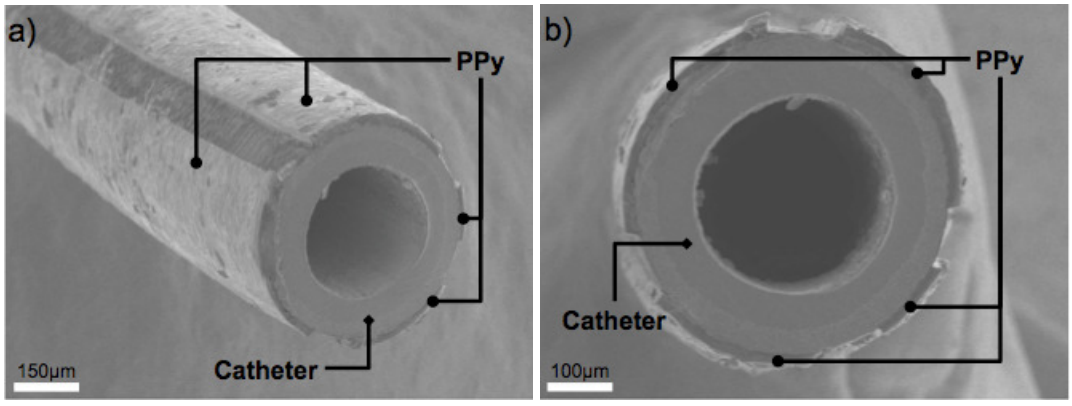

Figure 6.4: SEM images of polypyrrole coated catheter laser ablated to form four polymer electrodes.

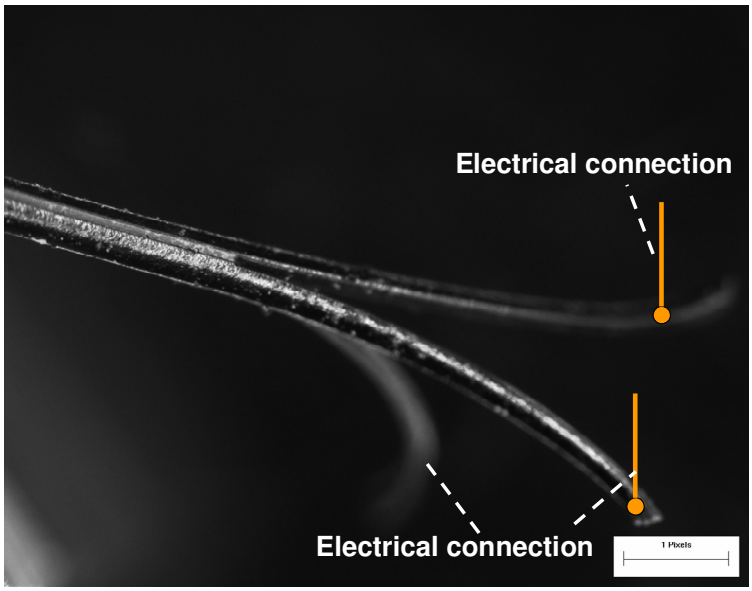

Figure 6.5: Image of the fabricated catheter showing the banana-shaped cut and electrical connections.

6.4 Experimental catheter actuation

As was suggested in section 6.2.1, the positioner catheter was coated with 40 µm thick polypyrrole and the scanner catheter was coated with 10 µm thick polymer, as was suggested by the developed model.

6.4.1 Positioner catheter

The polymer coated positioner catheter was actuated inside the electrolyte by applying a step potential of +0.5 V versus Ag/AgCl reference electrode (within the voltage range proposed in Chapter 2) and a bending radius of R=16.8 mm was achieved in 32 seconds. Figure 6.6 shows the initial and final positions of the catheter. The model for predicting the radius of curvature (Equation 6.1) is compared to experimental results to verify that it can provide a reasonable description of the

response, and then it is used to predict conditions under which the desired 10 mm radius of curvature can be achieved.

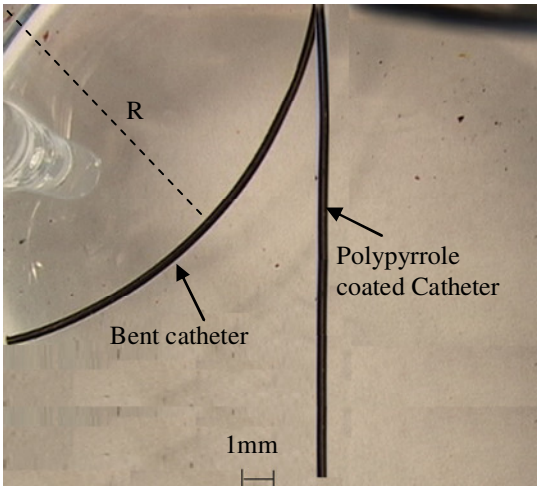

Figure 6.6: Catheter tip position at two states: initial, bent.

Curvature improvement

According to Equation 6.1, curvature can be improved by applying a higher voltage. Figure 6.6 illustrates the effect of actuation voltage on the radius of curvature. In this model a Young's modulus of 350 MPa and 65 MPa for the polypyrrole coating and the catheter were respectively used from our previously measured mechanical parameter (reported in Chapter 5). Voltage, *V*, was increased in order to decrease the radius of curvature (shown as points in Figure 6.7). As shown in this figure, a radius of curvature of R=9.8 mm was achieved by applying 1.2 V across the two polymer electrodes to change the polymer potential from -0.4 V to +0.8 V, versus an Ag/AgCl reference electrode_ the range determined in Chapter 2. This is similar to the curvature achieved in wire guided catheters used at present. Further

increases in voltage were found to lead to better curvature, but shorter lifetimes, and were thus avoided [30].

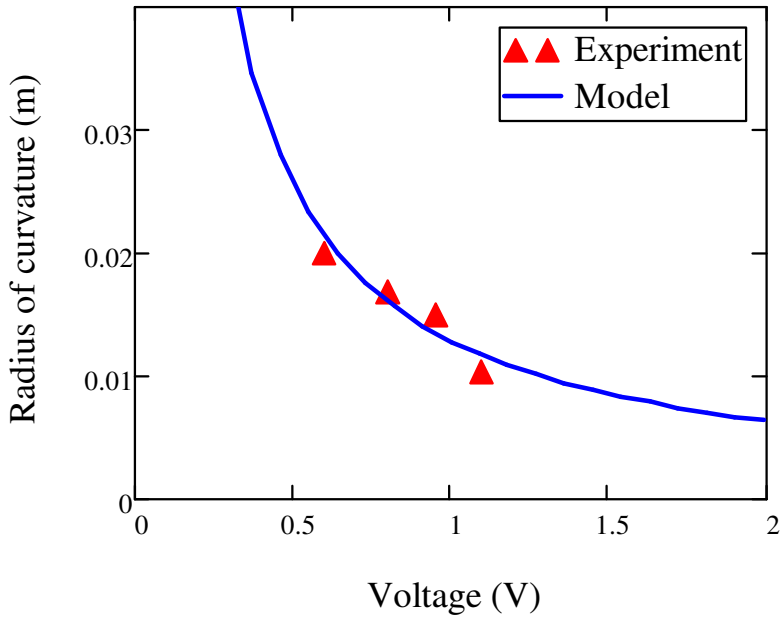

Figure 6.7: Experimental and simulated bending radius versus strain for 40 µm thick polymer

6.4.2 Scanner catheter

The scanner catheter with 4 polymer electrodes was also tested in the same electrolyte (aqueous-$NaPF_6$) by applying potential across the two facing polymer electrodes. In this experiment two potential sources are used (see Figure 6.8); one applies an alternating voltage across the two facing electrodes with high frequency which causes the catheter to move back and forth in y direction relatively quickly; the other source simultaneously applies a potential with a slower frequency to the second polymer electrode pairs resulting in x direction actuation.

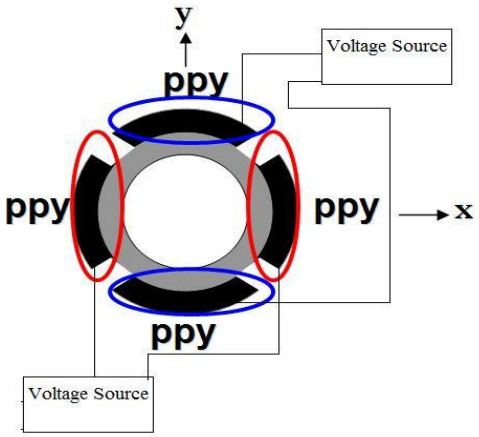

Figure 6.8: Schematic cross-section of the scanner catheter with 4 polymer electrodes.

The primary demonstration of the scanner was performed with a speed of 0.1 Hz in the x direction and 1 Hz in y direction. Figure 6.9 is a view of the scanner tip at initial and final positions with the arrows showing the route of the scanning.

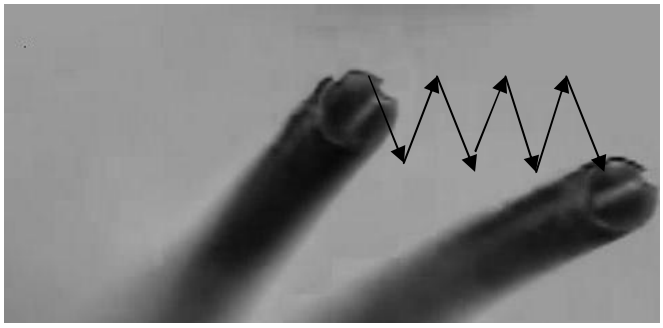

Figure 6.9: Scanner catheter tip position at two states: initial, end of the scanning. Arrows show the scanning path.

A preliminary image was obtained by inserting a ball-lensed fiber optic into the polypyrrole based active catheter. The fibre was connected to a commercially available OCT system. The experiment was performed inside an aqueous solution of 1M AQ- $NaPF_6$ and the optical fiber was actuated back and forth with an applied voltage of -0.5 V to 0.5 V, versus an Ag/AgCl reference electrode, at 1 Hz. Although

voltages below -0.4 V were found to limit charging, (as reported in Chapter 2) the high actuation speed of >1 Hz let us exceed this limit, since the bias time is too short for the polymer to reach that level. An Infra red card (as a test object) was scanned which was placed 1 mm away from the optical fiber. The resulting image shown in Figure 6.10 shows the resolution needed for effective medical imaging [35].

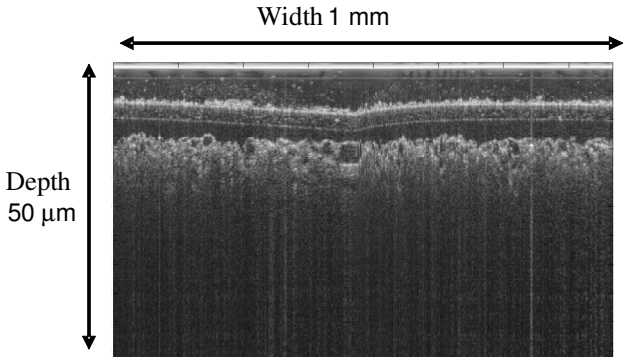

Figure 6.10: OCT image of an infrared card taken using the polypyrrole driven scanner catheter.

Speed improvement

In many medical procedures constant monitoring in real time is essential for the surgical operation, particularly when operating inside a non-stationary environment such as the coronary arteries. In order to achieve real time OCT imaging the scanner catheter requires scanning with higher speed (10-30 Hz) over a 1 mm distance. Figure 6.11 illustrates the catheter displacement as a function of frequency when an actuation potential of -0.5 V to 0.5 V, versus an Ag/AgCl reference electrode, is applied on a 2 cm long scanner catheter. Equation 6.4 was used to predict the actuation response, where in calculating $Z(\omega)$, an ionic conductivity of $\sigma_i = 2.2\times10^{-3}$ S/m, an electronic conductivity of $\sigma_e = 8000$ S/m and a volumetric capacitance of $C_v =$

2×10^8 F/m^3 were used (Chapter 5)[25]. According to the experimental data, a 1 mm displacement was achieved at 1 Hz under ±0.5 V alternating potential. The scanning at 1 Hz was tested over 1 hour and a relatively stable actuation performance was achieved.

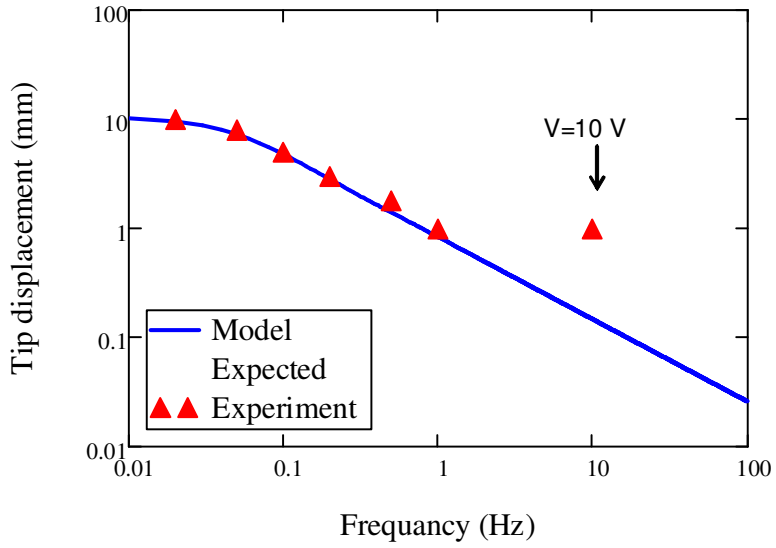

Figure 6.11: Measured and predicted catheter tip displacement as a function of frequency (The model prediction shown is for the applied voltage of 1 V (From -0.5 V to 0.5 V versus Ag/AgCl reference electrode)).

According to the model, tip displacement of 1 mm at 10 Hz can be achieved if the applied voltage is increased to 10 V. Our experimental result (shown in Figure 6.11), also showed that the scanning speed of 10 Hz is possible by applying a high actuation potential (10 V), however the number of scanning cycles was limited due to short polymer lifetime at this potential.

Equations 6.2 - 6.4 were used to study the feasibility of achieving high scanning speed (10 Hz – 30 Hz) of an optical fiber (with a diameter of 55 µm) which is in the lumen of an UltraflowTM HPC catheter, providing that the applied voltage is

within the range suggested in Chapter 2. As mentioned in section 6.2, impedance $Z(\omega)$ is a function of physical properties of the polymer [25]. According to this model, characteristics of the conducting polymer such as electronic conductivity, ionic conductivity and electrochemical strain to volumetric charge ratio need to be improved to achieve the desired catheter scanning speed (i.e. 30 Hz) for real time imaging. Table 1 illustrated the current values of these parameters and the model suggested values needed for obtaining a 1 mm displacement at 30 Hz actuation using the polymer actuator fabricated on the UltraflowTM HPC catheter. Table 6.1 also contains recommendations for achieving the required electrochemical characteristics.

Parameters	**Current value**	**Required value**	**Methods**
Electronic conductivity	0.8×10^{4} S/m	10×10^{4} S/m	-Add a metal coating
Ionic conductivity	2×10^{-3} S/m	8×10^{-3} S/m	-Increase polymer porosity -Use fast mobile ions
Strain/volumetric Charge	4×10^{-11} m^3/C	12×10^{-11} m^3/C	-Use larger mobile ions

Table 6.1 Electrochemical parameters of the polypyrrole driven catheter; current values, model suggested value for achieving 30 Hz actuation and recommendations for improving the mentioned parameters.

There are trade offs in achieving the best performance of the actuator. For instance adding a metal backing to increase the electronic conductivity will lead to an increase in the stiffness of the device which may result in smaller displacement. Using large ions increases the strain to charge ratio but likely leads to a slower rate of response. Therefore careful modification of these properties is required to achieve the best performance.

An alternative is to replace the commercial catheter with a tube-shaped material which has optimum mechanical properties. According to the model, 30 Hz scanning

speed can be achieved (without the requirement of enhancing the polymer ionic conductivity and strain to charge ratio), by using a flexible coating (with a Young's modulus of 1MPa or lower and a thickness of 220 μm or more) around the fiber onto which a thin layer of polypyrrole (~1 μm) is deposited. The only factor that needs to be improved to make this approach work, is the electronic conductivity along the length, which must reach 100,000 S/m. Adding a very thin layer of metal (e.g. 1 nm of gold) on to the polymer was found to have negligible effect on the structural stiffness, thus might be effectively employed to increase the conductivity. The next generation design can reach the desired scanning speed by eliminating the commercial catheter and using such a flexible tube with thin and highly conductive polypyrrole active layers for deflecting the optical fiber inside a rigid encapsulation.

According to the results presented in this section, the polypyrrole driven catheter was successful as a "positioner" in producing the minimum radius of curvature required for cardiovascular catheterization. However, its application as a scanner catheter in real time imaging application is limited by the slow actuation speed of polypyrrole. In order to develop a practical scanner using the commercial catheter investigated, improvements in the material electrochemical properties are required. An alternative approach is to replace the relatively stiff commercial catheter with a flexible coating around the optical fiber onto which a thin and highly conductive polypyrrole is grown. Further work is needed to encapsulate these designs, as will be discussed briefly in the next chapter. The scanner design will be fit within a 2 mm diameter stiff tube containing electrolyte and capped by a lens. The positioner design may be best accomplished by again replacing the commercial

catheter body, this time with an ionically conductive material, thereby enabling ion transport internal to the device.

6.5 Polypyrrole sensor on the catheter

The positioner catheter needs to be bent to a large degree and remain stationary for the surgical operation to be performed on the lesion. The scanner catheter needs to scan the optical fiber over only a 1mm distance. Therefore drift in catheter position should be minimized. In addition the catheter tip may strike the artery wall during the positioning step, which if detected can improve the accuracy and efficiency of the operation.

Currently, x-ray imaging is used to monitor the catheterization process from outside the body. In order to improve the performance of the active catheters, a feedback control system that obtains information on the catheter position from a built-in sensor is very useful. One interesting property of polypyrrole actuators is that they can also be used in reverse mode of operation as a force sensor, as described in Chapter 4. We investigate the feasibility of using polyprrole as both an actuator and a sensor on the catheter. This combination could enable a compact integrated design capable of multitasking without sacrificing the actuation performance (other available sensors are often stiff and impede the actuation). Furthermore, this will be a step towards mimicking natural muscles where all elements of the feedback loop are made of similar high molecular weight materials.

The studies performed in Chapter 4 show that the output voltage, V, of the polypyrrole sensor is $V = -\sigma \cdot \alpha$, where, σ, is the stress to be sensed as applied to the

sensors and α is the strain to charge density ratio of the polymer. The voltage sensitivity of the polymer sensor to stress is therefore determined by the ratio, α, which is measured to be $3.6 \pm 0.8 \times 10^{-11}$ m^3/C (or equivalently V/Pa). In order to detect changes in the catheter position of 50 μm, stresses of about 0.02 MPa need to be detected. This was estimated by relating the catheter tip displacement to its corresponding curvature and stress on the catheter. For detecting stresses <0.02 MPa, voltages <1 μV need to be sensed. According to our measurement of the sensor response at high frequencies, the sensitivity drops to 1.7×10^{-11} - 1.5×10^{-11} V/Pa at frequencies from 10 Hz -30 Hz. This implies the need for detection of even lower voltages for scanner catheter, where 10-30 Hz speed of actuation is required. On the other hand the polypyrrole sensor sharp step response (Figure 4.2) makes it suitable for high frequency sensing applications. Therefore polypyrrole generated voltage needs to be amplified to be employed in practical devices.

In addition to polypyrrole load sensing capability, this polymer can generate a response to the external force applied to it while the polymer itself is actuating [34, 35]. This effect is investigated with its application in detecting the catheter strike to the arterial wall in mind. A sudden increase in the load applied to the polypyrrole electrode during the positioning operation, likely implies that the catheter has struck the arterial wall. Since any further pressure can lead to a puncture of arterial walls and internal bleeding, it will be of great assistance to the person operating the catheter to be provided with a feedback signal corresponding to the load applied on the artificial muscle.

To verify that polypyrrole can sense forces while actuating an experiment was conducted. A step in potential was applied to a polypyrrole free standing film clamped into the Aurora Scientific muscle analyzer, while the external load on the polymer was cycled between 0 and 7 g (equivalent variation in stress of 1.75 MPa). The high-load half-cycle lasted 40 seconds, while the low-load half-cycle lasted 60 seconds. The resulting current from the combined effect of the potential and load change (monitored via Solatron potentiostat) is plotted in Figure 6.12. The inset shows the variations in load. Using signal processing, it is possible to detect the rising and falling edges resulting from the changes in load. Such data can be used by the operator to detect interactions between the catheter and the arterial walls to avoid applying excessive pressure in the wrong direction. This can lead to safer operation.

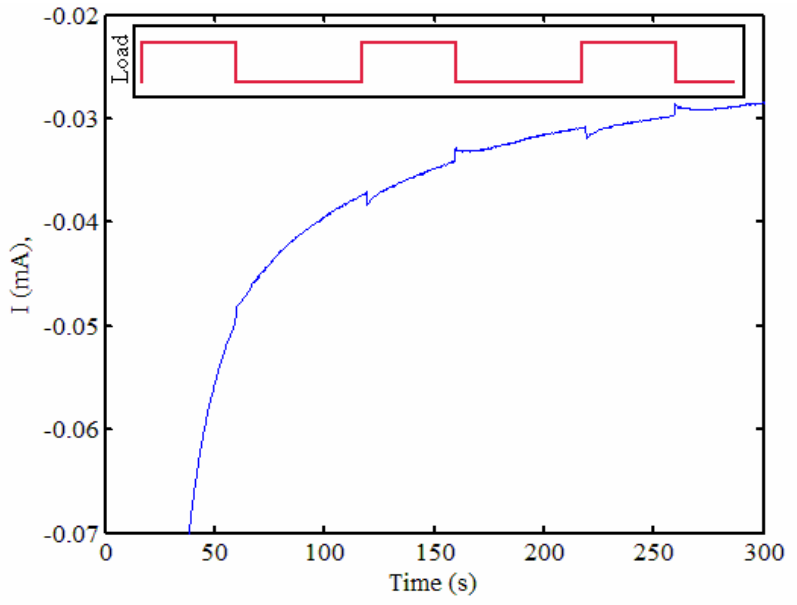

Figure 6.12: The combined effect of actuation and changing the external load on the current going through the cell.

The fabricated positioner catheter was actuated inside the electrolyte and an obstacle was placed on its way, representing the arterial wall. Unfortunately no

measurable current was observed when the catheter bending was stopped by the obstacle, unless we pushed the obstacle manually to hit the catheter hard.

The polypyrrole electrodes of the positioner catheter actuating to a radius of 10 mm, if strikes the arterial wall, undergoes a stress change of ~ 10 kPa. In order to detect this stress a current in the order of 10 nA needs to be sensed, which is practically challenging. The results of this feasibility study show the potential of polypyrrole in sensing load and position; however a sophisticated instrument capable of detecting low voltages and or currents is required.

6.6 Conclusion

Two polypyrrole based active catheters, as a positioner and a scanner, were designed and fabricated for maneuvering and imaging applications inside artery. The bending of the positioner catheter using polypyrrole actuators was demonstrated in an aqueous solution of $NaPF_6$ by applying a step in potential across the two polymer electrodes. A bending radius of 9.76 mm was achieved in 30 seconds which is sufficient for manoeuvring through most vessels' branches. The scanner catheter was also tested and a 2-D motion with a speed of 1 Hz in y direction and 0.1 Hz in x direction was demonstrated. An *ex vivo* OCT image was generated by scanning an optical fiber over a test object using the developed catheter. A scanning speed of 10 Hz is achieved with a tip displacement of 1mm using over-potential actuation, which degraded the polymer within few cycles. The primary challenge in achieving an effective polypyrrole driven scanner catheter for real time OCT imaging is to demonstrate high scanning speed with reasonable liftetime. According to a developed

model, improving the polymer electrochemical properties (i.e. increasing ionic and electronic conductivities, and electrochemical strain) will result in a high speed scanning of the commercial catheter suitable for real time imaging applications. An alternative is to replace the commercial catheter with a flexible tube containing the optical fiber. According to the model, a thin polypyrrole layer with a conductive backing on the tube, can provide the speed required in the imaging application investigated (i.e. 30 Hz) without modification of the material electrochemical properties. Finally a feasibility study on employing polypyrrole as position and load sensors on the catheter was performed which showed a proof of concept. However the sensitivity of polypyrrole sensor was found to be too small to be applied in catheters.

References

[1] J.D.W. Madden, N.A. Vandesteeg, P.A. Anquetil, P.G.A Madden, A. Takshi, R.Z Pytel, S.R. Lafontaine, P.A. Wieringa, I.W. Hunter, "Artificial muscle technology: physical principles and naval prospects" IEEE Journal of Oceanic Engineering, vol. 29, n 3, pp. 706-28, July 2004.

[2] C. Immerstrand, K. Holmgren-Peterson, K.E. Magnusson, E. Jager, M. Krogh, M. Skoglund, A. Selbing, O. Inganäs, "Conjugated-polymer micro- and milliactuators for biological applications" Source: MRS Bulletin, vol. 27, n 6, pp. 461-464, June 2002.

[3] D. Zhou, G.G. Wallace, G.M. Spinks, "Actuators for the cochlear implant", Synth. Met., vol. 135-136, pp. 39–40, 2003.

[4] A. Gursel, G. Daniel, "A bio-inspired robotic locomotion system based on conducting polymer actuators" IEEE/ASME International Conference on Advanced Intelligent Mechatronics, AIM, pp. 998-1004, 2009.

[5] K. Ren, S. Liu, M. Lin, Y. Wang, Q.M. Zhang, "A compact electroactive polymer actuator suitable for refreshable braille display" Proceedings of SPIE - The International Society for Optical Engineering Electroactive Polymer Actuators and Devices (EAPAD), vol. 6524, 2007.

[6] G. Spinks, G. Wallace, J. Ding, D. Zhou, B. Xi, J. Gillespie, "Ionic liquids and

polypyrrole helix tubes: bringing the electronic braille screen closer to reality" Proceedings of SPIE - The International Society for Optical Engineering, vol. 5051, pp. 372-380, 2003.

[7] E. Smela, "Conjugated polymer actuators for biomedical applications" Advanced Materials, vol. 15, n 6, pp. 481-494, March 17, 2003.

[8] A. Mazzoldi, D. De Rossi, "Conductive polymer based structures for a steerable catheter", in Proc. SPIE–The International Society for Optical Engineering, vol. 3987, pp. 273-80, 2000.

[9] Y. Haga, M. Esashi, "Biomedical microsystems for minimally invasive diagnosis and treatment", Proc. of the IEEE, vol. 92, n 1, pp. 98-114, 2004.

[10] K. Ikuta, M. Tsukamoto, S. Hirose, "Shape memory alloy servo actuator system with electric resistance feedback and application for active endoscope", in Proc. IEEE Int. Conf. Robotics and Automation, pp. 427–430, 1988.

[11] D. Reynaerts, J. Peirs, H. V. Brussel, "Design of a shape memory actuated gastrointestinal intervention system", in Proc. 5th Int. Conf. New Actuators, pp. 26–28, 1996.

[12] W. C. McCoy, Steerable and aimable catheter, U.S. Patent 4543 090, 1985.

[13] S. Kaneko, S. Aramaki, K. Arai, Y. Takahashi, H. Adachi, K. Yanagisawa, "Multi freedom tube type manipulator with SMA plate", in Proc. Int. Symp. Microsystems, Intelligent Materials and Robots, pp. 27–29, 1995.

[14] M. Salimuzzaman, A. Matani, O. Oshiro, K. Chihara, M. Asao, "Visualization of a blood vessel using a micromotor", in Proc. Tech. Dig. 14th Sensor Symp. pp. 279–280, 1996.

[15] H. Lehr, W. Ehrfeld, B. Hagemann, K.-P. Kamper, F. Michel, Ch. Schulz, Ch. Thurigen, "Development of micro and millimotors", Min. Invas. Ther. Allied Technol, vol. 6, pp. 191–194, 1997.

[16] S. Gue, T. Fukunda, K. Kosuge, F. Arai, K. Oguro and M. Negoro, "Micro Catheter System with Active Guide Wire", in Proc. IEEE International Conference on Robotic and Automation, Nagoya, Aichi, JAPAN, vol.1, pp. 79-84,1995.

[17] S. Guo, T. Nakamura, T. Fukuda, "Microactive guide wire using ICPF actuator-characteristic evaluation, electrical model and operability evaluation", in Proc. of the IEEE IECON 22nd International Conference on Industrial Electronics, Control, and Instrumentation, Taipei, pp. 1312–1317, 1996.

[18] K. Onishia, Sh. Sewaa, K. Asakab,N. Fujiwarab, K. ogob, "Bending response of polymer electrolyte actuator", in Proc. SPIE Smart Structures and Materials, vol. 3987, pp. 121-128, 2000.

[19] J. Carey, A Fahim, M. Munro, "Design of braided composite cardiovascular catheters based on required axial, flexural, and torsional rigidities" Journal of Biomedical Materials Research - Part B Applied Biomaterials, vol. 70, n 1, pp. 73-81, 2004.

[20] Yang V.X.D., Tang S.J., Gordon M.L., Qi B., Gardinar G., Kortan P., Haber G.B., Kandel G., Vitkin I.A., Wilson B.C., and Marcon N.E., "Endoscopic Doppler optical coherence tomography: first clinical experience with a novel imaging technique", Gastrointestinal Endoscopy, 61, pp. 879-90, 2005.

[21] Munce, Nigel R. , Mariampillai, Adrian; Standish, Beau A.; Pop, Mihaela; Anderson, Kevan J.; Liu, George Y.; Luk, Tim; Courtney, Brian K.; Wright, Graham A.; Vitkin, I. Alex; Yang, Victor X.D. "Electrostatic forward-viewing scanning probe for Doppler optical coherence tomography using a dissipative polymer catheter" Optics Letters, vol. 33, n 7, pp. 657-659, April 1, 2008.

[22] A. Mazzoldi, A. Della Santa, D. De Rossi, "Conducting polymer actuators: properties and modelling" OSada, Yoshihito and De Rossi, Danilo E., Polymer Sensor and Actuators. Heidelberg:Springer Verlag, 1999.

[23] R. H. Baughman, R. L. Shacklette, R. L. Elsenbaumer, "Micro electromechanical actuators based on conducting polymers". Lazarev, P. I., Editor. Topic in Molecular Organization and Engineering, Molecular Electronics. Dordrecht, Kluwer, vol. 7, pp.267, 1991.

[24] J.D.W. Madden, G. A. Peter, I.W. Hunter, "Conducting polymer actuators as engineering materials" Proceedings of SPIE 9th Annual Symposium on Smart Structures and Materials: Electroactive Polymer Actuators and Devices, Yoseph Bar- Cohen, Ed., SPIE Press, pp.176-190, 2002.

[26] T. Shoa, D. Yoo, J. Madden, "A dynamic electromechanical model for

electrochemically driven conducting polymer actuators", submitted to IEEE Transactions on Mechatronics, 2010.

[26] M. Prosi, K. Perktold, Z. Ding, M. Friedman, "Influence of curvature dynamics on pulsatile coronary artery flow in a realistic bifurcation model" in Journal of Biomechanics, vol. 37 , Issue 11 , pp. 1767 – 1775.

[27] R. V. Gregory, W. C. Kimbrell, H. H. Kuhn, "Conductive textiles" Synthetic Metals, vol. 28, n 1-2, pp.823-835, Jan 30, 1989.

[28] M. Yamaura, T. Hagiwara, K. Iwata, "Enhancement of electrical conductivity of polypyrrole film by stretching: counter ion effect" Synthetic Metals, 26, pp.209-224, 1988.

[29] M. Cole, J. D. Madden, "The effect of temperature exposure on polypyrrole actuation" Materials Research Society Symposium Proceedings, vol. 889, pp.105-110, 2006.

[30] T. Shoa, M. Cole, V. Yang, J. D. Madden, "Polypyrrole actuator operating voltage limits in aqueous NaPf6" in Proc. SPIE: Smart Structures and Materials: Electroactive Polymer Actuators and Devices, vol. 6524, pp. 652421, 2007.

[31] E.W.H. Jager, E. Smela, O. Inganas, "Microfabricating conjugated polymer actuators" Science, 290, 1540–5, 2000.

[32] Y. Wang, M. Bachman, G.P. Li, S. Guo, B.J. F. Wong, Z. Chen, "Low-voltage

polymer-based scanning cantilever for *in vivo* optical coherence tomography" Optics Letters 30, n 1, 53-55, 2005.

[33] T. F. Otero, M. T. Cortes, "A sensing muscle" Sensors and Actuators, B: Chemical 96, 152-156, 2003.

[34] T. F. Otero, M. T. Cortes, "Artificial muscles with tactile sensitivity" Advanced Materials 15, 279-282, 2003.

[35] K. Lee, N.R. Munce, T. Shoa, L.G. Charron, G.A. Wrigh, J.D. Madden, V.X.D. Yang, "Fabrication and characterization of laser-micromachined polypyrrole-based artificial muscle actuated catheters" Sensors and Actuators, A: Physical, vol. 153(2), pp. 230-236, 2009.

[36] J.D.W. Madden, B. Schmid, M. Hechinger, S.R. Lafontaine, P.G.A. Madden, F.S. Hover, R. Kimball, I.W. Hunter, "Application of polypyrrole actuators: Feasibility of variable camber foils" IEEE Journal of Oceanic Engineering, 29,3: 738-749, 2004.

[37] A. Della Santa, A. Mazzoldi, D. De Rossi, "Steerable microcatheters actuated by embedded conducting polymer structures" Journal of Intelligent Material Systems and Structures, 7- 292-300, 1996.

CHAPTER 7: CONCLUSIONS

7.1 Significance of the research

Polypyrrole actuators are being investigated for applications in robotics and devices. Their biocompatibility, low cost, large strain, low actuation voltage and ability to be miniaturized have made this polymer particularly promising for biomedical applications. Advanced biorobotics and minimally invasive medical procedures where a miniaturized active element is needed to provide a controllable movement of a surgical tool inside the body could significantly benefit from this technology. Although the polypyrrole artificial muscle has shown great potential to be used in this application, it needs to be further characterized and modelled as an engineering material. This characterization has been a focus of the thesis contributions, as has the initial study of the feasibility of application of polypyrrole actuators in active catheters.

The significance of this research is in its contributions in three main subjects:

1. Characterization of polypyrrole artificial muscles in terms of electrochemical stability, dependence of the mechanical properties on operational conditions and performance as a mechanical sensor. These studies are crucial in developing practical devices using a polypyrrole artificial muscle.

2. Development of two physical models; one is a semi-empirical model which describes the electromechanical coupling in polypyrrole artificial muscle, and the other is an analytical model which predicts the dynamic actuation response. These models are expected to serve as effective design tools for artificial muscle engineers.

3. Demonstratoin of the feasibility of using polypyrrole to deform a catheter sufficiently for eventual use in minimally invasive diagnostic procedures, whose potential medical outcomes (particularly in optical biopsy and early detection of cancer) could have a significant impact on health.

The contributions are outlined in more detail at the end of the introduction section. In the remarks that follow these contributions are further discussed and future work outlined, including efforts needed to make the catheter a medically practical device.

7.2 Concluding remarks

Characterization studies were included in the first three chapters (Chapter 2-4). In Chapter 4, in addition to the characterization study on polypyrrole sensors, a model for electromechanical coupling was also proposed. An analytical model was presented in Chapter 5, and application of polypyrrole in active catheters was described in Chapter 6. In this section conclusions of the thesis work are summarized.

In order to determine the range of applications that are appropriate for polypyrrole actuators, a key factor is the electrochemical stability. We investigated

polypyrrole electrochemical stability in aqueous-$NaPF_6$ which is known to provide large stable strains. This was done by cycling the polymer film between fixed voltages and measuring the charge transfer. In Chapter 2 it is reported that, voltages higher than +0.8 V (versus an Ag/AgCl reference elerctrode) result in a rapid irreversible reduction in the polymer charging capability, and this reduction may be due to a permanent degradation of the polymer. Reduction in charge transfer at voltages less than -0.4 V (versus an Ag/AgCl reference electrode) is also observed, likely due to a decrease in the polymer conductivity. Therefore potentials higher than +0.8 V (versus an Ag/AgCl reference electrode) should be avoided for the stable operation of the actuator. Potentials lower than -0.4 V (versus an Ag/AgCl reference electrode) lead to slower actuation. A stable actuation performance was achieved over this potential range for at least 30 min.

When a material is under load, a change in stiffness will lead to a deformation. In Chapter 3 it was shown that the stiffness of polypyrrole is a function of charge state (oxidation state), frequency and load. The magnitudes of the electro-stiffening, frequency dependence and load dependence are important to understand in order fully describe the actuation of polypyrrole. According to the measurements, polypyrrole acts like a viscoelastic material, thus its complex Young's modulus including storage and loss components was studied. Uniformity of doping was ensured by allowing enough time to reach steady state charge levels, and the creep during measurements was minimized by using preconditioning cycles. The results of this study show that storage modulus decreases (from 1 GPa to 0.80 GPa) as the polypyrrole oxidation potential increases (from -0.4 V to +0.4 V versus Ag/AgCl reference electrode). The

loss modulus, on the other hand, increases from 55 MPa to 80 MPa. An increasing trend in the Young's modulus is also observed with the applied load. The storage modulus increases from 0.65 GPa to 1 GPa by increasing the applied load from 0.2 MPa to 2.5 MPa. The modulus is found to be history dependent and increase with time through the experiment, which may be due to stretch alignment of the polymer. It is also observed that the complex Young's modulus increases in proportion to the logarithm of frequency. In addition the modulus is found to decrease during actuation, perhaps due to the additional perturbation by the passage of the charge.

All these variations in the modulus as a function of voltage, load, frequency, history and actuation happen simultaneously in the polypyrrole driven catheter, however, their effective contribution to the active strain is very small (<0.2% strain). In short, providing that the loads are modest (< 5 MPa), variations in the modulus will have a relatively small impact on the overall mechanical response. In cases where larger stresses are encountered, and or high precision in strain is needed, then variation in modulus will need to be taken into account. This will be made more difficult by history dependence of the mechanical properties.

The sensing ability of polypyrrole is another attractive feature which mimics natural muscles, in that all the functional elements are integrated into the actuator. For the catheter under investigation it could serve as a position sensor in a feedback loop. It could also be used as a force sensor to detect the catheter strike onto the arterial wall by sensing sudden increases in the load applied to the polymer. In Chapter 4 the properties of polypyrrole sensors were investigated and a link between actuation and sensing was demonstrated. It was shown that the same constant of proportionality

describes the response in both actuation and sensing. A new mechanism for electromechanical coupling is suggested that can be exploited in materials that are both ionically and electronically conducting. Based on this finding a semi-empirical model of the electromechanical coupling was proposed. The model suggests that the insertion of ions into the polymer requires mechanical work to elastically deform the matrix. The external application of stress alters the internal stress on ions, helping insert or remove charge, and change voltage. The frequency dependence of the relationship between stress and voltage was also investigated. The sensor response is relatively stable at frequencies between 0.1 Hz and 100 Hz. The results and models presented enable the prediction of polypyrrole sensor and actuator responses. The results of this study are used in Chapter 6, to investigate the feasibility of using polypyrrole sensor on active catheters. It is found that polypyrrole is able to sense sudden changes in load during actuation; however the sensing effect is not strong enough to provide force feedback when polypyrrole actuators are used to drive catheters.

In designing artificial muscle driven devices, a physical model capable of accurately predicting the actuation response is needed. The existing models mostly focus on the static operation of the actuator; however in many applications dynamic behaviour governs the performance of the device. The scanner catheter described in Chapter 6, for instance, needs to be accurately modelled in the high frequency regime of operation so that its performance in rapid scanning can be evaluated. In Chapter 5 an analytical model was presented to predict the dynamic actuation response of electrochemically driven structures. A 2D impedance model was first presented

which uses the conducting polymer RC transmission line equivalent circuit to predict the charge transfer during actuation. The predicted electrochemical charging was then coupled to a mechanical model to find the actuation response of a bending structure. The advantage of this model compared to existing models is that it represents the two dimensional charging of the polymer, namely through the thickness of the polymer structure and along its length. The model considers both ion 'diffusion' through the thickness and electronic resistance along the length. An output of the model is the prediction of charge density in the polymer as a function of position and time, which is then used to estimate free strain via the strain to charge ratio. Given the modulus of the polymer and of passively deformed structures, time dependent deformation is then determined. The complete electromechanical model is a function of ionic and electronic conductivities, dimensions, volumetric capacitance, elastic modulus, and strain to charge ratio, all of which are measured independently. The full electro-mechanical model was shown to provide a good description of the response of bending polymer catheter when comparing with experimental results. The model can be effectively used as a design tool for electrochemically driven devices, and was used later in Chapter 6 to design polypyrrole driven catheters.

Results of the characterization studies (presented in Chapter 2-4) along with the analytical model proposed in Chapter 5 were used to evaluate the feasibility of using polypyrrole to drive a commercial catheter for manoeuvring and imaging applications inside arteries. In Chapter 6 design, fabrication and demonstration of two active catheters are presented; 1) a "positioner catheter" for the manoeuvring application which is meant to be bent to a minimum curvature of 10 mm, 2) a "scanner catheter"

for imaging application which is meant to move an optical fiber back and forth in two dimensions with a relatively high speed (10-30 Hz). The polypyrrole actuated structure produced enough bending moment on the positioner catheter to provide a curvature radius of <10 mm, sufficient for manoeuvring through most vessels' branches. The actuator produced a 2-D scanning motion of the catheter tip repeatedly with a rate of 1 Hz in one dimension and 0.1 Hz in the other dimension. It was used to scan an optical fiber over a test object to generate an *ex vivo* OCT image. Although the scanner catheter showed potential to be used in imaging applications, its scanning speed is too slow to produce images in real time. A scanning speed of 10 Hz was achieved by applying 10 V versus an Ag/AgCl reference electrode (exceeding the safe potential range reported in Chapter 2), which as was expected degraded the polymer within few cycles. According to the developed model improving the polymer electrochemical properties (i.e. increasing ionic and electronic conductivities, and electrochemical strain) will result in a fast scanning of the commercial catheter suitable for real time imaging applications. The model also suggests replacing the commercial catheter with a flexible tube to encompass the optical fiber. A thin polypyrrole layer with a conductive backing can then be fabricated on the flexible tube, to provide the speed required in the imaging application investigated (i.e. 30 Hz), without modification of the material electrochemical properties.

At the end of the chapter a feasibility study was performed to evaluate the performance of polypyrrole sensors on the catheter as an active element of a feedback

loop. As was mentioned above, the sensitivity is too low to be used in this application.

7.3 Implications of the research findings

The results obtained from characterization studies and the models developed for polypyrrole sensor and actuator are relevant to virtually any application of polypyrrole as an actuator or mechanical sensor. Some of the potential applications are now described.

- The results of the studies on electrochemical stability of polypyrrole could be used to define the appropriate range of potential for electrochemically driven polypyrrole devices (e.g. actuators and supercapacitors) which operate in aqueous-$NaPF_6$. The choice of the proper voltage range depends on the application of the device. For instance, if short life cycles are acceptable (e.g. disposable devices) a broader voltage range may be used.

  The method described to find the safe voltage range can be applied to study the electrochemical stability of other electrochemically driven materials (such as carbon nanotubes, hydrogels, ionic polymer composites and other types of conducting polymers) in different electrolytes.

- The findings from the study of polypyrrole Young's modulus dependency on voltage, load and frequency could be used in developing effective polypyrrole actuators and sensors. This work serves as a ground work for modelling the mechanical behaviour of artificial muscle actuators.

We have gone to great lengths in this study to ensure that oxidation of the polymer sample is homogenous and known. The approach used to ensure homogenous and known oxidation state could be of benefit to others seeking to measure properties of conducting polymers as a function of oxidation state.

- The study performed on the sensing ability of polypyrrole and our proposed semi-empirical model of the sensor/actuator electromechanical coupling can be used in other electrochemically driven materials that are both ionically and electronically conducting. The findings of this study could lead to development of an integrated device where polypyrrole is used as both sensor and actuator. This could be an important step towards mimicking natural muscle in that all the functional elements are integrated into the actuator.

- The dynamic 2D impedance model proposed in this thesis for polypyrrole actuators can potentially be used as a design tool for other electrochemically driven devices, where the operation of the device is based on charging an imperfectly conductive electrode inside an electrochemical cell. Supercapacitors, batteries and other artificial muscle actuators are examples of electrochemical devices where the 2D impedance model can be employed to understand and predict their charging behaviours.

- The application of the active catheter developed in this research was initially targeted towards cardiovascular interventions. The final catheter is meant to access the lesions in narrow and curved blood vessels where a conventional guide wire cannot reach. The catheter tip should then be bent

actively to access the lesion. A flexible wire is then inserted through the lumen of the catheter to navigate through the lesion and open a channel for passage of blood. The whole process is monitored using angiography from the outside and intravascular imaging from the inside simultaneously. The intravascular imaging is meant to be performed using the scanner catheter equipped with an OCT optical fiber. OCT imaging using the scanner catheter provides a 3D high resolution (close to cellular level) image from the lesion which is very useful for treatment purposes. This imaging technology is expected to be used as optical biopsy in near future for early detection of diseases.

Although the polypyrrole driven catheter was primarily designed for cardiovascular applications, its application can likely be extended to other catheterization and endoscopic procedures such as brain catheterization, ablation catheters, bronchoscopy, colonoscopy and so on. Miniaturizing the device enables accessing narrow and complicated vessels inside the body that are not accessible using the current technology. In brain catheterization, for instance, a miniaturized active catheter could be extremely beneficial.

7.4 Suggestions for future research and development of catheters

Polypyrrole artificial muscle shows great potential to be employed on catheters to provide controllable manoeuvrability inside the body. However, actuation of this device involves using electrolytes and electrical currents which in most medical applications mandates encapsulation, especially since only very limited currents are permitted to be applied *in vivo* [1]. We can also extend the application of the active

catheters to reach tissues in narrow complex passages (e.g. blood vessels of the brain and tertiary bronchi of the lung) by further miniaturizing the design. Multiple imaging probes can be embedded inside the catheter to obtain more information from the diseased tissue, which required some design modifications.

Despite the attractive characteristics of polypyrrole artificial muscle in developing active catheters, a key challenge remains the slow actuation speed, which limits the performance of the scanner catheter in real time imaging. Although design optimization can be performed to achieve the speed required for real time imaging as was suggested in Chapter 6 (i.e. replacing the catheter with a flexible tube coated with a conductive backing and thin polypyrrole actuators), improving the actuation speed of the polymer material itself can significantly enhance its applicability. In order to address this issue we need to improve the electrochemical properties of the polymer as was found from the model predictions. In the following subsections some ideas for solving the remaining challenges with the catheter are explored.

7.4.1 Encapsulation

Passing substantial currents through the blood is incompatible with medical standards and is unlikely to produce the optimum actuation performance. For this reason an encapsulated design is sought before *in vivo* testing can begin. The scanner catheter could be encapsulated inside a rigid tube filled with the electrolyte. A lens is embedded in front of the catheter tip to amplify the angular scanning as shown in Figure 7.1 (similar to Figure 6.1A). The total outer diameter of the catheter tip including encapsulation needs to be small (< 3 mm).

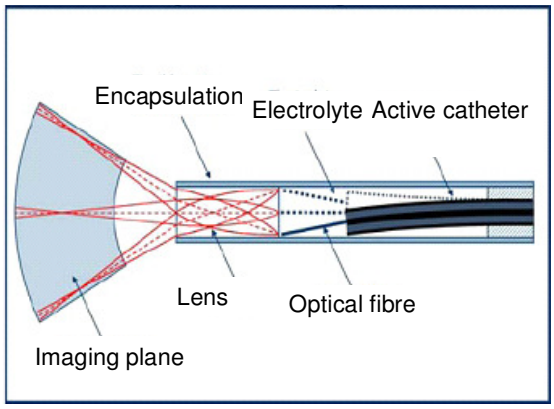

Figure 7.1: Schematic of an encapsulated scanner catheter.

Encapsulation of the positioner catheter is more challenging, since the encapsulation material is a part of the bending structure. This material needs to flexible so that it does not impede the performance of the polymer actuator in bending the device. A design is presented in Figure 7.2, where the active catheter is encapsulated inside a coating that is impermeable to ions. Four polypyrrole actuators are used in this design to provide bending moment in two directions, as shown in Chapter 6, Figure 6.4. The four polymer strips are patterned on a gel electrolyte layer, which itself surrounds a central tube. An encapsulant will be added creating a completely encapsulated device that can be bent in either of two directions.

The model presented in Chapter 5 (Equation 5.6) was modified for the proposed geometry and suggested the following parameters in order to achieve the bending radius of 10 mm on a commercial catheter (Ultraflow^{TM} HPC): tube Young's modulus of 20 MPa with an outer and inner diameter of 1mm and 0.8 mm respectively, electrolyte gel Young's modulus of 1MPa with a thickness of 0.3 mm. The Ultraflow catheter has a Young's modulus of 65 MPa and an outer and inner diameter of 0.5mm and 0.28 mm respectively. According to the model prediction a

minimum bending radius of 10 mm can be achieved in ~ 30 s with a polymer electrode thickness of 40 μm capable of generating an electrochemical strain of 4%.

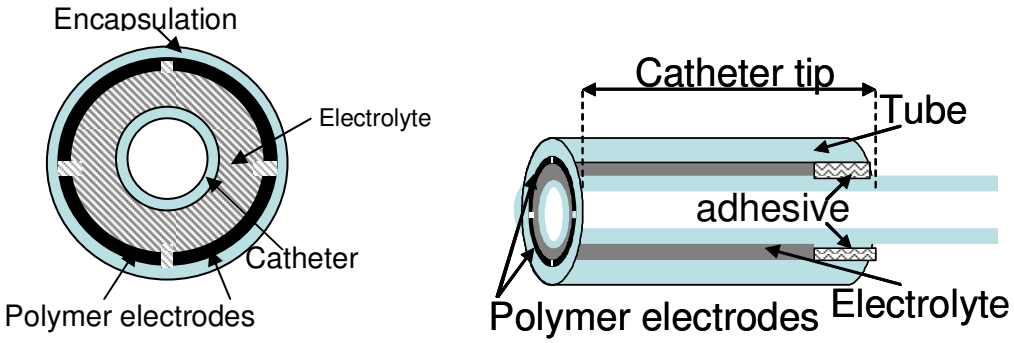

(a) (b)

Figure 7.2: Encapsulated design for active catheters: a) cross section view, b) side view.

7.4.2 Miniaturizing the device

In order to further miniaturize the design to enable access to narrow and torturous blood vessels, fabricating the catheter in house with optimum mechanical properties and tip flexibility is suggested. Fabricating a flexible tube containing an optical fiber onto which highly conductive polymer actuators are fabricated is also beneficial for high speed scanning of the optical fiber as was suggested in Chapter 6. Figure 7.3 shows an optical fiber embedded catheter made of silicone which we developed during this research. Polypyrrole electrode will be formed on to the catheter and an encapsulant will be added similar to the approach suggested in Figure 7.2. A thin layer of gold can also be deposited onto the polypyrrole electrode to enhance its electronic conductivity and thus the actuation speed.

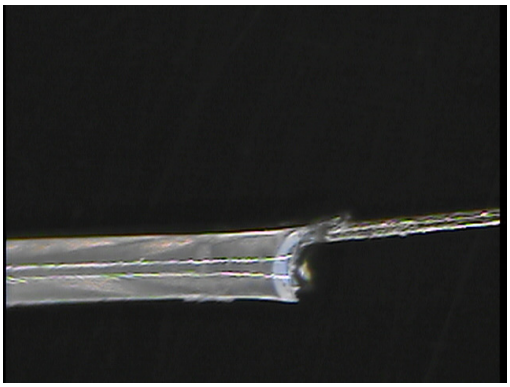

Figure 7.3: Picture of a silicone catheter with an embedded optical fiber

A more efficient design would be a catheter body which is itself an ion conductor such as a solid electrolyte [2,3] or a gel electrolyte [4]. The catheter body serves as both the mechanical tubing needed for passing medical tools and as the electrolyte for the polypyrrole actuators. Previous work has demonstrated the use of such polymer and gel based structures in bending bilayers and trilayers, so the primary challenge is to form these layers as tubes. Another challenge is to maintain high ionic conductivity for the polymer fast scanning capability.

7.4.3 Improving the actuation speed

In order to improve the polypyrrole actuator speed, which is mostly limited by the material ionic and electronic conductivities, as discussed in Chapter 6, adding a conductive backing to the polymer, or incorporating conductive nano-particles (i.e. metals and carbon nanotubes) into the polymer material is suggested for reducing electronic resistance limited charging, while increasing the porosity of the material by modifying the growth condition or post processing of the synthesized polymer (e.g.

cutting holes) to enhance ionic conduction is recommended for increasing rates of ion transport.

Analysis suggests that it will be difficult to use these techniques to push frequency response much beyond 100 Hz. Where faster scanning is needed in one axis, combining actuator technologies to form a hybrid device, such that the polypyrrole actuator provides large catheter bending of the beam structure for example and another actuator (e.g. a piezoceramic) provides fast catheter axial scanning is worth investigating as it plays to the advantages of the actuator technologies (fast motion for piezoelectrics and large bending for polypyrrole). This configuration might be used to create a scanning confocal or multiphoton probes.

In summary, polypyrroler artificial muscle driven catheters show potential to be used in future biorobotics and minimally invasive surgery. Its application in controllable manoeuvrings for guiding surgical tools seems promising, but its actuation speed needs to be improved for real time imaging applications. Miniaturization of the encapsulated active catheter could facilitate accessing narrow and deep vessels leading to useful clinical applications.

References

[1] Shoa, T., Madden, J.D, Munce, N.R., Yang, V.X.D. Chapter 11, Biomedical applications of electroactive polymer actuators, Ed. F. Carpi and E. Smela, Wiley book: 229-248, 2008.

[2] Della, A. Santa, A. Mazzoldi, D. de Rossi (1996) "Steerable microcatheters actuated by embedded conducting polymer structures", J. Intelligent Mat. Syst. Struc., 7, 3, 292–300.

[3] F Vidal, C Plesse, G Palaprat, A Kheddar, J Citerin, D, Conducting IPN actuators: From polymer chemistry to actuator with linear actuation", Volume 156, Issues 21-24, 1 December 2006, p.1299-1304.

[4] Madden, John D.W; Cush, Ryan A.; Kanigan, Tanya S.; Brenan, Colin J.; Hunter, Ian W. "Encapsulated polypyrrole actuators" Synthetic Metals, v 105, n 1, p 61-64, August 16, 1999.

APPENDIX 1[6]: CHALLENGE WITH OPEN CIRCUIT EXPERIMENT ON POLYPYRROLE

In Chapter 3 we studied polypyrrole Young's modulus dependency on oxidation state, load and frequency. This study was performed by biasing the polymer at different oxidation states (from -0.4 V to +0.4 V versus an Ag/AgCl reference electrode) and measuring the polymer stiffness by applying load (from 0.7 MPa to 2.5 MPa) over a range of frequency. During the measurements of the polymer stiffness at each oxidation state the bias voltage was kept constant. The experiments performed in Chapter 3 were also repeated under open circuit condition where the bias voltage was disconnected. This case was studied for conditions where polypyrrole needs to be operated in open circuit mode, such as a polypyrrole sensor that generates voltage in response to a detected force or displacement.

In each case, the cell was open circuited after the charging at each oxidation state had been complete. Cycling with a sinusoidal wave to stabilize the load at various load levels seems to have been successful at constant-potential experiments. However, considerable drift in position is observed during open-circuit tests. Figure A1.1a and b show the measured displacement in open circuit mode in response to a sinusoidal load applied on the polymer film after being biased at -0.4 V and +0.4 V.

[6] This is originally the appendix to the manuscript on which chapter 3 is based.

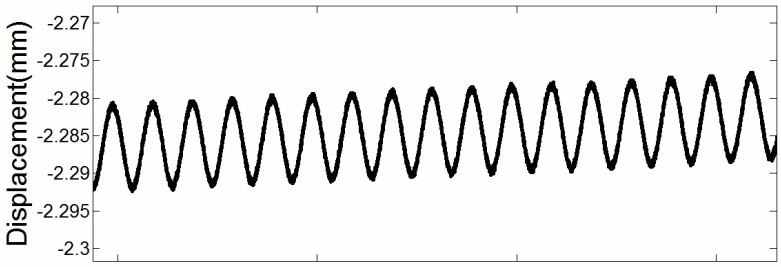

(a)

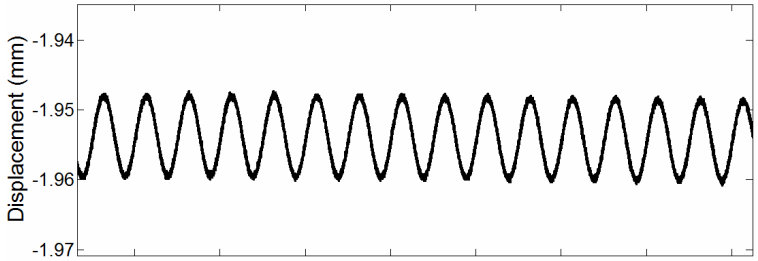

(b)

Figure A. 1 : The measured polymer displacement in response to sinusoidal wave in load at open circuit after being biased (a) at -0.4 V and (b) at +0.4 V (during the last 150 sec.)

The amount of creep is more significant when the polymer was biased at the reduced state of -0.4 V. In order to investigate this effect the potential of the polymer at open circuit was recorded during open circuit measurements. Figure A1.2a and b depict the polymer potential in open circuit mode after being biased at -0.4 V and +0.4 V respectively. According to Figure A1.2a, polypyrrole potential rises towards higher oxidation states at open circuit, even after having been biased at a reduced state of -0.4 V. This drift in the OC potential may be due to a gradual charge loss, caused by Faradaic reactions involving impurities or reactants (e.g. dissolved oxygen) at the polypyrrole/electrolyte interface [1-6]. As shown in Figure A1.1a, the direction of the creep after biasing at -0.4 V, is also upward which suggests volume increase

during the open circuit experiment. This can be the result of ions insertion into the polymer to balance the induced charge from the rising potential shown in Figure A1.2a. Figure A1.1b and 2b suggest the opposite phenomenon for the polymer which was at a potential higher than the equilibrium of 0.3 V. If fixing the position of the actuator is desired, keeping the potential constant can effectively achieve that goal, while leaving the actuator at open circuit leads to a slow creep.

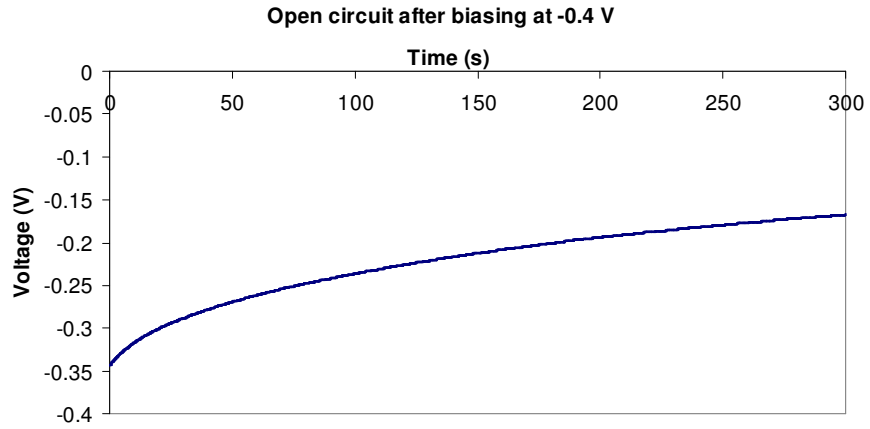

(a)

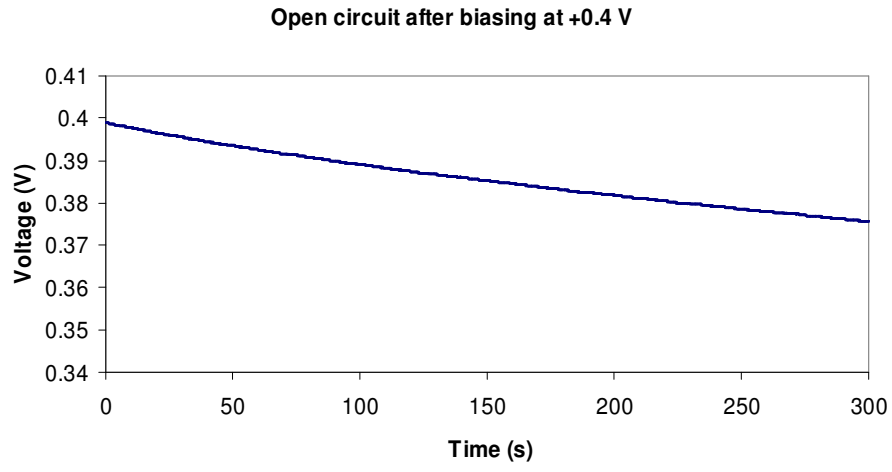

(b)

Figure 7.4: The measured polymer open circuit potential after being biased (a) at -0.4 V and (b) at +0.4 V.

The measured Young's modulus under open circuit experiment is in the same order as the constant potential experiment with a slight difference most pronounced at reduced states (not shown here). This difference is expected since the potential of the polymer when reduced rises rapidly at open circuit experiment, as shown in Figure 3.12a, and hence the oxidation state does not remain the same as the constant potential condition.

References

[1] J He, D E. Tallman, G. P. Bierwagen, Journal of The Electrochemical Society 151,12 (2004) B644-B651.

[2] M. Agata; N. Urszula, M. Krzysztof, Journal of Electrochimica Acta 46 (2001) 4113-4123.

[3] P. Pfluger, M. Kronubi, G.B. Street, G. Weiser, J. Chem. Phys. 78 (1983) 3212.

[4] Y. Son, K. Rajeshwar, J. Chem. Soc. Faraday Trans. 88 (1992) 605.

[5] J. Lei, C.R. Martin, Chem. Mater. 7 (1995) 578.

[6] B. E. Conway, Electrochemical Supercapacitors: Scientific Fundamentals and Technological Applications. (1999) Springer.

APPENDIX 2: COMPARISON OF THE 2D IMPEDANCE MODEL WITH IMPEDANCE SPECTROSCOPY OF POLYPYRROLE

Electrochemical Impedance Spectroscopy is a method employed to characterise the dynamic behaviour of electrochemical cells. In this method the impedance of the electrochemical cell is measured over a range of frequency. A fitting routine can be used to find an equivalent circuit whose impedance has a similar dependence on frequency as the measured impedance response. The standard equivalent circuits for electrochemical cells which includes one capacitor does not provide a good fit for the artificial muscle electrodes and exhibits deviations from the experimentally measured response. In Chapter 5 we presented a 2D transmission line equivalent circuit model including lumped RC elements (Figure 5.1) for polypyrrole actuators and proposed an analytical model based on the solution of the impedance of the transmission line. This model was then coupled to a mechanical model to predict the dynamic actuation response. In this appendix the validity of the 2D impedance equivalent circuit in providing a good fit to the polymer impedance spectroscopy measurement is verified.

Electrochemical impedance spectroscopy (described in section 1.6.3) of a 15 μm thick polypyrrole film with a dimension of 50 mm × 2.7 mm on an insulating backing was performed inside an aqueous solution of $NaPF_6$ (as shown in Figure A2.1). The insulating backing on one side was used to block ions from penetrating

into that side, since it is assumed in the model that ion diffusion through the polymer thickness occurs only from one side (similar to the case of polymer coated catheter).

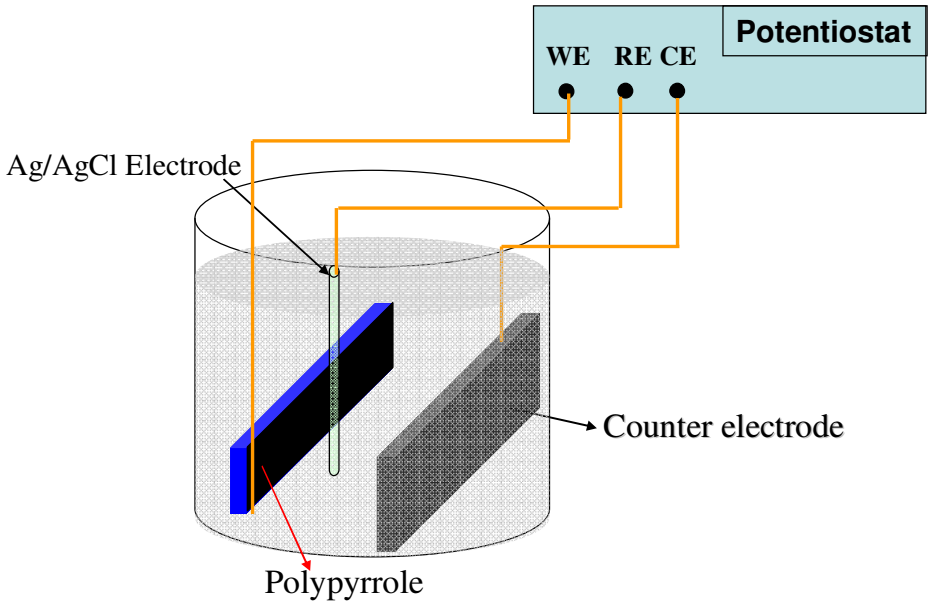

Figure A2. 1 Experimental set up for electrochemical impedance spectroscopy of polypyrrole

The polymer film was connected to the working electrode of the potentiostat via a gold wire attached to the end of the polymer film (as shown in Figure A2.1). An Ag/AgCl reference electrode was placed between the polymer and a counter electrode (here, a carbon fiber paper). A small sinusoidal voltage is applied versus the polymer and the reference electrode. The frequency of the sinusoidal signal is varied from 1000 Hz down to 0.0004 Hz and the impedance of the cell is measured by measuring the resulting current at various frequencies. The Bode plot of the impedance and the model predictions are shown in Figure A2.2.

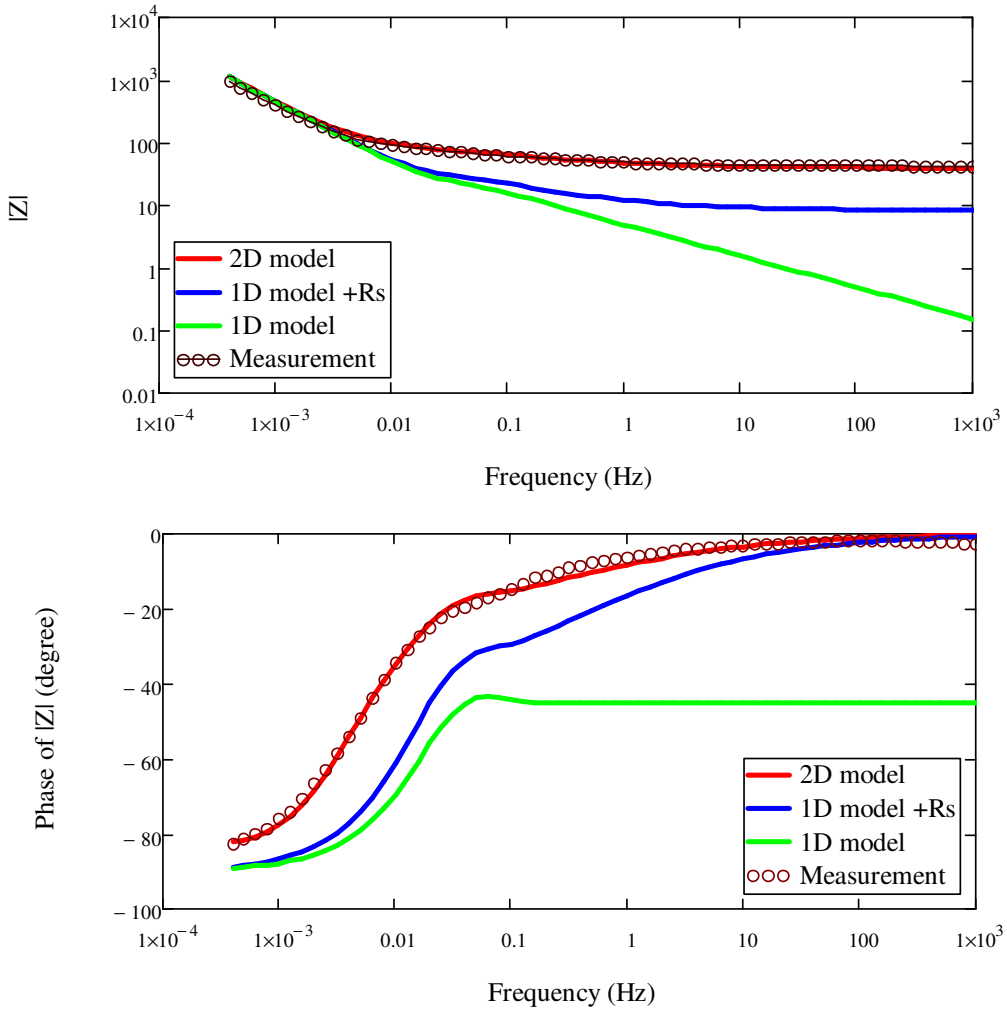

Figure A2.2: Electrochemical impedance spectroscopy of polypyrrole, above is the magnitude and below is the phase.

This Figure illustrates three cases of model predictions. The "1D model" represents the case where ionic resistance through the polymer thickness is only considered (Equation A2.1). In the "1D+Rs model", the effect of solution resistance is also taken into account (Equation A2.2), and in the "2D model" electronic resistance through the polymer length is added (Equation A2.3).

$$Z_{1D}(s) = \frac{\coth\left(\sqrt{\frac{s.C_V}{\sigma_i}}.h\right)}{A.\sigma\sqrt{\frac{s.C_V}{\sigma_i}}} \tag{A2.1}$$

$$Z_{1D+Rs}(s) = \frac{\coth\left(\sqrt{\frac{s.C_V}{\sigma_i}}.h\right)}{A.\sigma_i\sqrt{\frac{s.C_V}{\sigma_i}}} + \frac{d}{\sigma_s A} \tag{A2.2}$$

$$Z_{2D}(s) = \sqrt{\frac{1}{\sigma_e w.h}\left(\frac{\coth\left(\sqrt{\frac{s.C_V}{\sigma_i}}.h\right)}{A.\sigma\sqrt{\frac{s.C_V}{\sigma_i}}} + \frac{d}{\sigma_s A}\right)}.\coth\left(\sqrt{\frac{\frac{1}{\sigma_e w.h}A.\sigma_i\sqrt{\frac{s.C_V}{\sigma_i}}.\sigma_s A}{\coth\left(\sqrt{\frac{s.C_V}{\sigma_i}}.h\right).\sigma_s A + dA.\sigma_i\sqrt{\frac{s.C_V}{\sigma_i}}}}.L\right) \tag{A2.3}$$

The values used for the parameters of the above equations are as follows; ionic conductivity is σ_i = 2.2 × 10^{-3} S/m, solution conductivity is σ_s = 8 S/m, electronic conductivity is σ_e = 8000 S/m and volumetric capacitance is C_v = 2 × 10^8. These parameters are all directly measured minimizing the need for fitting.

We can see from Figure A2.2, that the "1D model" predicts a linear increase in impedance from 1000 Hz to 0.1 Hz with a phase of -45° implying a charge transfer response. The phase approaches -90° at lower frequencies and the magnitude rises, showing a trend towards a capacitive response. This can also be seen from the Nyquist plot of Figure A2.3, where a straight line parallel to the imaginary axes appears at low frequencies. Considering the solution resistance, the "1D + Rs model" provides a more reasonable prediction of the impedance at high frequencies where a pure resistive behaviour is observed followed by a transition to a capacitive response. This model, however, underestimates the transition time over which polymer

charging is complete (fast transition towards the capacitive response). Prediction of the "2D model" shows the best agreement with the measured impedance by taking the effect of the electronic resistance into account. An additional resistor (14 kΩ) parallel to the transmission line of Figure 5.1 was also considered in this model representing the leakage of the charge at very low frequencies. The effect of leakage can also be observed from the Nyquist plot of Figure A2.3, where the response deviates from a straight line at low frequencies.

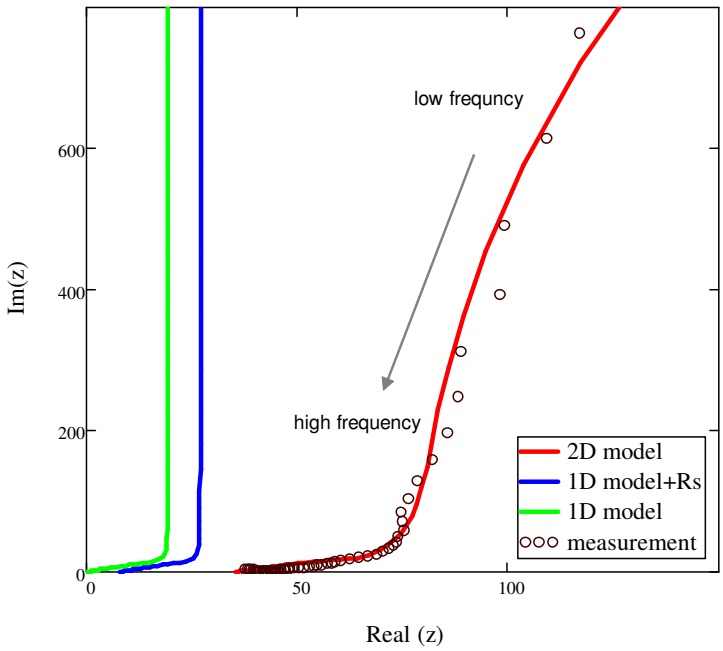

Figure A2.3: Nyquist plot of the impedance.

The good match between the 2D impedance model and the measurement results confirms the accuracy of the model in predicting the polymer electrochemical response. Although this model is primarily developed to predict the dynamic charging behaviour of electrochemically driven conducting polymer actuators, it can be

generalized to be used as an effective design tool for other electrochemical devices that work based on mass transport of species into a conductive electrode, such as supercapacitors and batteries.

APPENDIX 3: EFFECT OF BODY TEMPERATURE (37ºC) ON POLYMER ACTUATION [7]

The polypyrrole driven catheter will ultimately be operated inside the body, where it experiences a temperature of ~ 37 °C. Therefore information about the effect of body temperature on the actuation performance is critical for this application. Actuation of polypyyrole during and after exposing to high temperatures (up to 100°C) [2] has been previously studied by others as summarized below.

M. Cole has reported a temporary increase in actuation strain and strain rate during cycling at elevated temperatures (from 25 °C to 80 °C) likely due to higher charging amplitude and rate [1]. A loss of charge capacity and hence strain was observed over cycles (capacity drops by 50% at 80 °C in 3 hours) [1]. In another study he observed a reduction in strain rate after exposing the polymer to 80 °C for a long period of time (5000 s) [2]. This slow response was postulated to be due to decrease in polymer ionic conductivity as a result of structural compaction after being exposed to high temperatures. Another study by N. Vandesteeg [3] has suggested that the induced stress increases with temperature as it is increased from 25 °C to 100 °C during at least the first 270 seconds, but eventually decreases with cycling. An increase in the actuation speed and charging over the first cycles was also observed in these studies [3,4]. M. Christophersen, and E. Smela [5] have reported an increase in bending curvature of a polypyrrole/gold bilayer structure at elevated temperatures

[7] The experimental work of this study was performed by Kevin Lannon as part of his summer project under supervision of the Author.

(from 25 °C to 55 °C). These studies suggest that high temperature may increase the polymer actuation stress, strain and speed during first cycles of actuation, but eventually leads to slower response and smaller actuation stress with prolonged exposure to high temperatures.

According to the results reported in the above studies, substantial effects on polypyrrole electrochemical and mechanical properties have been mostly observed at temperatures higher than 37 °C. We are interested in application of polypyrrole at body temperature (37 °C). In this study, polypyrrole was exposed to 37 °C and its charging behavior was investigated.

Polypyrrole film was deposited onto a glassy carbon substrate using the electrochemical deposition method described in section 1.6. The charging behavior of the polymer was studied at room and body temperatures, and the results were compared. A cycling experiment similar to what was described in Chapter 2 (Section 2.2) was performed on the polymer film.

1. The film was first biased to +0.15 V versus an Ag/AgCl reference electrode (average of cycling from 0 to +0.3 V) for 10 min, at room temperature (20°C).

2. The polymer was then cycled from 0 to 0.3 V, and its charge transfer was recorded.

3. Steps 1-2 were repeated at 37 °C.

4. Step 3 was repeated at room temperature for the second time.

All measurements were relative to a Ag/AgCl reference electrode.

Figure A3.1 illustrates the charge transfer during cycling from 0 to 0.3 V. According to the measurement results exposure to 37 °C does not show a noticeable change in the amount and rate of charge transferred. Cycling experiments at other

potentials were also performed and their results suggest similar charging behavior continued over a period of 3 hours at 37 °C.

The polymer of this experiment was coated on a rigid substrate (i.e. glassy carbon), and the effect of temperature on the mechanical strain, and the stress was not directly measured. We assumed that the electrochemical charging at 37 °C is the main factor in determining the actuation performance of polypyrrole at this temperature. This assumption is valid according to literature [2,4], where the loss of actuation at high temperature was found to be mostly due to the loss of charging [2], and changes in stress at elevated temperature were reported to be dependent upon the ionic conductivity as opposed to changes in mechanical stiffness [4].

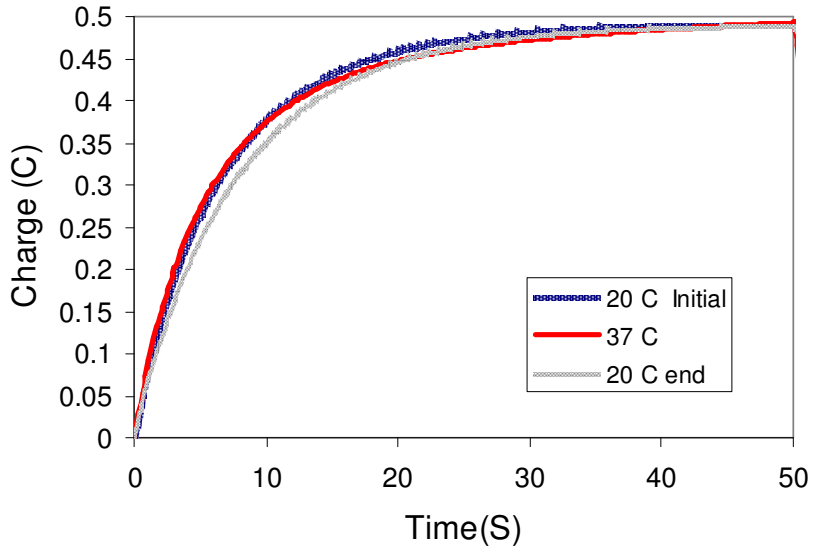

Figure A3.1: Amount of charge transferred in response to step in voltage from 0 to +0.3 V, at room and body temperatures.

It can be concluded that exposure to body temperature will not influence the charging amplitude and rate during at least 3 hours of operation at 37 °C in polypyrrole as grown and actuated. Further investigations of the actuator's

mechanical performance and cycle life are needed prove that there is little effect on actuation at 37 °C, but based on charge transfer results it appears likely that actuation will not be significantly affected.

References

[1] M. Cole, Master's Thesis, UBC, 2006

[2] M. Cple, J. Madden, "The Effect of Temperature Exposure on Polypyrrole Actuation" Materials Research Society Symposium Proceedings 889, 105-110, 2006.

[3] N. Vandesteeg, PhD Thesis, MIT 2007.

[4] Y Keng, PV Pillai, IW Hunter, "Characterizing the Effect of Temperature Increase on Polypyrrole Active Strength and Stress Rate" Proc. of ASME on Smart Materials, Adaptive Structures and Intelligent Systems, 53-60, 2009.

[5] M. Christophersen, and E. Smela , "Polypyrrole/Gold Bilayer Microactuators: Response Time and Temperature Effects" Proc. of SPIE, Electroactive Polymer Actuators and Devices (EAPAD) Vol. 6168, 61680V, 2006.

APPENDIX 4: ACTUATION IN PHOSPHATE BUFFERED SALINE AS A STEP TOWARDS SIMULATING OPERATION IN BLOOD[8]

The polypyrrole actuator based catheter designed in Chapter 6 was initially designed to use blood as the electrolyte, where the ions inside the blood were to be used to cause actuation in polypyrrole. In order to investigate actuation of polypyrrole in blood, an experiment was performed inside a phosphate buffered saline (PBS) solution which is commonly used in biological research and contains salts that are present in the blood, including sodium chloride, sodium phosphate, and potassium chloride and potassium phosphate. The ion concentrations of the solution usually match those of the human body.

As depicted in Figure A4.1 a free standing polypyrrole film is clamped into an electromechanical test apparatus (Dual Mode Lever System, Aurora Scientific, 300B). A square wave potential wave (from -0.4 V to 0.4 V versus an Ag/AgCl reference electrode) was applied (via the Solatron potentiostat) to the polymer film inside the PBS solution versus a Ag/AgCl reference electrode. The resulting strain is recorded using a data acquisition card.

[8]The results shown in Figure 4A.2 is the work done by Niloofar Fekri, as part of a summer undergraduate research project under supervision of the author.

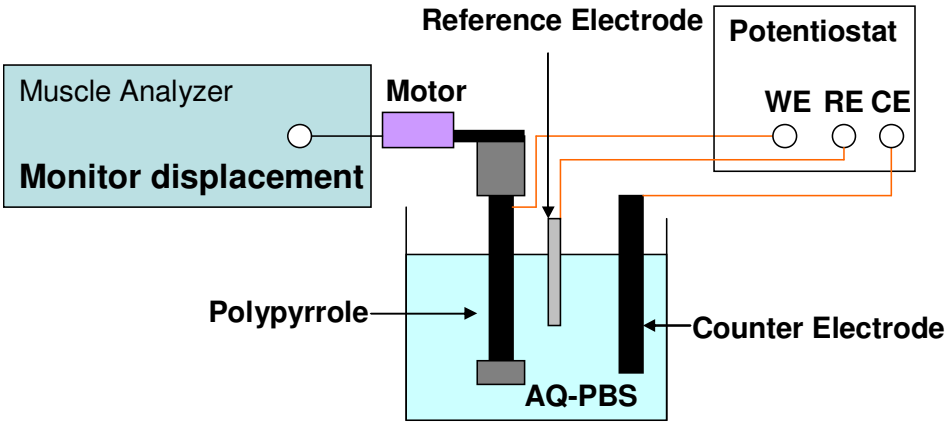

Figure A4. 1: Experimental set up for actuation of polypyrrole inside PBS.

Figure A4.2 depicts the measured electrochemical strain in response to the applied voltage. We can see that polypyrrole initially contracts in response to the step potential from -0.4 V to + 0.4 V versus an Ag/AgCl reference electrode, but it starts to expand after about 1 sec. This mixed contraction/expansion response is likely due to involvement of more than one mobile ion species during actuation [1]. The polypyrrole coated catheter was also tested inside the PBS solution and its bending response showed a similar behaviour (bending towards one side first and changing direction after ~1 s). This behaviour is not desired for applications. Furthermore, the electrochemical strain of polypyrrole actuated in PBS is very small (as shown in the figure it is almost 10 times smaller than the strain generated in $NaPF_6$). In addition to small strain and undesired actuation behaviour, there is a safety (and regulatory) issue involved with directly applying an electrical current through the blood (especially close to the heart) [2,3]. The maximum current allowed is 50 µA [3]. Therefore encapsulation of the active catheter within an insulating material containing a suitable

electrolyte, which results in the best performance of the actuator, was found to be the most practical approach.

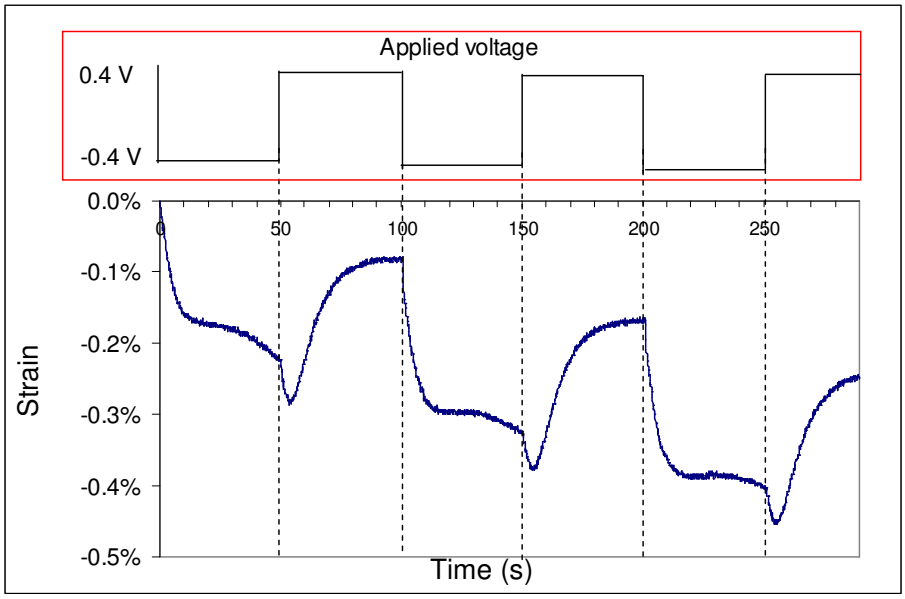

Figure A4. 2: Polypyrrole electrochemically induced strain in response to voltage square wave (from -0.4 V to +0.4 V) in PBS solution.

References

[1] P. Qibing, O. Inganas, "Electrochemical applications of the bending beam method; a

novel way to study ion transport in electroactive polymers" Solid State Ionics, 60, 1-3:161-166, 1993.

[2] www.americanheart.org.

[3] M. Levin, "Safe current limits for electromedical equipment and hazards to patients", Journal of the American hear association, Circulation, 2160, 1994.